

**DESIGNING OF ION-IMPRINTED CRYOGELS AND THEIR  
USE FOR HEAVY METAL REMOVAL**

**İYON BASKILANMIŞ KRIYOJELLERİN TASARIMI VE  
AĞIR METAL UZAKLAŞTIRILMASI AMACIYLA  
KULLANIMI**

**MİTRA JALİLZADEH**

**PROF. DR. SERAP ŞENEL**

**SUPERVISOR**

Submitted to Institute of Science of Hacettepe University

as a Partial Fulfillment to the Requirements

for the Award of the Degree of Doctor of Philosophy

in Chemistry

2014

## ETHICS

In this thesis study, prepared in accordance with the spelling rules of Institute of Graduate Studies in Science of Hacettepe University,

I declare that

- all the information and documents have been obtained in the base of the academic rules
- all audio-visual and written information and results have been presented according to the rules of scientific ethics
- in case of using others works, related studies have been cited in accordance with the scientific standards
- all cited studies have been fully referenced
- I did not any distortion in the data set
- and any part of this thesis has not been presented as another thesis study at this or any other university.

30/01/2014

Mitra JALILZADEH

To my parents

## ABSTRACT

### DESIGNING OF ION-IMPRINTED CRYOGELS AND THEIR USE FOR HEAVY METAL REMOVAL

Mitra JALILZADEH

Doctor of Philosophy, Department of Chemistry

Supervisor: Prof. Dr. Serap ŞENEL

January 2014, 150 pages

Heavy metals generally are toxic for animal and human body. Heavy metals due to stability and resistance to degradation are classified as environmental toxins. Therefore these metals should be removed from wastewaters.

Cryogels are polymeric gel matrices. Cryogels generally have interconnected supermacroporos spongy structure, high pore density, and large pores. Due to their large surface area and low flow resistance, they can be used for fast and high capacity separation.

Due to specific ion recognitions ion-imprinted cryogels were used as stationary phases in chromatography. Interaction of template molecule to functional monomer with non-covalent interaction is organized and provides solid materials which have functional groups, then by removing of template ions forms template ion specific regions in polymer.

In present study, four different ion-imprinted supermacroporose 2-hydroxyethyl methacrylate (HEMA)-based cryogels: [PHEMA-N-methacryloyl-(L)-cysteine-Cd (II), PHEMA-N-methacryloyl-(L)-aspartic acid-Pb(II), magnetic PHEMA-N-methacryloyl-(L)-histidine-Cu (II) and non-magnetic PHEMA-N-methacryloyl-(L)-histidine-Cu (II)], were synthesized. These cryogels were characterized by surface

area measurements (BET), swelling tests, scanning electron microscopy (SEM), EDX, and FTIR. The surface areas of ion-imprinted cryogels (106, 43.6, 92.0, and 78.5 m<sup>2</sup>/g ) were higher than those of non-imprinted cryogels (78.5, 18.6, 47.0, and 29.3 m<sup>2</sup>/g). These cryogels were used for adsorption of Cd(II), Pb(II) and Cu(II) ions from aqueous solutions, respectively. Adsorption of heavy metals by these cryogels and effects of pH, initial concentration, contact time, temperature on adsorption capacity were examined. The maximum adsorption capacities of the ion-imprinted cryogel membranes were 77.2 mg/g for Cu(II) by Cu(II) ion-imprinted non-magnetic cryogel, 182.7 mg/g by magnetic Cu(II) ion-imprinted cryogel, 86.7 mg/g for Cd(II) by Cd(II) ion-imprinted cryogel, and 122.7 mg/g for Pb(II) by Pb(II) ion-imprinted cryogel, respectively. Heavy metal ions adsorption behavior was examined by Langmuir and Freundlich isotherms. The adsorptions were best fitted by Langmuir isotherms. First and second-order kinetic models were applied for these adsorptions. Pseudo-second order kinetic model was suitable for these adsorptions and indicated that adsorption was chemically controlled. Thermodynamic values ( $\Delta H^\circ$ ,  $\Delta G^\circ$ ,  $\Delta S^\circ$ ) were calculated and thermodynamic possibility of adsorption was evaluated. Selectivity studies for ion-imprinted and non-imprinted cryogels were studied. Competitive adsorption studies by eight metal ions (Cu(II), Cd(II), Pb(II), Zn(II), Ca(II), Co(II), Ni(II), Fe(III)) were examined. Adsorption and desorption studies were repeated for three times, and reusability of the cryogels was proved without a significant loss in adsorption capacity.

Keyword: ion imprinted cryogel, PHEMA-N-methacryloyl-(L)-cysteine-Cd (II), PHEMA-N-methacryloyl-(L)-aspartic acid-Pb(II), magnetic PHEMA-N-methacryloyl-(L)-histidine-Cu, non-magnetic PHEMA-N-methacryloyl-(L)-histidine-Cu (II)

## ÖZET

# İYON BASKILANMIŞ KRİYOJELLERİN TASARIMI VE AĞIR METAL UZAKLAŞTIRILMASI AMACIYLA KULLANIMI

**Mitra JALİLZADEH**

**Doktora, Kimya Bölümü**

**Tez Danışmanı: Prof.Dr.Serap ŞENEL**

**Ocak 2014, 150 sayfa**

Genelde ağır metaller insan ve hayvan vücudu için toksik madde olarak tanımlanmışlardır. Ağır metaller dayanıklılık, kararlılık ve kimyasal bozunmaya karşı direnç göstermek gibi özellikleri nedeniyle, çevresel toksinler olarak sınıflandırılmışlardır. Bu nedenle ağır metaller su kaynaklarından uzaklaştırılmalıdır.

Kriyojeller, polimerik jel matrikslerdir. Kriyojeller genellikle birbiriyle bağlı süpermakrogözenekli süngerimsi bir yapıya, yüksek gözenek yoğunluğuna ve geniş gözeneklere sahiptirler. Geniş yüzey alanı ve düşük akış direnci sağladıklarından, yüksek kapasitede hızlı ayırma özelliğine sahiptirler.

İyon baskılanmış kriyojeller spesifik iyon tanıma özeliği nedeniyle kromatografide sabit faz olarak kullanılırlar. Kalıp iyon etrafında fonksiyonel monomerlerin kovalent olmayan etkileşimlerle organize edilmesi ve kimyasal fonksiyona sahip katı malzemelerin oluşturulması sağlanır. İşlem sonrasında kalıp iyonun uzaklaştırılması ile yapıda kalıp iyon özgü bölgeler oluşmuş olur.

Bu çalışmada, dört farklı iyon baskılanmış süpermakrogözenekli 2-hidroksietil metakrilat (HEMA) bazlı kriyojeller [PHEMA-N-metakriloil-(L)-sistein-Cd(II),

PHEMA-N-metakriloil-(L)-aspartik asit-Pb(II), manyetik PHEMA-N-metakriloil-(L)-histidin-Cu(II) ve manyetik olmayan PHEMA-N-metakriloil-(L)-histidin-Cu(II)], sentezlenmiştir. İyon baskılanmış kriyojeller yüzey alanı ölçümleri (BET), şişme testleri, taramalı elektron mikroskobu (SEM), EDX ve FTIR çalışmaları ile karakterize edilmiştir. İyon-baskılanmış kriyojellerin yüzey alanları (106, 43.6, 92.0, ve 78.5 m<sup>2</sup>/g) iyon-baskılanmamış kriyojellerin yüzey alanlarından (78.5, 18.6, 47.0, ve 29.3 m<sup>2</sup>/g) daha yüksektirler. Bu kriyojellere, sırasıyla sulu çözeltilerden Cd(II), Pb(II) ve Cu(II) iyonlarının adsorpsiyon çalışmaları gerçekleştirilmiştir. Ağır metal iyonlarının iyon baskılanmış kriyojel membranlar ile adsorpsiyonuna pH'ın, ağır metal derişiminin, adsorpsiyon süresinin ve sıcaklığın etkisi incelenmiştir. İyon-baskılanmış kriyojel membranların maksimum adsorpsiyon kapasiteleri Cu(II) için 77.2 mg/g Cu(II) iyon-baskılanmış kriyojelle, 182.7 mg/g Cu(II) için Cu(II) iyon- baskılanmış manyetik kriyojelle, 86.7 mg/g Cd(II) için Cd(II) iyon-baskılanmış kriyojelle, ve 122.7 mg/g Pb için Pb(II) iyon-baskılanmış kriyojelle elde edilmiştir. Ağır metal iyonlarının adsorpsiyon davranışları Langmuir ve Freundlich izotermi kullanarak incelenmiştir. Sonuçların Langmuir izotermiyle uyumlu olduğu gözlemlenmiştir. Birinci ve ikinci derece kinetik modelleri bu adsorpsiyonlar için uygulanmıştır. Sözde-ikinci derecenin bu adsorpsiyonlar için daha uygun olduğu ve adsorpsiyonların kimyasal kontrollü olduğu gösterilmiştir. Termodinamik parametreler ( $\Delta H^\circ$ ,  $\Delta G^\circ$ ,  $\Delta S^\circ$ ) bu adsorpsiyonlar için hesaplanmış ve adsorpsiyon proseslerinin olasılığı, termodinamik değerlere göre incelenmiştir. Seçicilik çalışmaları, iyon baskılanmış ve baskılanmamış kriyojellerle gerçekleştirilmiştir. Yarışmalı adsorpsiyon çalışmaları, sekiz metal iyonunun bulunduğu çözeltide (Cu(II), Cd(II), Pb(II), Zn(II), Ca(II), Co(II), Ni(II), Fe(III)) yapılmıştır. Adsorpsiyon ve desorpsiyon işlemi üç kez art arda tekrarlanmıştır ve kriyojel membranların adsorpsiyon kapasitesinde önemli bir kayıp olmadan tekrar kullanım için uygun olduğu gözlemlenmiştir.

Anahtar kelimeler: iyon baskılanmış kriyojel, PHEMA-N-metakriloil-(L)-sistein-Cd(II), PHEMA-N-metakriloil-(L)-aspartik asit-Pb(II), manyetik PHEMA-N-metakriloil-(L)-histidin-Cu(II) ve manyetik olmayan PHEMA-N-metakriloil-(L)-histidin-Cu (II).

## **ACKNOWLEDGEMENT**

I would like to thank to my supervisor Prof. Dr. Serap ŞENEL for her help, encouragement, kindness, criticism, advice, and sensibility.

I would like to express my deepness gratitude to Prof. Dr. Adil DENİZLİ for his kindness, advice, help, encouragement, and sensibility.

In addition, I would like to express my deepness gratitude to Assoc. Prof. Dr. Lokman Uzun for his endless help, patience, advice, comments and suggestions about this research. He was always with me in during of my PhD education. I want to thank him for his helpful behaviors, enormous contribution, understandings, and effective advises.

I would like to express my thanks to Assoc. Prof. Dr. Handan Yavuz Alagöz for her advice and kindness.

I would like to thank my friends in Biochemistry Research Group and chemistry department, Recep Üzek, Mehmet Emin Çorman, Canan Armutcu, Turkan Mammadova, Esmâ Sari, Huma Ishaq, Dr. Fatma Yılmaz, Dr. Nilay Bereli, Dr. Müge Andaç, Dr. Ali Derazshamshir, Dr. Gözde Baydemir, Gülsu Şener, Bahar Ergün, Dr. Işık Perçin Demirçelik, Emel Tamahkar, Özlem Şahin, Masoomeh Mehrnia, Matin Yazdani, Mohammadreza Ghafarlu, Fatma Kartal, Dr. Veyis Karakoç, Mine Dursun, Çiğdem Çiçek, Dilara Saçlıgil, Yeşeren Saylan, Duygu Çimen, Ilgım Göktürk, Tuğba Doğan, Gizem Uzunoğlu, Binaz Demirci, Erdoğan Özgür, Sevgi Aslıyüce, Kemal Çetin, Senem Çulha and Semra Akgönüllü for their help, trustful and providing me a friendly atmosphere to work in.

I am especially grateful to Assoc. Prof. Dr. Selim Sanin, Dr. İlknur Durukan, Dr. Anies Satti, and Ömer Arslan for their help.

My greatest thanks to my family, my brother, Ramez Jalilzadeh, my sister, Raana Jalilzadeh, my nephew, Hamed, and my nieces, Razieh, Ayshin, Elay for their kindness, patience and understanding...

Mitra JALİLZADEH

## **CONTENTS**



	<b><u>PAGES</u></b>
ABSTRACT.....	i
ÖZET.....	iii
ACKNOWLEDGEMENT.....	v
CONTENTS .....	vi
FIGURE LEGENDS.....	xi
TABLE LEGENDS.....	xvii
1. INTRODUCTION.....	1
2. GENERAL INFORMATION.....	4
2.1. Heavy Metals.....	4
2.1.1. Heavy Metals Toxicity.....	4
2.1.2. Removal of Heavy Metals.....	5
2.1.3. Conventional Refinement Techniques.....	5
2.1.3.1. Chemical Precipitation .....	6
2.1.3.2.2. Electrochemical process.....	7
2.1.3.3. Liquid-Liquid Extraction.....	7
2.1.3.4. Flotation.....	8
2.1.3.5. Coagulation and Flocculation .....	8
2.1.3.6. Ion-exchange.....	8
2.1.3.7. Membrane Processes.....	9
2.1.4. New Methods for Removing Heavy Metals.....	9
2.1.4.1. Adsorption.....	10
2.1.4.1.1. Adsorption on Modified Natural Materials.....	13
2.1.4.1.2. Adsorption on Industrial by-Products.....	12
2.1.4.1.3. Adsorption on Polymers.....	12
2.1.4.1.4. Modified Biopolymers.....	13
2.1.4.1.5. Hydrogels.....	13
2.1.4.1.6. Cryogels.....	14

2.1.4.1.6.1. Cryogels in Treatment of Water and Wastewater.....	16
2.1.4.1.6.2. Composite Systems.....	17
2.1.4.2. Membrane Filtration.....	17
2.1.4.3. Electrodialysis.....	18
2.1.4.4. Photocatalysis.....	18
2.1.4.5. Metal Chelating Method.....	19
2.1.5. Cadmium.....	21
2.1.6. Copper.....	21
2.1.7. Lead.....	22
2.1.8. Polymer Based Adsorbents for Removal of Metals.....	23
2.1.9. Determination of Heavy Metals.....	25
2.1.9.1. Atomic Absorption Spectrometry.....	26
2.1.9.2 Absorption Principles.....	26
2.2. Molecular Imprinting Technology.....	27
2.2.1. Covalent Imprinting.....	29
2.2.2. Non-Covalent Imprinting.....	29
2.2.3. Semi-Covalent Imprinting.....	30
2.2.4. Sythesis Methods of MIP.....	33
2.2.5. Surface Imprinting.....	33
2.2.6. Novel Technologies for MIP.....	34
2.2.6.1. Controlled/Living Free Radical Polymerization(CLRP).....	34
2.2.6.2. Block Copolymer Self-assembly.....	35
2.2.6.3. Microwave-assisted Heating Method.....	35
2.2.6.4. Ionic Liquid as porogen.....	35
2.2.7. Ion Imprinted Polymer(IIP).....	36
2.2.7.1. Different Approches for IIP.....	36
2.2.7.2. The Crosslinking of Linear Chain Polymers Carrying Metal-binding Groups.....	37
2.2.7.3. Chemical Immobilization.....	37
2.2.7.4. Surface Imprinting.....	38

2.2.7.5. The History of Ion Imprinted Polymers.....	39
3. MATERIALS AND METHODS.....	41
3.1. Materials.....	40
3.2. Preparation of Ion Imprinted Cryogels.....	40
3.2.1. The Cryogels for Cu(II) Ions.....	43
3.2.1.1. Synthesis of Functional Monomer.....	43
3.2.1.2. Preparation of MAH-Cu(II) Pre-Complex.....	43
3.2.1.3. Preparation of Cu(II) Ion Imprinted and Non-Imprinted Non-Magnetic Cryogels.....	43
3.2.1.4. Preparation of Cu(II) Ion Imprinted and Non-Imprinted Magnetic Cryogels.....	45
3.2.2. The Cryogels for Cd(II) Ions.....	46
3.2.2.1. Synthesis of Functional Monomer.....	46
3.2.2.2. Preparation of MAC-Cd(II) Pre-Complex.....	46
3.2.2.3. Preparation of Cd(II) Ion Imprinted and Non-Imprinted Cryogels.....	47
3.2.2. The Cryogels for Pb(II) Ions.....	48
3.2.3.1. Synthesis of Functional Monomer.....	48
3.2.3.2. Preparation of MAsp-Pb(II) Pre-Complex.....	49
3.2.3.3. Preparation of Pb(II) Ion Imprinted and Non-Imprinted Cryogels.....	49
3.3. Characterization Studies.....	51
3.3.1. Swelling Properties of Cryogels.....	51
3.3.2. FTIR Studies.....	51
3.3.3. Surface Morphology.....	51
3.3.4. X-Ray Analysis.....	51
3.3.5. Surface Area Measurements.....	52
3.3. Heavy Metal Ion Adsorption from Singular Aqueous Solutions.....	52
3.3. Selectivity Studies for Metal ion Imprinted Cryogels.....	53
3.6. Desorption and Reuse.....	54
3.7. Competitive Heavy Metal Adsorption/Enrichment.....	54
4. RESULT AND DISCUSSION.....	55

4.1.1. Swelling Characterization of Cryogels.....	55
4.1.2. FTIR Analyses.....	56
4.1.3. Surface Area Measurements.....	58
4.1.4. Surface Morphology.....	62
4.1.5. X-Ray Analysis (EDX).....	63
4.2. Adsorption Studies with Ion Imprinted Cryogels.....	63
4.2.1. Effective Parameters on Heavy Metal Adsorption Performances of Molecularly Imprinted Cryogels.....	63
4.2.1.1. Effect of pH.....	63
4.2.1.2. Effect of Initial Concentration.....	67
4.2.1.3. Effect of Temperature.....	71
4.2.1.4. Effect of Contact Time.....	79
4.2.1.5. Adsorption Isotherms.....	82
4.2.1.5.1. Langmuir Isotherm.....	83
4.2.1.5.2. Freundlich Isotherm.....	84
4.2.1.6. Adsorption Thermodynamics.....	92
4.2.1.7. Adsorption Kinetics.....	107
4.2.2. Magnetic vs Non-Magnetic Cu(II)-Imprinted Cryogels.....	116
4.2.3. Selectivity Studies.....	117
4.2.3.1. Ion Imprinted vs Non-Imprinted Cryogels.....	117
4.2.3.1.1. Cu(II) Ion-Imprinted Magnetic vs Non-Imprinted Cryogels.....	117
4.2.3.1.2. Cu(II) Ion-Imprinted vs Non-Imprinted Cryogels.....	118
4.2.3.1.3. Cd(II) Ion-Imprinted vs Non-Imprinted Cryogels.....	119
4.2.3.1.4. Pb(II) Ion-Imprinted with Non-Imprinted Cryogels.....	120
4.2.3.2. Competitive Adsorption by Ion-Imprinted Cryogels.....	122
4.2.3.2.1. Adsorption of Cu(II), Cd(II), Pb(II), and Zn(II) by Cu(II) Ion-Imprinted Magnetic Cryogel.....	122
4.2.3.2.2. Adsorption of Cu(II), Cd(II), Pb(II), and Zn(II) by Cu(II) Ion-Imprinted Non-Magnetic Cryogel.....	123
4.2.3.2.3. Adsorption of Cd(II), Cu(II), Pb(II), and Zn(II) by Cd(II) Ion-Imprinted Cryogel.....	124

4.2.3.2.4. Adsorption of Pb(II), Cu(II), Cd(II), and Zn(II) by Pb(II) Ion-Imprinted Cryogel.....	126
4.2.4. Simultaneous Competitive Adsorption on Ion Imprinted Cryogels.....	126
4.4. Desorption and Reuse.....	127
4.5. Comparison with Literature.....	127
5. CONCLUSION.....	129
REFERENCES.....	133
CURRICULUM VITAE.....	150

## FIGURE LEGENDS

	<u>PAGES</u>
Figure 2.1. Schematic diagram of cryogels formation.....	16
Figure 2.2. Methods for synthesis of functional polymers.....	20
Figure 2.3. Schematic diagram of the molecular imprinting process.....	28
Figure.2.4. Structure of commonly used functional monomers and cross-linkers	32
Figure 2.5. Schematic representation of IIP synthesis.....	36
Figure 2.6. Schematic representation of surface imprinting.....	39
Figure 2.7. Number of published articles about IIP in the last 10 years.....	39
Figure 3.1. Possible formula of MAH-Cu(II) complex.....	43
Figure 3.2. Possible formula of MAC-Cd(II) complex.....	47
Figure 3.3. Possible formula of MAAsp-Pb(II) complex.....	49
Figure 3.4. Optic photos of ion imprinted cryogels in different shapes. (A) Pb(II), (B) Cu(II), (C) magnetic Cu(II), (D) Cd(II), imprinted cryogels.....	50
Figure 3.5. Atomic absorption spectroscopy instrument.....	53
Figure 4.1. Swelling ratio of cryogels (Asterisk superscript is involved for magnetic cryogel).....	55
Figure 4.2. FTIR spectra of Cu(II) ion imprinted poly(HEMA-MAH) cryogels.....	57
Figure 4.3. FTIR spectra of Cd(II) ion imprinted poly(HEMA-MAC) cryogels.....	58
Figure 4.4. FTIR spectra of Pb(II) ion imprinted poly(HEMA-MAAsp) cryogels.....	58
Figure 4.5. SEM photographs of cryogels: A) Cu(II) ion imprinted; (B) Non-imprinted; (C) Cu(II) ion imprinted magnetic; (D) Non-imprinted magnetic;.....	60
Figure 4.6. SEM photographs of cryogels: A) Cd(II) ion imprinted; (B) Non-imprinted; (C) Pb(II) ion imprinted; (D) Non-imprinted;.....	61

Figure 4.7. EDX spectra of cryogels after desorption of metal ions: (A) Cu(II) imprinted; (B) Cu(II) non-imprinted; (C) Pb(II) imprinted; (D) Pb(II) non-imprinted; .....	62
Figure.4.8. The effect of pH on adsorption of Cu(II) by Cu(II) ion-imprinted magnetic cryogel membranes. Concentration: 60 ppm; incubation period: 120 min; T: 25°C.....	65
Figure 4.9. The effect of pH on adsorption of Cu(II) by Cu(II)-ion imprinted non-magnetic cryogel membranes; Concentration: 60 ppm; incubation period: 120 min; and T: 25°C.....	66
Figure 4.10. The effect of pH on adsorption of Cd(II) by ion imprinted cryogel membranes; Concentration: 60 mg/L; incubation period: 120 min; and T: 25°C...66	66
Figure 4.11. The effect of pH on the adsorption of Pb(II) by ion imprinted cryogel membranes; Concentration: 60 mg/L; incubation period: 120 min; T: 25°C.....	66
Figure 4.12. The effect of initial concentration on adsorption of Cu(II) by ion-imprinted magnetic cryogel membranes; pH: 5.5; incubation period: 120 min and T: 25°C.....	69
Figure 4.13.The effect of initial concentration on adsorption of Cu(II) by ion imprinted non-magnetic cryogel membranes; pH: 5.5; incubation period: 120 min and T: 25°C.....	70
Figure 4.14. The effect of initial concentration on the adsorption of Cd(II) by ion-imprinted cryogel membranes; pH: 5.5; incubation period: 120 min; and T: 25°C.....	70
Figure 4.15. The effect of initial concentration in adsorption of Pb(II) by ion-imprinted cryogel membranes, pH: 5.5; incubation period: 120 min; and T: 25°C.....	70
Figure 4.16. The effect of temperature on adsorption of Cu(II) by ion-imprinted magnetic cryogel membranes; Concentration: 30 ppm; pH: 5.5 and incubation period: 120 min.....	72
Figure 4.17. The effect of temperature on adsorption of Cu(II) by ion-imprinted magnetic cryogel membranes; Concentration: 130 ppm; pH: 5.5 and incubation period: 120 min.....	73
Figure 4.18. The effect of temperature on adsorption of Cu(II) by ion-imprinted magnetic cryogel membranes; Concentration: 400 ppm; pH: 5.5 and incubation period: 120 min.....	74

Figure 4.19. Effect of temperature on the adsorption of Cu(II) by Cu(II) ion imprinted non-magnetic cryogel membranes; pH: 5.5; incubation period: 120 min; and concentration (A): 30 ppm, (B): 130 ppm and (C): 400 ppm.....	76
Figure 4.20. The effect of temperature on the adsorption of Cd(II) by ion imprinted cryogel membranes; pH: 5.5; incubation period: 120 min; and concentration (A): 30 ppm; (B): 130 ppm; (C): 400 ppm.....	77
Figure 4.21. The effect of temperature on the adsorption of Pb(II) by ion imprinted cryogel membranes; pH: 5.5; incubation period: 120 min; and concentration (A): 30 ppm; (B): 130 ppm; (C): 400 ppm.....	78
Figure 4.22. The effect of contact time on adsorption of Cu(II) by ion-imprinted magnetic cryogel membranes; Concentration: 60 ppm; pH: 5.5; and T: 25°C.....	80
Figure 4.23. The effect of contact time on adsorption of Cu(II) by ion imprinted non-magnetic cryogel membranes; Concentration: 60 ppm; pH: 5.5 and T: 25°C.....	81
Figure 4.24. The effect of contact time on the adsorption of Cd(II) by ion imprinted cryogel membranes; Concentration: 60 ppm; pH: 5.5 and T: 25°C.....	81
Figure 4.25. The effect of contact time for adsorption of Pb(II) by ion imprinted cryogels; Concentration: 60 ppm; pH: 5.5; incubation period: 120 min; and T: 25°C.....	82
Figure 4.26. Langmuir isotherm model for adsorption of Cu(II) by ion imprinted magnetic cryogel membranes.....	86
Figure 4.27. Freundlich isotherm model for adsorption of Cu(II) by ion imprinted magnetic cryogel membranes.....	87
Figure 4.28. Langmuir isotherm models for adsorption of Cu(II) by ion-imprinted non-magnetic cryogel membranes.....	89
Figure 4.29. Freundlich isotherm model for adsorption of Cu(II) by ion-imprinted non-magnetic cryogel membranes.....	89



Figure 4.30. Langmuir isotherm model for adsorption of Cd(II) by ion imprinted cryogel membranes.....	90
Figure 4.31. Freundlich isotherm model for adsorption of Cd(II) by ion-imprinted cryogel membranes.....	90
Figure 4.32. Langmuir isotherm model for adsorption of Pb(II) by ion imprinted cryogel membranes.....	91
Figure 4.33. Freundlich isotherm model for adsorption of Pb(II) by ion-imprinted cryogel membranes.....	91
Figure 4.34. Langmuir isotherms of ion imprinted magnetic cryogels (Cu*-1, Cu*-2, Cu*-3) at different temperatures (4, 25, 32, 40°C).....	96
Figure 4.35. Langmuir isotherms of ion imprinted magnetic cryogels (Cu*-4, Cu*-5, Cu*-6) at different temperatures (4, 25, 32, 40°C).....	97
Figure 4.36. Langmuir isotherms of ion imprinted magnetic cryogels (Cu*-7, Cu*-8, Cu*-9) at different temperatures (4, 25, 32, 40°C).....	98
Figure 4.37. Van't Hoff plots for adsorption of Cu(II) on the ion imprinted magnetic cryogels.....	99
Figure 4.38. Langmuir isotherms for adsorption of Cu(II) by ion imprinted non-magnetic cryogel membranes at different temperatures.....	101
Figure 4.39. Van't Hoff plot for the adsorption of Cu(II) by imprinted non-magnetic cryogel membranes.....	102
Figure 4.40. Langmuir isotherms for adsorption of Cd(II) by ion imprinted cryogels at different temperatures (4, 25, 32, 40°C).....	103
Figure 4.41. Van't Hoff plot for the adsorption of Cd(II) by imprinted cryogel membranes.....	104
Figure 4.42. Langmuir isotherms for adsorption of Pb(II) by ion imprinted cryogels at different temperatures.....	106

Figure 4.43. Van't Hoff plots for the adsorption of Pb(II) by ion imprinted cryogels.....	107
Figure 4.44. Pseudo first-order kinetic model for adsorption of Cu(II) by ion imprinted magnetic cryogel membranes.....	110
Figure 4.45. Pseudo second-order kinetic model for adsorption of Cu(II) by ion imprinted magnetic cryogel membranes.....	111
Figure 4.46. Pseudo first-order kinetic model plots for adsorption of Cu(II) by ion imprinted non-magnetic cryogels.....	112
Figure 4.47. Pseudo second-order kinetic model plot for adsorption of Cu(II) by ion imprinted non-magnetic cryogels.....	113
Figure 4.48. Pseudo first-order kinetic model for adsorption of Cd(II) by ion imprinted cryogel membranes.....	114
Figure 4.49. Pseudo second-order kinetic model for adsorption of Cd(II) by ion imprinted cryogels.....	114
Figure 4.50. Pseudo first-order kinetic model for adsorption of Pb(II) by ion imprinted cryogel membranes.....	115
Figure 4.51. Pseudo second-order kinetic model for adsorption of Pb(II) by ion imprinted cryogel membranes.....	116
Figure 4.52. Comparison of adsorption capacities of ion imprinted magnetic and non-magnetic cryogels; pH: 5.5; incubation period: 120 min and T: 25°C.....	117
Figure 4.53. Comparison of adsorption capacities of magnetic Cu(II) ion-imprinted with non-imprinted cryogels; pH: 5.5; T: 25°C; and incubation period: 120 min..	118
Figure 4.54. Comparison of adsorption capacities of Cu(II) ion imprinted with non-imprinted cryogels; pH: 5.5; T: 25°C; and incubation period: 120 min.....	119
Figure 4.55. Comparison of adsorption capacities of Cd(II) ion-imprinted and non-imprinted cryogels; pH: 5.5; incubation period: 120 min; and T; 25°C.....	120

Figure 4.56. Comparison of adsorption capacities of Pb(II) ion imprinted with non-imprinted cryogels; T: 25°C; pH: 5.5; incubation period: 120 min.....121

## TABLE LEGENDS

	<u>PAGES</u>
Table 2.1. Physical methods for the removal of heavy methods.....	6
Table 3.1. Summarizing the strategy for cryogel synthesis.....	42
Table 3.2. Composition of Cu(II) ion imprinted non-magnetic cryogels.....	44
Table 3.3. Composition of Cu(II) ion imprinted magnetic cryogels.....	46
Table 3.4. Composition of Cd(II) ion imprinted cryogels.....	48
Table 3.5. Composition of Pb(II) ion imprinted cryogels.....	50
Table 4.1. Swelling ratio of PHEMA cryogels.....	56
Table 4.2. Surface area measurements (BET) of ion imprinted and non-imprinted cryogels.....	59
Table 4.3. Langmuir and Freundlich models parameters for adsorption of Cu(II) by Cu(II) ion-imprinted magnetic cryogels.....	88
Table 4.4. Langmuir and Freundlich models parameters for adsorption of Cu(II) by ion imprinted non-magnetic cryogels.....	88
Table 4.5. Langmuir and Freundlich model parameters for adsorption of Cd(II) by ion imprinted cryogel membranes.....	90
Table 4.6. Langmuir and Freundlich models parameters for adsorption of Pb(II) by ion imprinted cryogel membranes.....	91
Table 4.7. Langmuir model parameters for adsorption of Cu(II) by Cu(II) ion imprinted magnetic cryogels at 4°C and 25°C.....	94
Table 4.8. Langmuir model parameters for adsorption of Cu(II) by Cu(II) ion imprinted magnetic cryogels at 32°C and 40°C.....	95
Table 4.9. Thermodynamic parameters for adsorption of Cu(II) by ion imprinted magnetic cryogels.....	100

Table 4.10. Langmuir model parameters for adsorption of Cu(II) by ion imprinted non-magnetic cryogels at different temperatures.....	100
Table 4.11. Thermodynamic parameters for adsorption of Cu(II) by ion imprinted non-magnetic cryogels.....	102
Table 4.12. Thermodynamic parameters for adsorption of Cu(II) by ion imprinted non-magnetic cryogels.....	104
Table 4.13. Thermodynamic parameters for adsorption of Cd(II) by ion imprinted cryogels.....	105
Table 4.14. Langmuir model parameters for adsorption of Pb(II) by ion imprinted cryogels at different temperatures.....	105
Table 4.15. Thermodynamic parameters for adsorption of Cd(II) by ion imprinted cryogels.....	107
Table 4.16. Pseudo first-order and second-order kinetic models parameters for adsorption of Cu(II) by ion imprinted magnetic cryogel membranes.....	112
Table 4.17. Pseudo first-order and second-order kinetic models parameters for adsorption of Cu(II) by ion imprinted non-magnetic cryogel membranes.....	113
Table 4.18. Pseudo first-order and second-order kinetic models parameters for adsorption of Cd(II) by ion imprinted non-magnetic cryogel membranes.....	115
Table 4.19. Pseudo first-order and second-order kinetic models parameters for adsorption of Pb(II) by ion imprinted non-magnetic cryogel membranes.....	116
Table 4.20. Comparison of selectivities of ion imprinted with non-imprinted cryogels.....	121
Table 4.21. Competitive adsorption of heavy metal ions by Cu(II) magnetic ion imprinted cryogel from multi-metal ions solution.....	122
Table 4.22. Competitive adsorption of heavy metal ions by Cu(II) magnetic ion imprinted cryogel from multi-metal ions solution.....	123

Table 4.23. Competitive adsorption of heavy metal ions by Cd(II) ion imprinted cryogel from multi-metal ions solution.....	124
Table 4.24. Competitive adsorption of heavy metal ions by Pb(II) ion imprinted cryogel from multi-metal ions solution.....	125
Table 4.25. Simultaneous competitive adsorption of heavy metal ions by Pb(II), Cu(II), and Cd(II) ion imprinted cryogel from multi metal ions solution.....	126
Table 4.26. Adsorption/desorption/regeneration cycles for ion imprinted cryogels.....	127
Table 4.27. Comparison of this study with other studies.....	128

## 1. INTRODUCTION

Most of heavy metals are necessary in small amounts for body but in high concentrations are toxic [1]. There isn't any agreed definition of authority units, such as IUPAC for heavy metals, but elements such as Zn, Fe, Cu, Cr, Co, Pb, Cd, Ni, Pd, Ag, Hg, Pt, Au, As, etc. are classified in this group of metals [2]. Accumulation of these metals in living organisms causes serious health problems. These metals after being absorbed by body make connection to cellular units with vital important ones such as proteins, enzymes and nucleic acids and inhibit their functions [3]. Toxicity of these metals most commonly affects the brain and kidneys, but some metals such as arsenic clearly cause cancer [4].

Removal of heavy metals from water is necessary, because these pollutant materials can't be changed to harmless material as organic pollutants. Many methods have been used for removal of heavy metals. There are many traditional methods, such as chemical precipitation, adsorption, electrochemical process, extraction, floatation, coagulation, ion exchange etc., but these methods are generally expensive or risky [5]. Nowadays, new adsorbents are used for adsorption. Purposes of adsorption with these materials are development of cheaper and more effective process for removal of heavy metals from water [6]. Adsorbents such as lignin, tannin, chitin, chitosan, dead biomass, zeolite, clay, by-products of agricultural industry, activated carbon, carbon nanotubes and synthetic polymer-based ones have been used for adsorption of heavy metals from water [7]. Adsorbent materials have usually a porous structure, and the sorption process generally takes place in the pore walls or in specific locations within the particles [8]. Modified biopolymers that have functional groups have been used because of their widespread presence in nature but, synthetic polymers have been preferred as new generation of adsorbents [9]. These synthetic polymers can be designed for removing specific metals. Hydrogels and cryogels have been used for removing of heavy metals because of their ability of expanding their volumes due to their high swelling capacity in the solvent. These polymers have advantages such as preparation in different shapes, combination with various materials for getting desired properties and resistant to degradation [10].

Cryogels are supermacroporous hydrogels which are formed at subzero temperature by radical polymerization of monomers [11]. Due to their polymeric network with interconnected macropores, they show very low flow resistance and the solution can diffuse into these matrices easily. Generally the pore size depends on the concentration of monomer, ratio of crosslinker, their physicochemical properties and the freezing conditions [12]. Cryogels have a high density of pores. Macroporous structures of cryogels allow transportation of undesirable particles from containing fluid through the gels. Composite cryogels can be formed in order to increase the capacity of the cryogels in water and wastewater treatment applications [13].

Molecular imprinting technology (MIT) is a technique for preparing materials with cavities that are able to recognize a certain molecule according to its shape, size and chemical functionality. Polymerization occurs around the interested molecules called as template. After removal of template molecules, a three dimensional cavity is formed. Specific sites for many molecules such as metal ions, organic molecules, proteins in a synthetic polymer can be created by via MIT [14].

Ion imprinted polymers (IIP) are prepared by copolymerization of monomer, ligand-metal complex and cross-linker. After removing of the template ion, these polymers have high selectivity towards the target ion due to the affinity of the ligand for imprinted metal ions [15]. The first ion- imprinted polymers have been introduced in 1976, but the real development of IIP is more in the last 10 years [16].

This study consists of two main parts; (i) preparation of various ion imprinted cryogels (Cu(II), Cd(II) and Pb(II)) and Cu(II) imprinted magnetic cryogels and use of these cryogels for removing of specific metal ions from aqueous solutions; (ii) thermodynamic and kinetic parameters for these processes. For this purpose, the functional monomers N-methacryloyl-L-histidine (MAH), N-methacryloyl-L-cysteine (MAC) and N-methacryloyl-L-aspartic acid (MAAsp) were prepared by reacting appropriate amino acids with methacryloyl chloride and then, pre-complexes of these monomers with metal ions were prepared. Ion imprinted magnetic and non-magnetic cryogels were synthesized by bulk polymerization of metal ion pre-complex, 2-hydroxyethyl methacrylate (HEMA) and methylene bisacrylamide. The



cryogel membranes were characterized by surface area measurements, swelling test, scanning electron microscopy, and FTIR. These cryogels were used for adsorption of heavy metal ions from aqueous solutions in different concentrations, pHs, incubation times and temperatures and their effect on adsorption dynamics was studied. The thermodynamic values such as  $\Delta H^\circ$ ,  $\Delta G^\circ$ ,  $\Delta S^\circ$  for adsorption were calculated and then thermodynamic possibility of adsorption was indicated. The selectivity of ion imprinted cryogels for each of ion imprinted cryogel and specific ion in presence of other ions was studied. Reuse of this cryogels was examined with repeated adsorption-desorption cycles. Kinetics of the processes was studied as well.

## **2. GENERAL INFORMATION**

### **2.1. Heavy Metals**

For identification of heavy metals there aren't any agreed criteria as density, toxicity and atomic weight or definition of authority units, such as the IUPAC. All transition elements, transuranium elements, elements which have metallic property except those required by body and all of p-elements are called toxic metals [1]. However in this group, there are also non-metals such as arsenic that is known as a semi-metal. Heavy metals are adsorbed in soils and sediments. Degree of adsorption depends on electronic structures, diameters, degree of hydration, pH, concentrations, adsorbent structure, oxidation and concentrations of other metals. Heavy metals have very different properties; some of them are used in machine manufacturing, electronics, different parts of our daily life or high-technical jobs [17]. Heavy metal ions in domestic and industrial waste water are very important because of their damage for health of living organisms and ecological systems. The accumulation of these non-biodegradable components in living organisms causes serious health problems. Heavy metals are grouped as toxic (Hg, Cr, Pb, Zn, Cu, Cd, Ni, etc.), valuable (Pd, Au, Ag, Pt, etc.) and radionuclides (U, Th, Ra, etc.) [3].

The trace amounts of heavy metals can be determined in waste water samples using flame atomic absorption spectrometer (FAAS), graphite furnace atomic absorption spectrometer (GFAAS), inductively coupled plasma optical emission spectroscopy (ICP-OES), inductively coupled plasma mass spectrometry (ICP-MS), laser-induced breakdown spectroscopy (LIBS) and anodic stripping voltammetry.

#### **2.1.1. Heavy Metals Toxicity**

Many heavy metals are necessary in small amounts for the normal development of the biological cycles but in high concentrations are toxic. These metals which are called trace elements for example Zn, Fe, Cu, Cr and Co are necessary for body but the amount more than physiological concentration is known to have toxic side effects [1, 17]. There is another group of heavy metals such as arsenic, lead, cadmium and mercury that are highly toxic for human beings and other living beings even at trace levels [14]. Heavy metals generally are toxic but oxides of

heavy metals aren't toxic. Presence of heavy metal ions in rivers and lakes can cause of several health problems for animals, plants and human beings. The human body can not dispose the metals as a result they are deposited in various internal organs. Large deposits may cause adverse reactions and serious damage to the body [18]. The reason of extreme toxicity of heavy metals in organisms is that they are water-soluble in ions or compounds form and are easily absorbable by living organisms in nature. Generally toxic effect of heavy metals is due to their complexation with organic compounds. These metals after being absorbed by body get connected to cellular units with vital importance such as proteins, enzymes and nucleic acids and inhibit their functions [3]. These metals react with -SH groups of proteins, maybe this event chemically seems simple, but this is important in metabolism and can cause death [19]. In animal body because of their homeostatic mechanism, if concentration of metals doesn't go over the limit of tolerance or heavy metals don't affect metabolism for long time, metabolism can protect itself [19]. Toxicity of metals most commonly effects on the brain and kidneys but other manifestations can be appearing. Some metals such as arsenic clearly cause cancer [4].

### **2.1.2. Removal of Heavy Metals**

Presence of heavy metals in environmental waters is dangerous for human and other living beings. Organic pollutants can be changed to harmless material with biodegradation, but heavy metals don't change into harmless material with biodegradation [20]. Therefore removing of heavy metals from water is necessary. Many methods have been used for removal of heavy metals. Methods that are used widely for metals removal is shown below (Table 2.1).

### **2.1.3. Conventional Refinement Techniques**

Since ancient times there are traditional methods for removing heavy metals from the environment but some of these methods are expensive and risky due to the possibility of generation of hazardous by-products [18]. For removal of heavy metal ions from wastewater, physical, chemical or biological refinement technique or combined techniques can be selected. Several parameters such as the content and quantity of waste, chemicals and energy requirements, process performance,

process economics are considered. Amongst the available techniques, adsorption, ion exchange and membrane processes are frequently used.

Table 2.1. Physical methods for the removal of heavy metals

Base	Commonly used methods
Dimension	Filters, membranes, particles, gels
Density	Precipitation
Charge	Ion exchange resins, electrokinetic systems
Specific Affinity	Interactions between ligands with particles or macromolecules

### 2.1.3.1. Chemical Precipitation

This method is one of the old methods that were applied for heavy metal removal from water. It is used when economic recovery is not important and complex chemical compounds are not involved. This method is a good choice for high concentrations of heavy metals, but it is not effective for concentrations of less than 50 mg/L [21]. The method is based on conversion of metal ions to the insoluble precipitate such as hydroxide, sulfide, phosphate or carbonate by suitable agents, and removing the precipitate from medium. Organic polymers and alum as coagulants can improve the performance of process. Besides the advantages of cheapness and simplicity, this method has the disadvantages of formation of a large volume of precipitate having a low density, amphoteric character of some metal hydroxides, and inhibition effect of reagents having the ability to form complexes in refining environment.

To form the precipitate in hydroxide salt, alkaline reagents such as NaOH,  $\text{Ca(OH)}_2$  or  $\text{NH}_4\text{OH}$  are used. Most metal hydroxide precipitates are formed in the pH range of 8.0-11.0. If  $\text{Ca(OH)}_2$  is used as precipitating agent, secondary precipitates such as  $\text{CaSO}_4 \cdot 2\text{H}_2\text{O}$  may be formed. So, precipitation agent having capability to form soluble by-products should be preferred [22], especially when metal recovery is important. Precipitation agents such as FeS and  $\text{H}_2\text{S}$  are used

for sulfide precipitates. Typically, the metal sulfide solubility value is less than that of metal hydroxide; therefore operation efficiency for metal sulfides gives the better result. To prevent  $\text{H}_2\text{S}(\text{g})$  formation, neutralization of acidic waste is required before the precipitation process. Carbonate precipitates that are obtained with  $\text{Na}_2\text{CO}_3$  and  $\text{CaCO}_3$  have larger solubility values than that of hydroxide forms. Phosphate precipitates are formed by adding phosphate or soluble salts of hydroxyl apatite. Blais et al. used dithiocarbamate (DTC), xanthatediethyl dithiocarbamate (DDTC) as reagents to perform the precipitation due to chelate formation [18]. Dean et al. used precipitation method for removing metals such as copper, zinc, iron, manganese, nickel, and cobalt as the hydroxide [21].

### **2.1.3.2. Electrochemical Process**

This method is one of the most interesting traditional methods. In this method, an electrochemical cell is formed that is placed in mixture containing metal ions. Metal ions are deposited on the mercury cathode. High selectivity is the advantage of this method but the long duration of action (slow rate of accumulation) is its major disadvantage [21]. This method is used for recovery of metal ions in the form of pure metal or pure salt solution by electrolysis. Migration of toxic components toward the electrode depends on diffusion, convection and electrolytical migration. The ions having less negative potentials than water in solution fed to the cathode are reduced to metal. The presence of oxygen or other reducible elements decreases the current efficiency and increases the consumption of energy. Controlling the parameters for electrolysis, selectivity for metal ions may be obtained. If the reduction of metal ions is controlled by mass transfer, process performance increases. The electrode area, the mass transport regime and presence of turbulence promoters affect the process [22]. Electrocoagulation and electroflotation are the other options for electrochemical processes. But their investment and operating costs are very high.

### **2.1.3.3. Liquid-Liquid Extraction**

This is the widely used method for heavy metal treatment. In this method, chelating reagent is added to the aqueous phase for creating ion-specific complex of metal ion. Solubility of this complex in water is very low; hence complex is extracted by using an organic solvent such as hydroxyquinoline, diethyl

dithiocarbamate, and ammonium dithiocarbamate pyridine. The major disadvantages of this method are the use of little amount of organic solvent for increasing the efficiency of the aqueous phase separation factor and the difficulty of effective separation of these two phases after extraction.

#### **2.1.3.4. Flotation**

In flotation, a surface-non-active material with suitable surface-active agent is converted to removable surface-active material by means of gas bubbles formed in solution. Advantages of this method are simplicity and efficiency of the method. Ions that are converted to hydrophobic precipitates by surface-active agents form foam by connecting to gas bubbles.

#### **2.1.3.5. Coagulation and Flocculation**

Coagulation is destabilization and initial coalescing of colloidal particles and flocculation is the formation of larger particles (floc) from smaller particles. In coagulation process, charge neutralization and bridging mechanisms are important [23]. Following these processes, treatment process is completed by sedimentation and filtration. Coagulation for hydrophobic colloids and suspended particles gives better results. Chemical requirement and tangle volume are disadvantages of this method.

#### **2.1.3.6. Ion-Exchange**

This physical method is based on exchange of ions between the solution phase and the solid matrix. The method has advantages of high decontamination capacity, treatment efficiency, fast kinetics and cost effectivity. Several parameters such as temperature, pH, contact time and ionic charge effect on the rate of exchange. Ion-exchange resins that are insoluble in water and organic solvents can be synthesized by covalent binding of charged functional groups to the cross-linked polymeric matrices. The matrix is usually polystyrene that contains 3-8% divinyl benzene. The particle size is usually in the range of 20-25 mesh. For the strong acid cation exchanger ( $-\text{SO}_3\text{H}$ ), cation affinity increases with the cation charge and with the increasing atomic number for different ions having the same charge. Resins with weak acid type cation exchangers that have carboxyl functional groups follow a reversed affinity order for alkali and alkaline

earth metals. For strong base anion exchangers having quaternary ammonium ( $-N^+R_3$ ) groups, the ion exchange capacity increases with increasing ionic charge. The affinity order for weak base anion exchangers having secondary or tertiary amine groups is similar to the order reported for strong base anion exchangers. Amphoteric ion exchangers, such as AMF-IT and AMF-2M that exchange cation or anion depending on the solution pH can also be used [16]. If original sample contains ferrous ions, the adsorption of organic material will cause the reduction in performance due to chlorine and the possibility to form ferric hydroxide are the disadvantages of the method.

#### **2.1.3.7. Membrane Processes**

Membrane process is based on the recovery of metal ions from diluted wastewater with semi-permeable membranes. Membrane processes that are used for the removal of heavy metal ions are ultrafiltration (UF), reverse osmosis (RO), nano filtration (NF), microfiltration (MF) and electro-dialysis (ED). Pore sizes of the membranes for MF and UF applications are (0.1 to 3  $\mu\text{m}$ ) and (0.01-0.1  $\mu\text{m}$ ), respectively [5]. Higher metal recovery performance in NF applications can be achieved due to narrow pore size (0.001- 0.01  $\mu\text{m}$ ). In the RO, metallic or polymeric-based membranes are used, and pressure or electric current being the driving force for the passage of solution through the membrane. Less space of apparatus, performance of process and little need for chemicals are the advantages of the method. Requirement of high energy, blockage of membrane pores and the necessity of membranes to renew in about five years are the disadvantages. Juang et al. reported removal of Cu(II) and Zn(II) ions from synthetic wastewater by chitosan-enhanced membrane filtration [24].

#### **2.1.4. New Methods for Removing Heavy Metals**

Generally purposes of new methods are development of cheaper and more effective technologies eventually, to decrease the amount of by-product and to improve the quality of the treated water. These new methods are adsorption with new adsorbents, membrane filtration, electrodialysis, metal chelating, and photocatalysis [6].

#### **2.1.4.1. Adsorption**

This method is one of the common methods for metal removal from water. Adsorption is adhesion of particles to a surface. Adsorbed substance is adsorbate and the substance that having capacity or tendency to adsorb particle is adsorbent [25]. According to interaction between the adsorbent and adsorbate, adsorption is classified into three kinds; Physical, Chemical and Ionic adsorption. Physical adsorption is a result of attraction power between the solid surface and adsorbed substance. Here weak van der Waals forces are active and adsorption occurs as multilayer and reversible manner [26]. Chemical adsorption occurs when there is chemical interaction between functional groups on the solid surface and adsorbed substance. This type of adsorption is single-layered and not reversible. Ionic adsorptions happen when ions with electrostatic forces adsorb in complementary charged zones. In this type of adsorption, ions with high charge and small diameter are adsorbed better than the other ions. When an adsorption phenomenon takes place, there isn't only one kind of adsorption, maybe there are two kinds or three kinds simultaneously. Adsorption also depends on structure of the adsorbed substance, concentration, pH, and temperature. A material in the case of one component in solvent adsorb better than multi components in solvent on the surface of adsorbent.

Adsorption is similar to equilibrium reaction and continues until the concentration of substance on adsorbent surface and solution is balanced. After balancing, concentration of adsorbed substance is constant in solution. Adsorption depends on concentration of adsorbed substance and temperature. Generally adsorption process is performed at a constant temperature to examine the concentration effect in process. The amount of adsorbed substance is plotted against the concentration of adsorbed substance in solution and this mathematical expression is called adsorption isotherm. The Freundlich and Langmuir isotherms are the mostly used adsorption isotherms [25, 26]. Generally in adsorption method first metal ion forms a complex then this complex, is adsorbed on the adsorbent. This method is the sorption of components from gaseous or liquid phases onto the surface of the solid substrate. Besides of design and flexibility, lack of pollutant formation, low investment costs and regeneration of adsorbent are the advantages of this method. In this process, lignin, tannin, chitin, chitosan, dead



biomass, zeolite, clay, by-products of agricultural industry, activated carbon, carbon nanotubes and synthetic polymer-based adsorbents can be used. Adsorbents may be grouped as carbon adsorbents (activated carbon, activated carbon fibers, carbon molecular sieves, fullerenes, hetero fullerenes, nano-materials), mineral adsorbents (silica gels, zeolites, clay minerals, inorganic nano-materials, metal oxides, metal hydroxides, activated alumina) and other adsorbents (synthetic polymers, composite adsorbents and mixed adsorbents) [27,28].

Adsorbent materials have usually a porous structure, and the sorption process generally takes place in the pore walls or in specific locations within the particles. The overall rate of process is controlled by diffusion rate of adsorbed substances into the capillary pores and varies with the square root of contact time with the adsorbent [29].

Selection of adsorbent depends on sorption rate and capacity of adsorbent, surface area for particulate adsorbents, mechanical strength, low cost, regeneration and re-usability. Porosity can be obtained by emulsion polymerization of monomers in solvents capable to solve monomer but a poor swelling agent for polymer. In creating nitrogen, oxygen, or sulfur containing binding sites for the polymeric sorbent, a suitable ligand is attached to the support by means of a suitable activation procedure, or a copolymer of a suitable functional monomer having the desired functional coordination sites is synthesized. If the concentration of metal ions in aqueous solution is in the range of 1-100 mg/L, chemical precipitation and electrochemical process are not effective. Ion exchange, activated carbon adsorption and membrane technology are expensive for wastewater having large volumes and containing low concentration of metal ions. In recent years efforts have been made to search low-cost adsorbents that have metal-binding capacity [30]. In adsorption of heavy metals on adsorbent there are three steps, first, the transport of heavy metals to surface of adsorbent; second, adsorption on the adsorbent surface; and third, the transport of adsorbent and adsorbate from solution.

#### **2.1.4.1.1. Adsorption on Modified Natural Materials**

Natural zeolites due to their ion exchange capability gained a significant interest. Clinoptilolite has high selectivity for certain heavy metal ions such as Pb(II), Cd(II), Zn(II), and Cu(II) [26,29]. In recent years synthetic zeolites for heavy metals removal have been reported [28]. Clay–polymer composites, different phosphates calcined at 900°C, activated phosphate with nitric acid, and zirconium phosphate have been employed as new adsorbents for removal of heavy metals from aqueous solution [28,29,30].

#### **2.1.4.1.2. Adsorption on Industrial by-Products**

Chemical modification can improve removal performance of industrial by-products for metal removal from water. Alinnor et al. used fly ash for removal of Cd(II) and Ni(II) from synthetic solution [30]. Uysal et al. used 1, 5-disodium hydrogen phosphate modified sawdust for adsorption of Cr(VI) from ground water [31].

#### **2.1.4.1.3. Adsorption on Polymers**

Some polymers besides carbon and hydrogen atoms have other atoms such as oxygen (O), silicon (Si), nitrogen (N) or phosphorus (P) atoms in their chains, these polymers are called "inorganic polymers". Polymer chains can be in linear or branched structure. Increase in branching of polymers causes decrease in their solubility. If these branches bind another main chain, cross-linked polymers are formed. Poly(HEMA) is a polymer that is synthesized by adding methylol (-CH<sub>2</sub>OH) group to methyl methacrylate and polymerization of this monomer, 2-hydroxyethylmethacrylate (HEMA). Poly(HEMA) and poly(HEMA) with a small amount of cross-linking agent, ethyleneglycol dimethacrylate (EGDMA) can be used for heavy metal adsorption. Cross-linking prevents polymer from dissolving in water and this polymer is called "swollen hydrogel" [32]. One of the new approaches in metal removal methods is use of specific adsorbents [33]. These adsorbents consist of polymeric carrier matrix and ligands which can interact selectively with a metal ion (ion exchange or chelate-forming).

Some examples for these specific adsorbents can be given as follows [33];

Poly ( $\beta$ -diketone) adsorbents

- Polyhydroxyantraquinone adsorbents
- Polyphenylalanine adsorbent
- Macrocyclic polythioether adsorbents
- Polymeric adsorbent that have nitroresorcinol group
- Polymeric adsorbent that have oxime group
- Polymeric adsorbent that have tris-dithiocarbamates group
- Poly(allylamine) and polyacrylamide adsorbents
- Polyethyleneimine adsorbents
- Phosphorus-containing carbon adsorbents
- Sirorez-resin adsorbent

#### **2.1.4.1.4. Modified Biopolymers**

Biopolymers are used because of their ability to decrease transition metal ion concentrations to sub-parts per billion concentrations, widespread presence and non-detrimental nature to the environment; also having functional groups, such as hydroxyls and amines that increase the efficiency of metal ions uptake and the maximum chemical loading possibility. Cross-linked chitosan, cross-linked starch gel and immobilizing chitosan on the surface of non-porous glass beads are described as modified biopolymer adsorbents for the removal of heavy metals from the water [32]. Amine sites of chitosan are responsible for metal ion binding through chelation mechanisms. Chitosan is also a cationic polymer and it's also possible to sorb metal ions through anion exchange mechanisms.

#### **2.1.4.1.5. Hydrogels**

Hydrogels are cross-linked and hydrophilic polymeric structures that have ability of expanding their volumes due to their high swelling capacity in the water. Due to this capacity, they are widely used in the purification of wastewater [36]. Hydrogels are synthesized with polymerization of one or different kinds of monomers in large number. Hydrogels are insoluble because there are hydrogen bonds or van der Waals interactions between main chains. Hydrogels due to their superior properties have been used for medical application in last 30 years. Cross-linked poly(HEMA) is the most widely used hydrogel. Hydrogels have advantages such as resistant to degradation, not absorbed by body, sterilization by heat and preparation in different shapes and forms, also hydrogels can be

combined with various materials for getting desired properties. The first application of hydrogels was as lenses due to their mechanical stability, high oxygen permeability and appropriate refractive index. The other applications of hydrogels are artificial tendon materials, bio-adhesive agent in wound-healing, artificial kidney membranes, artificial leather and in advanced applications such as development of artificial muscles. Smart hydrogels can change electrochemical alerts into mechanical work, thus can function as human muscle tissue. In biotechnological applications, particularly bioactive hydrogel can be used in separation of proteins [10]. Various hydrogels were synthesized and applied for adsorption of heavy metals. Kesenci et al. prepared poly(ethyleneglycol dimethacrylate-co-acrylamide) hydrogel beads and used for removing of Pb(II), Cd(II) and Hg(II) from water [32]. Essawy et al. prepared poly(vinylpyrrolidone-co-methylacrylate) hydrogel and used for removal of Cu(II), Ni(II), and Cd(II) [29]. Barakt et al. prepared poly(3-acrylamidopropyl) trimethyl ammonium chloride hydrogel and used it for As(V) removal [33].

#### **2.1.4.1.6. Cryogels**

One of the polymer gels is 'cryogel' derived from Greek word Krios (Kryos) which means frost or ice. "Cryogels" are supermacroporous hydrogels which are formed at subzero temperature by radical polymerization of monomers [11]. Monomers, crosslinker, initiator and activator are dissolved in solvent such as deionized water. Mixture is immediately incubated under frozen conditions. At subzero temperature, the solvent freezes, forms ice crystals, and then these ice crystals interconnect to each other. Some part of solvent or solute molecules remains unfrozen. Monomers polymerize in liquid microphase, get crosslinked and form gel. After melting of cryogel, an interconnected polymeric network forms [34]. Due to interconnected macroporous structure indicating very low flow resistance, the solution can diffuse into these matrices easily. Pores give unique spongy structure to cryogels. Generally the pore size is 5-100  $\mu\text{m}$  and depends on the concentration of monomer, ratio of crosslinker, their physicochemical properties, and the freezing conditions [12]. Cryogels were first reported 50 years ago and because of properties, soon attracted attention due to large surface area and high density of pores. Cryogels provide high-capacity removal and provide convenience in working in viscous medium such as heavy metals industrial waste.

The biomedical and biotechnological potential of these materials has now been recognized by Lozinsky et al. [35]. Cryogels have advantages over other polymers as cryogels can be produced in different sizes and formats like discs, sheets, or monoliths with varying dimensions. Interconnected macroporous structure of cryogels makes them appropriate for the biomedical and biotechnological applications [36, 37]. Intermolecular bonds in the junctions of polymer network are different in gels and cryogels. Bonds of cryogels are chemical bonds as covalent, ionic or non-covalent. Methods which are used for heat-induced (thermotropic) gels cannot be used for the preparation of cryogels.

Steps in preparation of cryogels:

- The polymer solution containing gel-forming agents is frozen at temperatures, a few degrees below the solvent crystallization point. The frozen system looks as a single solid block, but essentially is heterogeneous and contains unfrozen liquid microphase with the crystals of the frozen solvent.
- The crystals of frozen solvent perform as a pore-forming agent. When melted, they leave pores. The surface tension between solvent and gel phase rounds the shape of the pores, making pore surface smoother.
- After melting, to form a system of interconnected pores arises inside the gel. The dimensions and shape of the pores depend on many factors; the most important is the concentration of initial materials.
- Micropores are formed in the polymeric phase. Thus, cryogels have both heterophase and heteroporous structure [38,39].

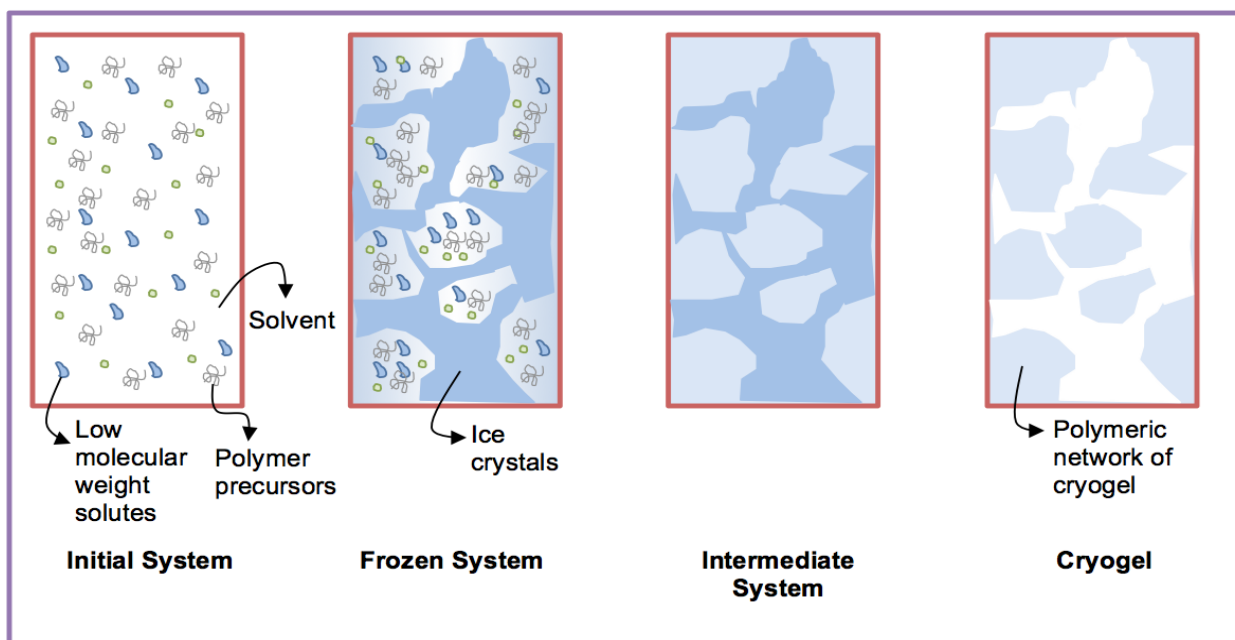


Figure 2.1. Schematic diagram of cryogel formation.

Cryogels are used in bioseparation ( in bed chromatography as stationary phase by Arvidsson et al. and Chase et al. [40-41]), for immobilization of biopolymers as enzymes by Kokufuta et al., polysaccharides by Hayashi et al., nucleic acids by Cocquemcot [42- 43], and as carriers for cell immobilization [44,45].

#### 2.1.4.1.6.1. Cryogels in Treatment of Water and Wastewater

For removal of heavy metals from water, the conventional methods are not always sufficient. Macroporous structure of cryogels allows transportation of undesirable particles from containing fluid through the gels. Composite cryogels can be formed in order to increase the capacity of the cryogels in water and wastewater treatment applications. Wang et al. used hydroxyapatite –PVA composite cryogels for removal of cadmium ions [13]. A cryogel having thiol functionalized groups on their surface for removing arsenic (V) from water was used. Composite cryogels containing MIP adsorbents have been used for water and wastewater treatment. The selectivity of MIP particles and the macroporous structure of cryogels make a unique combination for preparation of composite cryogels [46]. Hajizadeh et al. used composite cryogels containing activated carbon for treatment of water (phenol adsorption) [47]. Tekin et al. used composite cryogels containing imidazole group for removal of heavy metal ions such as Pb(II), Cd(II), Zn(II) and

Cu(II) from water [48]. Papancea et al. used PVA cryogel membranes for removal of metal ions [Cu(II), Ni(II) and Pb(II)] from aqueous solutions [49].

#### **2.1.4.1.6.2. Composite Systems**

Forming the multi-phase materials by two or more materials with maintaining their characteristics and limits can be defined as composite system. The composite materials have all properties of their components [50]. A new concept in chromatography is the preparation of sorbents that have high flow path and high surface area by embedding polymeric particles in various macroporous gels. Preparation of composite systems is preparation of cryogel with a higher surface area, the larger pore size and desired properties. Cryogels that are known as macroporous gels can be effective in removal of heavy metals from viscous industrial wastewater because of providing lower flow resistance and higher separation capacity. Because of their high flow rate they can be used in chromatographic column structure. Composite system in the structure of column was prepared by embedding molecular imprinted particles in the macroporous gels. This composite system without clogging was used in the removal of template molecule from wastewater due to its high flow rate [50].

#### **2.1.4.2. Membrane Filtration**

According to new membrane processes, treatment of wastewater containing copper and cadmium ions was accomplished by both of reverse osmosis (RO) and nanofiltration (NF) technologies. The results showed high removal efficiency of the heavy metals (98% and 99% for copper and cadmium, respectively) [51]. Multiple membrane process was used for selective separation. Commonly these processes are comprised of three steps; first, UF and microfiltration (MF) are used for separation of organic and suspended matters then, electrodialysis (ED) for desalination lastly, NF and RO are separately used to treat the concentrate from ED [52]. Recently polymer-supported ultrafiltration (PSU) technique has been shown that is favorable for effective removal of heavy metal ions from industrial influent [53]. Complexation-ultrafiltration is another technique that is used as an effective removal method for heavy metals by Petrov et al. [54], Barakat et al. [55] and Trivunac et al. [56]. Ferella et al. used surfactants-enhanced ultrafiltration process for removal of lead and arsenic by using cationic (dodecylamine) and

anionic (dodecyl benzene sulfonic acid) surfactants [57]. Recently modified UF blend membranes based on cellulose acetate (CA) with polyether ketone [58], sulfonated polyetherimide (SPEI) [59] and polycarbonate [60] were used for heavy metals removal from waste water. New integrated process combining adsorption, membrane separation, and flotation was developed for the selective removal of heavy metals from wastewater. This process contains three stages; first, heavy metal bonding (adsorption) in a bonding agent, then, wastewater filtration to separate the loaded bonding agent by cross flow microfiltration for low-contaminated wastewater or a hybrid process combining flotation and submerged microfiltration for highly contaminated wastewater lastly, bonding agent regeneration [61,62]. In another new hybrid process, flotation and membrane separation were developed by integrating specially designed submerged microfiltration modules directly into a flotation reactor [63]. Klaassen et al. and Madaeni et al. reported the other hybrid processes for heavy metals removal [64,65].

#### **2.1.4.3. Electrodialysis**

Electrodialysis (ED) in fact is a membrane separation in which ions in the solution are passed through an ion exchange membrane by applying an electric potential. Membranes have anionic or cationic characteristics and are in the form of thin sheets of plastic materials. In this method, solution with ions passes through the cell compartments, the ions cross anion exchange and cation-exchange membrane, anions migrate to cathode and cations migrate to anode [66]. Tzanetakis et al. removed Ni(II) and Co(II) ions from a synthetic solution by a high-performance membrane [67]. It was found that performance of an ED cell is almost independent of the type of ions and only depends on the operating conditions and the cell structure [68].

#### **2.1.4.4. Photocatalysis**

This method is based on two stages; first, to form electron–hole pairs ( $e^-/h^+$ ) in the conduction and the valence band of the semiconductor; second, migration of these charge carriers to the semiconductor surface then, reducing or oxidizing species in solution having suitable redox potential as organic pollute or heavy metal. This method was used with different semiconductors for removing different



heavy metals. Cu(II) was removed with TiO<sub>2</sub> (semiconductor) [69]. Heterogeneous photocatalytic oxidation of arsenide to arsenate in aqueous TiO<sub>2</sub> suspensions was applied for the remediation of arsenide contaminated water [70].

#### **2.1.4.5. Metal Chelating Method**

Specific polymeric adsorbents which are used in chromatography methods in view of conventional separation methods are gaining more and more importance with each passing day [71]. Metal chelating chromatography method in the removal of heavy metal ions from environmental waters is the best compared to other chromatography methods because of higher selectivity and sensitivity. Adsorbents in this method consist of a carrier matrix and a ligand which can attach selectively with the metal ions (chelate-forming) [72,73]. Commonly used first matrix carriers were inorganic (silica, aluminum oxide, glass, etc.), but in recent years synthetic polymers (polystyrene, polymethylmethacrylate, etc.) have been developed and reported [72].

These synthetic polymer matrices can be produced easily and in various forms (microsphere, membrane or fiber), also can be modified to various functional groups for effective interaction between metal and matrices. Ligands (materials which can be chelated) are attached to carrier matrices for specific interaction with metal ions and their removal from aqueous media. Usually chelate forming functional groups contain oxygen, nitrogen and sulfur atoms. Nitrogen in the structure of functional group can be in the form of primary, secondary and tertiary amine, nitro, nitroso, azo, diazo, nitrile, amide, and other groups. Oxygen can be in the form of phenol, carbonyl, carboxyl, hydroxyl, ether or phosphoryl groups and sulfur in the form of thiol, thioester, and disulfide groups. These groups can be attached on the polymer with chemical modification of the ligand or synthesis of sorbents by monomeric ligands. Functional polymers are synthesized by two different ways [72].

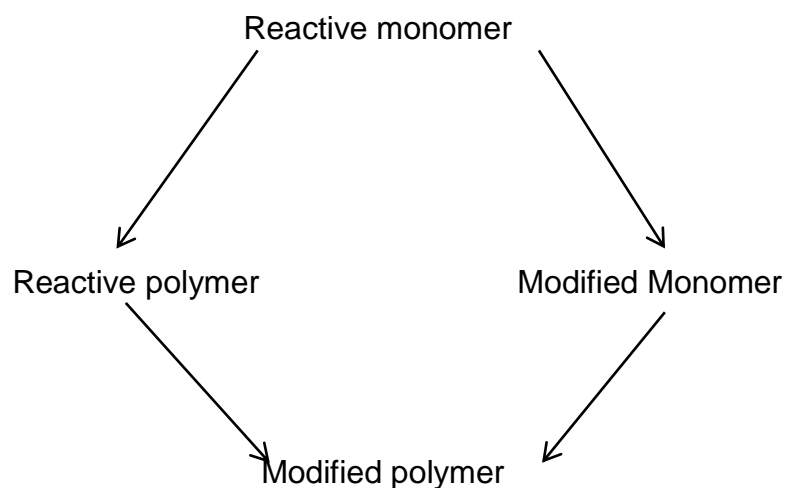


Figure 2.2. Methods for synthesis of functional polymers.

The heavy metal ions after chelating can be collected selectively by the sorbent in the result of fitting specific functional groups on the polymeric matrix [74]. In the carrier matrix (sorbent), non-specific interactions (electrostatic, etc.) are minimized, on the other hand these adsorbents are synthesized by an inert material (usually polymeric base) in the form of spherical particles. Some of commercially available matrices are produced in the form of porous materials to increase the surface area of interaction and to contain porous surface so that metal ions can enter easily. Besides mechanical strength and ease of use inside the column hydrodynamically, matrices should be inert, should not reduce specificity of specific adsorption and have suitable functional groups for ligand binding.

Principles of metal chelate chromatography are given as follows: Adsorption of metal ions is provided by feeding the solution that contains metal ions through column that is filled with the adsorbent. The second step, desorption of adsorbed metal ions by changing pH or ionic strength.

Selection of carrier matrix in metal chelate chromatography is very important. Briefly matrix should have these properties:

- Chemically inert
- Dimensions uniform, spherical and rigid
- Easily can be derivatized and clamped with a ligand

- In the column applications, resistant to 5 atm pressure and having suitable surface and size for adequate liquid phase flow rate in column.

### **2.1.5. Cadmium**

Cadmium is in the IIB group with an atomic weight of 112.41. This metal is present in the nature in the form of sulfide, carbonate or oxide in zinc, lead and copper ores. Density, melting point and boiling point of this metal are 8.65 g/cm<sup>3</sup>, 320.9°C and 765°C, respectively. This metal does not have any basic biological function for humans. Its biological half-life in human's body is 10-35 years. The U.S. Environmental Protection Agency (EPA) categorizes this metal in first category between 126 primary pollutants [75]. This metal is similar to zinc element in chemical properties. Cadmium can replace zinc that is an essential trace element for many plants, animals and micro-organisms and can disrupt metabolic processes. Cadmium is an active enzyme inhibitor. Cadmium is used in photography, TV phosphors, metal coating, anti-corrosion agent, pigments, and as a stabilizer in Ni-Cd cells. Cadmium can be delivered into water by waste batteries, paints, metal refinery facilities, galvanized pipe corrosion, soil and rock erosion, etc. The maximum allowable concentration of cadmium in water is 5 ppb [90] and minimum allowable discharge amount by WHO is 0.01 mg/dm<sup>3</sup>. When rate of hydrolysis is negligible, cadmium is in Cd(II) form. This form is the predominant form in the acidic, neutral and slightly alkaline medium. This metal forms inorganic complexes with anions such as carbonate, chloride and sulfate and organic complexes with humic acids. In the high pH values besides soluble ions [Cd(OH)<sup>+</sup>, Cd(OH)<sub>3</sub><sup>-</sup>] there are insoluble molecules such as Cd(OH)<sub>2</sub>. Amount of cadmium transferred from industrial wastes to the environment is estimated as 680 tons per year [76]. Cadmium can cause some health problems such as, kidney damage, cardiovascular disease, and high blood pressure [75].

### **2.1.6. Copper**

Copper is in the IB group with an atomic weight of 63.546. This metal is present in the nature in the form of sulfides, carbonate or oxide in the chalcopyrite, chalcocite, azurite, malachite and cuprite minerals. Density, melting point and boiling point of this metal are 8.96 g/cm<sup>3</sup>, 1084.62°C and 2562°C, respectively. Copper is essential to all living organisms as a trace element. The suggested safe

level of copper in drinking water for humans varies depending on the source, but tends to be pegged at 2.0 mg/L. The U.S. Environmental Protection Agency's Maximum Contaminant Level (MCL) in drinking water for copper is 1.3 mg/L. Cu is an essential micronutrient, is a component of several enzymes mainly participating in electron flow and is a catalyst in redox reactions. Copper is an excess of copper in the body [77]. Copper poisoning can occur from exposure to excess copper in drinking water or other environmental sources. Copper in body damages proteins, lipids, and DNA. Copper poisoning causes vomiting, hematemesis (vomiting of blood), hypotension (low blood pressure), melena (black "tarry" feces), coma, jaundice (yellowish pigmentation of the skin), and gastrointestinal distress [78]. Long-term exposure to copper can damage the liver and kidneys. According to the latest research at Sanford-Burnham Medical Research Institute, copper causes testicular cancer [79,80]. The copper is usually used in electrical wires, roofing, plumbing and industrial machinery.

#### **2.1.7. Lead**

Lead is in the IVA group with an atomic weight of 207.2. Density, melting point and boiling point of this metal are 11.34 g/cm<sup>3</sup>, 327.46°C and 1749°C, respectively. Metallic lead is rare in nature and found in ore with zinc, silver and (most abundantly) copper. The main lead mineral is galena (PbS), cerussite (PbCO<sub>3</sub>) and anglesite (PbSO<sub>4</sub>) [81]. Lead is used in building construction, lead-acid batteries, bullets, pewters, fusible alloys, and as a radiation shield. Lead is a poisonous substance to animals and humans. Lead is a highly poisonous metal (regardless if inhaled or swallowed), affecting almost every organ and system in the body. Lead can accumulate both in soft tissues and the bones. The main damage of lead is in the nervous system both in adults and children. Long-term exposure of adults can cause decrease in functions of the nervous system, also long-term exposure to lead or its salts (especially soluble salts or the strong oxidant PbO<sub>2</sub>) can cause nephropathy, and colic-like abdominal pains. It may also cause weakness in fingers, wrists, ankles, small increases in blood pressure, particularly in middle-aged and older people or anemial. Exposure to high levels of lead can damage the brain and kidneys in adults or children at least cause death. In pregnant women, exposure to high level of lead may cause miscarriage. Chronic, high-level exposure has shown to reduce fertility in males [82]. Lead

enters in drinking water with corrosion of house hold plumbing systems and erosion of natural deposits. Lead leaches into water through corrosion by a chemical reaction between water and plumbing system, also lead can leach into water from pipes, solder, fixtures and faucets (brass), and fittings. The amount of lead in drinking water also depends on the types and amounts of minerals in the water, staying time of water in pipes, the pipes wearing, acidity of water and its temperature. EPA estimates that 10 to 20 percent of human exposure to lead may come from lead in drinking water [82]. The U.S. Environmental Protection Agency's Maximum Contaminant Level (MCL) in drinking water for lead is 0.015 mg/L.

#### **2.1.8. Polymer Based Adsorbents for Removal of Metals**

Biological ligands which can be used for metal ion removal are peptides, macrocyclic chelating ligands and nucleobases (nucleic acids). Transition metals form coordinate covalent bond with protein ligands by electron pair in protein ligands. Commonly these ligands have S, N, and O atoms. These ligands have functional groups such as SH, -SS, -NH<sub>2</sub>, -NH, -OH, -OPO<sub>3</sub>H or carbonyl. The most common metal bonding units are Cys, His, Asp, Glu and more rarely Met, Asn, Gln, Ser, Thr and Tyr [83]. The coordination number of metals changes from one to eight depending on metal species. Protein groups capable of binding metal are called metallothionein, important units are cysteine (Cys) and sulfhydryl groups in cysteine, are responsible for metal binding. Thiols that have low molecular weight as cysteine's sulfhydryl group are reactive and range of their pKa is 8-1. The use of ion-imprinted inorganic polymers that are prepared by sol-gel process is very interesting, but because of different functional groups such as amine, organosilanes and thiols, different metal ion bonding locations occur. Passerini et al. used silanized glass matrix with immobilized glutaraldehyde and the cysteine containing system for pre-concentration of Cd(II), Co(II), Cu(II), Hg(II), Pb(II), and Zn(II) ions, and capacity values for these metals were 12.48, 5.50, 7.86, 6.06, 11.66 and 7.88 mmol /g, respectively [84]. Cd(II) imprinted (3-mercaptopropyl) trimethoxysilane-SiO<sub>2</sub> system prepared by sol-gel method was used for concentrations of 10, 20 and 50 mg/L of Cd<sup>2+</sup> and could remove 80% Cd(II) [85]. Li et al. modified the Cd(II) imprinted mercapto-silica polymer with tetraethyl ortho silicate for removing of Cd(II) and reported the capacity value as

83.89 mg/g [85]. Buhani et al. reported capacity value for Cd(II) removal as 53.3 mg/g by VA / HA composite cryogel [86]. Silica sol-gel matrices that are modified with polyethyleneimine, polyacrylic acid or EDTA can remove Cd(II) in the range of %90 [87]. Removal capacity value of bentonite–modified cysteine for Pb(II) and Cd(II) was 0.503 and 0.525 mmol/g, respectively [88]. Single imprinted 3-mercaptopropyl–trimethoxysilane was reacted with Cd(II) -chitosan complex that was cross-linked by epichlorohydrin then particle was cross-linked by tetraethoxysilane and double-imprinted adsorbent was synthesized. Capacity value for Cd(II) single- imprinted one was 342 mg/g whereas that for double-imprinted was 172 mg/g [86]. Özkütük et al. prepared the ion imprinted poly(HEMA-MAC) composite magnetic particles and reported capacity value as 28.45  $\mu\text{mol/g}$  for removal of Cd(II) [89]. Ion imprinted polymeric particles were synthesized by copolymerization of binary ligand (zz)-N, N'-bis (2-aminoethyl) but-2-enediamide, Cd(II) complex and pentaerythritol triacrylate crosslinker. Adsorption capacity value was 32.56 mg/g for Cd(II) [90]. 4-vinylpyridine (monomer) and ethyleneglycol dimethacrylate (cross-linker) in the presence of Cd(II) and quinaldic acid (complexing agent) were copolymerized and capacity value as 45.0 mg/g for Cd(II) was reported [91]. Capacity value for solid phase extraction by phenol-formaldehyde-Cd(II) -2-(p-sulfofenilazo)-1, 8- dihydroxy naphthalene-3, 6-disulfonate system ion imprinted polymeric system was reported as 270  $\mu\text{g/g}$ . This capacity value was more than the capacity value reported for non ion imprinted system [92]. Singh et al. prepared a new chemically modified cellulose microfiber through oxidation with sodium periodate and functionalized with N, N-bis(2-aminoethyl)-1, 2-ethanediamine and applied for removal of Cd(II) and reported the maximum sorption capacity as 4.59 mg/g [93]. Segatelli synthesized poly(EGDMA-HEMA) microspheres that used dye, Congo red as metal chelating agent and capacity value was obtained as 18.3 mg/g for Cd(II) removal [94]. Activated carbon sourced from BASS *Borassus aethiopum* (seed shells) and CONS *Cocos nucifera* (shells) were used for removal of Pb(II) and Cd(II) from wastewater. The adsorption capacity value for Pb(II) was found to be 12.19 mg/g and 24.39 mg/g for activated BASS and CONS respectively, also for Cd (II) was found to be 10.20 mg/g and 25.797 mg/g for activated BASS, and CONS, respectively [95]. Abollino et al. studied the adsorption of Cd, Cr, Cu, Mn, Ni, Pb and Zn on Na-montmorillonite (clay) in the presence of ligands. The

capacity of Na-montmorillonite for Cu(II), Pb(II), and Cd(II) was 3.04, 9.58, 5.20, and 3.61 mg/g [96], respectively. Coal fly ash as a low cost adsorbent was applied for removal of lead, cadmium and copper from aqueous solutions and capacity value was obtained as 10.0 mg/g, 5.0 mg/g and 2.8 mg/g, respectively [97]. Niñā et al. used calcium alginate (a natural polymer obtained from marine algae) microparticles for removal of Pb(II) and Cd(II) from synthetic wastewater samples and capacity values were 167 and 182 mg/g, respectively [98]. Zhang et al. synthesized a magnetic ion-imprinted polymer by using 3-(2-aminoethylamino) propyltrimethoxysilane (AAPTS) as the functional monomer, tetraethylorthosilicate (TEOS) as the cross-linker, and Pb(II) as the template and used for removal of Pb(II) from real environmental samples. The maximum adsorption capacity was found as 19.61 mg/g [99]. Zhu et al. synthesized lead ion-imprinted micro-beads with combination of two functional monomers (1,12-dodecanediol-O,O'-diphenylphosphonic acid (DDPA) and 4-vinylpyridine) and adsorbed lead ions by these polymers. The maximum adsorption capacity of the lead ion-imprinted micro-beads was calculated as 93.55 mg/g [100].

#### **2.1.9. Determination of Heavy Metals**

For determination of heavy metals in trace amounts in the water, wastewater, sediments, air, soil, plants, foods, fertilizers and animal tissues, there are various instrumental methods. Flame atomic absorption spectrometry (FAAS), electrothermal atomic absorption spectrometry (ETAAS), inductively coupled plasma atomic emission spectrometry (ICP-AES), inductively coupled plasma mass spectrometry (ICP-MS), instrumental neutron activation analysis (INAA) and cold vapor atomic absorption spectrometry (CVAAS) have been used in the analysis of samples [101]. Usually flame atomic absorption spectrometry (FAAS) is used for determination of metals in trace amount. This technique is typically used for determinations in the mg/L range, and may be decreased to  $\mu\text{g/L}$  for some elements. AAS can be used to determine over 70 different elements in solution or directly in solid samples. If the metal concentration is in the range of  $\mu\text{g/L}$ , electrothermal or graphite furnace atomic absorption spectrometry is used. Also hydride generation atomic absorption spectroscopy (HGAAS) should be used for determination of some metals such as As, Sb, Bi, Ge, Pb, Se, Te, and Sn. In this method, elements react with sodium tetrahydroborate ( $\text{NaBH}_4$ ) and form their

reduced hydrides. These hydrides are determined by hydride generation atomic absorption spectroscopy method [102].

### 2.1.9.1. Atomic Absorption Spectrometry

This method is based on absorption of optical radiation (light) by free atoms in the gaseous state and quantitative determination of elements. The electrons of the atoms that absorbed light can be promoted to the higher energy state for a short period of time (radiation of a given wavelength). Amount of absorbed light depends on amount of atoms [102].

### 2.1.9.2. Absorption Principles

Due to quantum theory, a photon with  $h\nu$  energy is absorbed by an atom and the electrons of atom in the base state are promoted to the higher energy state. Planck in 1999 described the energy difference between two energy states as:

$$\Delta E = E_i - E_0 = h\nu = hc/\lambda \quad (2.1)$$

$E_i$  = Energy of electron in transition state, J

$E_0$  = Energy of electron in base state, J

$h$  = Planck's constant,  $6.63 \times 10^{-34} \text{ m}^2 \text{ kg/s}$

$\nu$  = Frequency of the absorbed light, Hz

$C$  = Speed of light,  $3 \times 10^8$ , m/s

$\lambda$  = Wavelength of absorbed light, m

Lambert in 1760 found when a photon passes through the homogeneous medium, the intensity of light decreases but ratio of the transmitted light intensity to the incident light intensity is independent of the intensity of light [102].

$$I = I_0 \cdot e^{-Xd} \quad (2.2)$$

$X$  is absorption coefficient and depends on concentration.

$$X = k \cdot c \quad (2.3)$$

After Lambert, Beer improved the Lambert's law:



$$A = \log I_0/I = k.c.d \quad (2.4)$$

A= Absorbance

$I_0$ = the incident light intensity

I= the transmitted light intensity

K= absorption coefficient (depends on wavelength and medium), L/mol.cm

c= Concentration of absorbed substance, mol/L

d= the path length, cm

## **2.2. Molecular Imprinting Technology**

Every time environmental, pharmaceutical and biotechnology areas need fast and efficient novel methods for controlling the process and obtaining true product, therefore researchers search for better, more selective and sensitive analytical methods. Molecular imprinting technology (MIT) is preparing materials with cavities that are able to recognize a certain molecule according to shape, size and chemical functionality. Polymerization occurs around the interested molecules called as template. After removal of template molecules, a three dimensional cavity is formed in solid matrices. Specific sites for many molecules such as metal ions, organic molecules, proteins, and large species (cell, bacterie, etc) in a synthetic polymer can be created via MIT. This technique has been widely applied in many fields such as solid-phase extraction, chemical sensors and chromatographic separation due to their physical/chemical stability, thermal stability, low cost and easy preparation [103]. The first molecular imprinting material (silica gels) was synthesized in the early 1930.

Polymerization reaction is a very complex process and is affected by many factors such as type and concentration of the monomer, cross-linker, initiator, temperature, and time of polymerization, whether the presence or absence of magnetic field, and volume of the polymerization mixture. For obtaining ideal imprinted polymer, a variety of factors should be optimized. Sometimes preparation of imprinting polymer is a very time-consuming process [104].

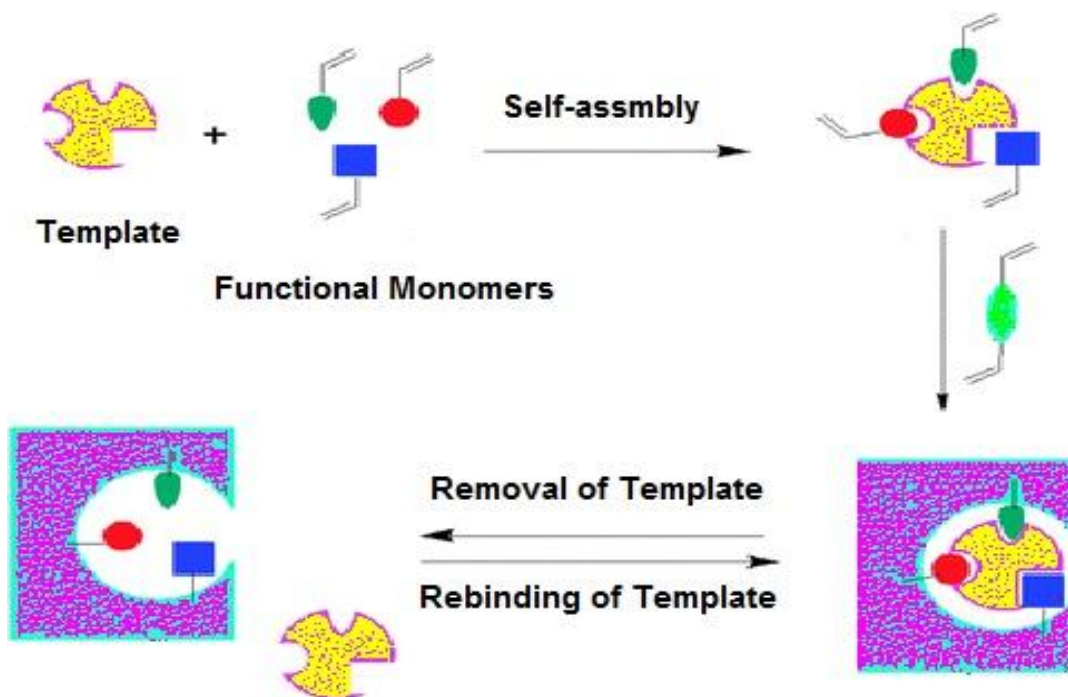


Figure 2.3. Schematic diagram of the molecular imprinting process [104].

Molecular Imprinting Method basically consists of three steps:

**STEP I (Pre-complexation):** Favorable monomers that can polymerize and have functional groups bind to the template or target molecule by covalent or non-covalent interactions and form a complex. In this interaction the three-dimensional structure of target molecule and chemical properties are important.

**STEP II (Polymerization):** Functional monomers, monomer-template complex by using a suitable cross-linker are polymerized and monomer-template complexes are located into solid matrices.

**STEP III (Removal of template molecule):** The template molecule is removed to form the cavities that target molecule can replace there. These cavities can identify the size, the structure and physicochemical properties of target molecule, and bind selectively and effectively to the target molecule. When ions are used as template which is called as ion imprinting method, the selectivity of polymeric adsorbent depends on the charge, the size, and the conditions, geometry of imprinted ion [105]. Molecular imprinting methods, basically due to the type of bond forming between the functional monomer and template molecule are divided into several methods: covalent, non-covalent, semi-covalent, etc.

### **2.2.1. Covalent Imprinting**

In covalent imprinting, typically the templates are bound to appropriate monomers by covalent bond and form pre-polymerized complex. After polymerization, the covalent linkage is cleaved and the template is removed from the polymer. If the guest molecule (template molecule) is in the medium, this molecule binds to the molecular imprinted polymer and the same covalent bond forms again. The greater stability of covalent bonds between template molecule and polymer results in more homogeneous distribution of binding sites through polymeric network. Covalent imprinting is also considered as a less flexible method because the formation of identical rebinding linkages requires rapidly reversible covalent interactions between templates and functional monomers. Therefore selecting favorable template is still challenge. In this method reaching to thermodynamic equilibrium is very difficult due to the strong nature of the covalent interactions and consequent slow binding and dissociation kinetics [106]. The polymerization conditions should be applied as desired (high temperature, high or low pH, and polar solvents, etc.) due to formation of covalent bonds, the kinetic of binding is slow.

### **2.2.2. Non-covalent Imprinting**

Functional monomer and template molecule bind by non-covalent interactions such as hydrogen bonding, hydrophobic, van der Waals interactions, and coordinated covalent bonds. After polymerization, the template molecule is removed then polymeric matrix can bind the target (template) by the same non-covalent interactions. The range of compounds which can be imprinted is greatly expanded. This method due to easy interaction between monomer and template molecule, easy removal of template molecule by solvent extraction, flexibility of functional monomer and template molecule choice advantages is widely spread method for imprinted polymer synthesis. But imprinted polymers synthesized by this method have heterogenic arises in the bonding positions due to depending of pre-complex stability to the affinity constant between the template and functional monomer and effecting polymerization conditions.

### 2.2.3. Semi-Covalent Imprinting

In this method, after removal of template molecule which is bonded by covalent interaction to functional monomer can also form non-covalent bond with functional monomer. This method is an intermediate alternative because the template is bound covalently and has high affinity of covalent binding to functional monomer as in the covalent approach, but the template rebind by non-covalent interactions and have mild operation conditions of non-covalent binding [107].

In the early years of imprinted method development, development of basic concepts and optimization of imprinted polymer were done by covalent interactions. Later, non-covalent interactions have become more attractive due to its easy application. Covalent interactions have a specific stoichiometric ratio between the template molecule and monomer. In non-covalent interactions, binding constants are lower and more binding sites of monomers during the process of imprinting in medium are desired. As a result, the binding sites don't replace in the cavities completely. Especially in catalytic applications and chromatographic studies, this situation is a disadvantage.

Therefore, when binding constants are high ( $K_a = 10^2-10^7$ ), in non-covalent interactions stoichiometric ratios are used. Nowadays in most efficient catalytic systems which are based on imprinted polymers, covalent and stoichiometric non-covalent interactions are used.

The relation between the target molecule and the cavities in imprinted polymers definition for enzyme and catalyst about hundred years ago is defined as key-lock by Emil Fischer. Although molecular imprinting method has many advantages and used in various applications, it has some potent disadvantages such as template leakage, incompatibility in aqueous media, low binding capacity, and slow mass transfer.

Different kinds of polymerization as radical, anion, cation, condensation, bulk, precipitation, suspension, emulsion, and dispersion are used for molecular imprinting process [108]. Radical polymerization techniques more than other techniques are used for imprinting process due to easy preparation and application. Generally, in bulk polymerization monolithic structures are formed by

free radical technique. Template, monomer, initiator and cross-linker are mixed and polymerized. The process lasts about 2-6 hours.

Peptide, amino acids, steroids, proteins, metal ions and organic molecules are used as template molecules. Methacrylic acid, acrylamide, vinyl pyridine and styrene monomers are mostly used as imprinting matrix and created acrylic or vinyl polymers. The other organic polymers such as poly(amino phenyl boronate), poly(phenylene diamine), polyurethanes can also be prepared. For selection of functional monomer FTIR, NMR, UV-Visible spectroscopic methods and computer simulation techniques are used. For stable complex formation, excessive amount of monomer forming coordination bonds and resulting in metal chelating monomer in polar solvents such as water for strong interaction, are used. Also in sol-gel imprinting method, silica and titanium oxide are used [109].

In non-covalent interaction, ethyleneglycol dimethacrylate (EGDMA), N-divinyl benzene (DVB) and N,N'-methylene bisacrylamide are the most widely used cross-linking reagents. The most common used solvents are toluene, acetonitrile, chloroform, ethanol, carbon tetrachloride, tetrahydrofuran, and dichloromethane. In most applications non-polar solvents are selected. When hydrophobic interactions are dominant, water and the other polar solvents can be used.

In radical polymerization, polymerization begins by the thermal decomposition of initiators. Usually 2,2'-azobis (isobutyronitrile) (AIBN) and 2, 2'-azobis (2, 4-dimethylvaleronitrile) (ADVN) are commonly used. When non-covalent interactions between monomer and template molecule are very weak, the reaction temperature can't be increased too much. In this condition, instead of thermal degradation, UV degradation should be preferred.

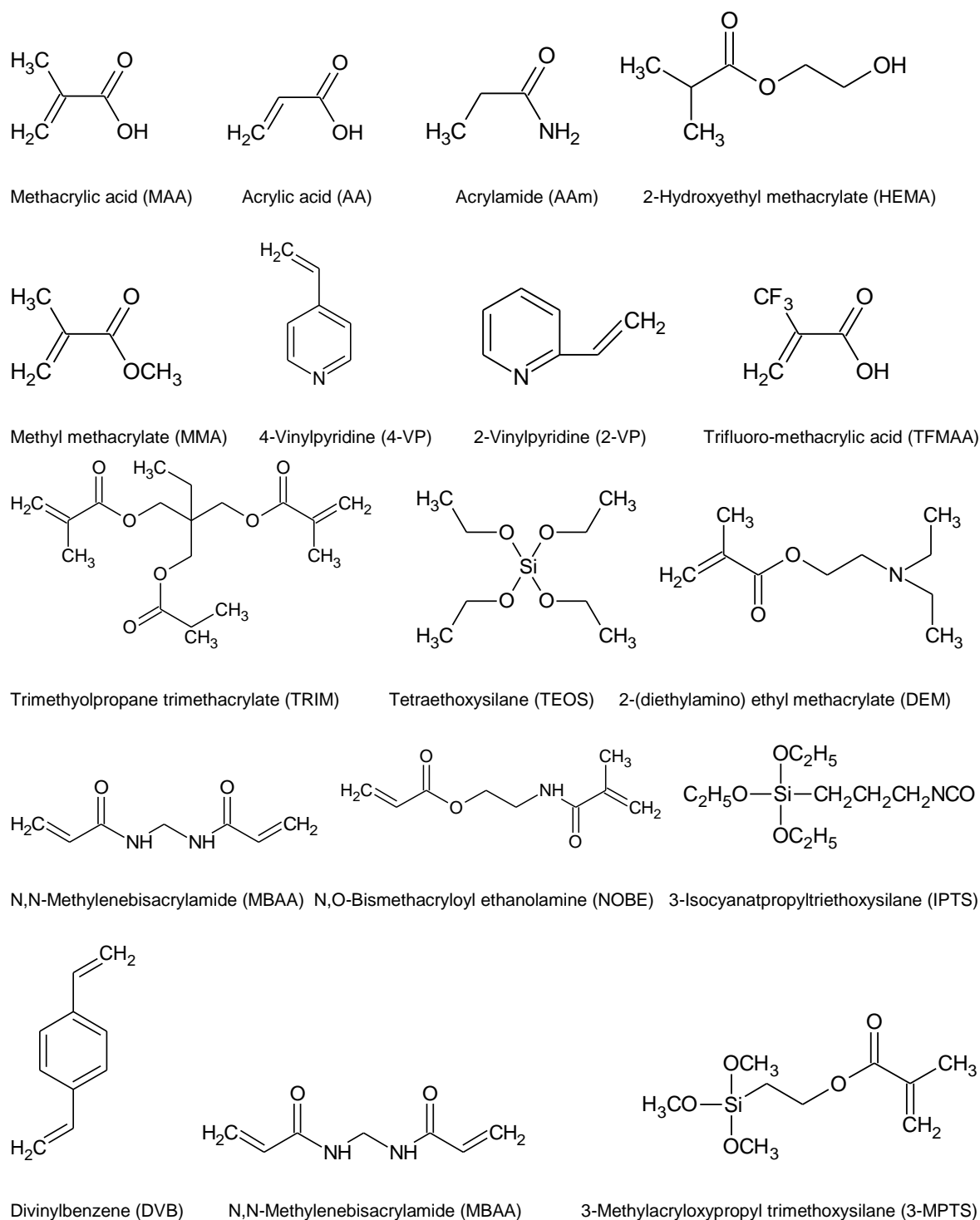


Figure 2.4. Structures of commonly used functional monomers and cross-linkers [109].

Reagents are important in preparation of imprinted polymers. An ideal template molecule for imprinting polymerization should have these properties; 1, It should not contain groups that prevent polymerization; 2, it should be stable chemically

during the polymerization reaction; 3, it should contain functional groups that adapted to functional groups of monomers [109].

Imprinted polymers are used for determination of quinolones in urine by Sun et al. [110], milk by Yan et al. [111], river water by Benito-Peña et al. [112], serum by Sun et al. [110], determination of propranolol by Hu et al. [113], tetracycline by Jing et al. [114], digoxin by González et al. [115], dopamine by Chen et al., [116] and sulfonamides by Li et al. [117] and removal of antibody or enzyme [118]. Metal ion imprinted polymers were used for determination of various metal ions [119].

#### **2.2.4 Synthesis Methods of MIP**

The formation mechanism of molecular imprinting polymer (MIP) is free-radical polymerization or sol–gel process. Bulk polymerization is preferred due to rapidity and simplicity in preparation. Also the other kinds of radical polymerization such as suspension polymerization, emulsion polymerization, seed polymerization and precipitation polymerization are used [105].

#### **2.2.5. Surface Imprinting**

This method is preferred due to the disadvantages of other methods such as incomplete removal of template molecule, small binding capacity and slow mass transfer [120]. These problems can be resolved by surface imprinting. Template molecules which are imprinted by this method are situated at the surface or in the proximity of the imprinted polymer. Several methods for surface imprinting have been used as, using of immobilized template [120], initiator on supporting matrix [121], and combined surface imprinting with controlled/living radical polymerization (CLRP) [123]. Various materials have been used in the surface imprinting process as supporting material, such as activated silica gel [122], Fe<sub>3</sub>O<sub>4</sub> magnetic nanoparticles,[123,124], chitosan [125], activated polystyrene beads [126], quantum dots (QDs) [127,128], and alumina membranes [129].

Fast recovery, high efficiency, low cost and direct purification of crude product from a mixture are advantages of magnetic separation method. Magnetic composite modified MIPs have significant advantages compared to conventional methods [130]. In recent years, MIT is widely used in nanotechnology due to

enormous advantages. Imprinted nano material has been employed in biosensors, biocatalysis, biorecognition, and drug delivery.

### **2.2.6. Novel Technologies for MIP**

In recent years, novel technologies have been introduced in MIT for preparing attractive and competitive well-designed MIP.

#### **2.2.6.1. Controlled/Living Free Radical Polymerization (CLRP)**

Reversible addition-fragmentation chain transfer (RAFT) polymerization, metal-catalyzed atom transfer radical polymerization (ATRP), and nitroxide-mediated polymerization (NMP) are controlled/living radical polymerization (CLRP) methods that are used for the production of well-defined polymers with well defined molecular weight, low polydispersity, controlled composition, and functionality [131]. This method is basically conventional free radical polymerization with additional processes as a thermodynamically controlled process with negligible chain termination and much slower rate for the polymer chain growth. A homogeneous polymer network with a narrow distribution of the chain length was produced by this method. In recent years, this method is used to synthesize developed molecular imprinted polymers [132]. Sulitzky et al. studied a new method to graft MIP films on silica support containing surface-bound free radical initiators [133]. RAFT is commonly most used method due to versatility and simplicity, also the polymerization products are free from the contamination of metal catalysts used in ATRP. In RAFT method, molecular imprinted polymers are prepared by bulk polymerization by Southard et al. [134], precipitation polymerization by Pan et al., [135] and surface imprinting by Titirici et al. [132] and Lu et al. [136]. Molecular imprinted polymers by RAFT polymerization were synthesized and applied for determination of L-phenylalanine anilide by Titirici et al. [132]. Chen et al. reported a general protocol for preparing surface-imprinted core-shell nanoparticles by surface RAFT polymerization using RAFT agent functionalized silica nanoparticles as the chain-transfer agent by copolymerization of 4-VP and EDMA in the presence of 2, 4-D as template [137]. Pan et al. prepared molecular imprinted polymers by RAFT precipitation polymerization for determination of 2,4-D [135].



### **2.2.6.2. Block Copolymer Self-Assembly**

Recent years, block polymer self-assembly has been rapidly developed. MIP nanospheres were prepared by diblock copolymer self-assembly. In this method, the diblock copolymer was synthesized with one block containing functional groups for both hydrogen bond formation and cross-linking, then to form a hydrogen-bonding complex with the template, at last the block copolymer self-assemble to form spherical micelles in a selective solvent. The desired structure was locked by cross-linking. After removing template, complement sites to the template were formed in the core-shell structured nanospheres. A few molecular imprinted polymers were synthesized by the block copolymer self-assembly technique because of complicated procedure [138].

### **2.2.6.3. Microwave-Assisted Heating Method**

Magnetic molecular imprinted polymers (mag-MIP) beads were synthesized by this method and suspension polymerization. These beads were applied for separation of trace triazines in spiked soil, soybean, lettuce and millet samples by Zhang et al. [139]. These beads could analyze samples in trace amount. The polymerization time of this method is very short. The microwave heating techniques are simple integrated techniques for molecular imprinting and have many advantages compelling the other techniques.

### **2.2.6.4. Ionic Liquid as Porogen**

Ionic liquid was used as porogenic solvent and these solvents have promising advantages for preparation of molecular imprinted polymers. Room-temperature ionic liquids have some excellent properties such as low melting point, saturated vapor pressure, non-flammability, good thermal stability, flexible viscosity and miscibility with water and organic solvent. These liquids have been used as solvents in MIP preparation process. 1-butyl-3-methylimidazolium tetrafluoro borate as porogenic solvent by combining sol-gel process was used for selective recognition of testosterone by He et al. [140]. These ionic liquids are more environmental friendly than traditional organic solvents.

### 2.2.7. Ion Imprinted Polymer (IIP)

The general procedure for preparation of IIP consists of several steps such as the preparation of a ligand-metal complex, copolymerization of monomer, ligand-metal complex, and cross-linker and removal of the template ion after polymerization to create three dimensional recognition cavities inside the polymer network [141]. These imprinted polymers are mainly prepared by free radical polymerization.

Ion-imprinted polymers have high selectivity towards the target ion due to the affinity of the ligand for the imprinted metal ion and the size and shape of the generated cavities [142].

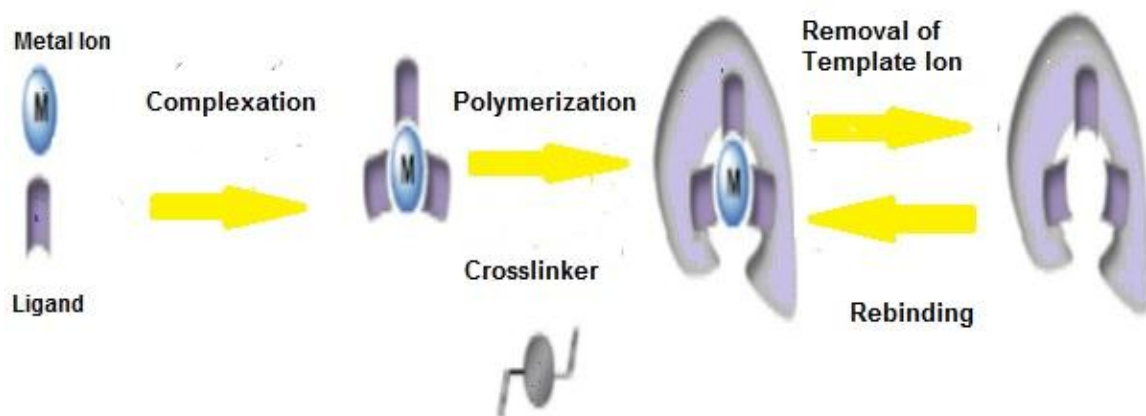


Figure 2.5. Schematic representation of an IIP synthesis [142].

#### 2.2.7.1. Different Approaches for IIP

Recent approaches for preparing IIP can be given as:

- crosslinking of linear chain polymers carrying metal-binding groups
- chemical immobilization of ligands, interacting with metal ions, by crosslinking
- surface imprinting conducted on aqueous-organic interface
- trapping of non-functionalized ligand inside the polymer network

### **2.2.7.2. The Crosslinking of Linear Chain Polymers Carrying Metal-Binding Groups**

This method is the oldest technique used to prepare ion imprinted polymers. Poly(4-vinylpyridine) was copolymerized with 1,4-dibromobutane in the presence of Cu(II), Fe(III), Co(II), Zn(II), Ni(II) or Hg(II) ions for separation of these metal ions. Chitosan deacetylate is a popular adsorbent for the removal of metal ions due to amino and hydroxyl complexing groups. Chitosan imprinted microparticles with template metal ions such as Cu(II), Zn(II), Ni(II), and Pb(II) and epichlorohydrin or glutaraldehyde as crosslinker was prepared by Chen et al. [142,143]. Shawky et al. prepared an Ag(I) ion imprinted membrane by crosslinking a mixture of chitosan and poly(vinyl alcohol) with glutaraldehyde [144]. Interpenetrating polymer networks (IPN), imprinted metal methacrylate, (Cu(II) or Pb(II)-MAA) was prepared by sequential polymerization of an epoxy resin with diethylenetriamine or triethylenetetramine and 1, 4-butanediol diacrylate in presence of AIBN by Wang et al. [145] and Pan et al. [146].

### **2.2.7.3. Chemical Immobilization**

First, binary complexes of metal ions with ligand which have vinyl groups are prepared, then isolated and polymerized with matrix-forming monomers [145]. Some of commercial monomers that are used in this method are: 4-VP by Alizadeh et al. [148] and by Ganjali et al. for Hg(II) [149] and for Cu(II) by Ng et al. [150], 1-vinylimidazole for Cd(II) by Segatelli et al. [151], acrylamide for Cu(II) by Baghel et al. [152] or acrylic acid for Fe(III) recognition by Singh et al. [153]. These monomers interact with the template (metal ion) by their nitrogen or oxygen atoms. A vinylated form of 1-hydroxy-9, 10-anthraquinone (HAQ) with EDMA in presence of uranyl ions was copolymerized and resulted in nano-sized particles [154]. The advantages of these synthesized monomers over the commercial monomers are the control of the structure and amount of species incorporated into the polymer. Amino acids or amino acid derivatives (histidine, cysteine, glutamic acid, and cysteine methylester) were used as chelating agents, formed complex with various metals i.e. for Al(III) by Andaç et al. [155], for Hg(II) by Andac et al. [156], for Cr(III) by Demiralay et al. [157], for Fe(III) by Luo et al. and by Fu et al.

[158,159], for Cd(II) by Li et al. [160], for Ni(II) by Milja et al., [161] and further copolymerized with a crosslinker, usually EDMA, in the presence of HEMA.

#### **2.2.7.4. Surface Imprinting**

Although, ion imprinted polymers which are prepared by the other processes (chemical immobilization or trapping) have high selectivity but have disadvantages such as low rebinding capacities because of restricted accessibility to the binding sites, embedding of template molecule inside the highly rigid polymer network [162,163]. Surface imprinting has solved these problems because in imprinted polymers that are imprinted by this method, binding cavities are onto or near the surface of polymer. Removal of template molecule is complete, accessibility to the target species is comfortable and mass-transfer resistance is low in this method [162,163]. In recent years a new method for preparation of surface imprinting was introduced, modification of small sized particles with the introduction of an imprinted layer on their surface leading to core-shell type particles. EDMA and the Cu(MAA)<sub>2</sub> complexes on the surface of polystyrene core were copolymerized by Dam et al [162,163]. Some other organic surface-imprinted materials have been prepared by grafting a polyethyleneimine layer on polypropylene fibers, after an activation step by a (meth)acrylic monomer, and further crosslinking it with epichlorohydrin in presence of Cu(II) ions [164,165]. Surface ion imprinted materials were prepared by the "grafting to" procedure by coupling chloropropylated silica with polyethyleneimine and further crosslinking it by epichlorohydrin in presence of Cu(II) or Cd(II) ions by Gao et al. [165], for Pb(II) by An et al [166] or for Co(II) ions by Liu et al. [167]. Milja et al. added a pre-polymerization mixture containing 4-VP, HEMA, EDMA, AIBN and UO<sub>2</sub><sup>2+</sup> ions in 2-methoxyethanol to silica particles which previously functionalized by quinoline-8-ol ligand and polymerized by precipitation polymerization [168]. The Cd(II) ions by Li et al. [169] and Pb(II) ions by Liu et al. [170] were imprinted on the surface of silica gel particles. For Co(II) [171] or for Cs(I) [172] ions by titanate whiskers which are used as support particles were imprinted on the surface of chitosan layer. Fu et al. mixed the mineral particles with deacetylated chitosan, GMPTS, and the template ion (Ce(III) or Sr(II)) after crosslinking by a sol-gel process and used for removal of metal ions [173]. Ren et al. prepared surface-imprinted Fe<sub>3</sub>O<sub>4</sub> particles by mixing magnetite nanoparticles with chitosan, Cu(II) ions and

epichlorhydrin in tripolyphosphate sodium solution [174]. Ion-imprinted magnetic beads were prepared by suspension copolymerization of N-methacryloyl-(L)-cysteine methylester-Cd(II) complex with HEMA and EDMA in presence of magnetite nanoparticles and used for the removal of Cd(II) ions from viscous human plasma by Candan et al. [175].

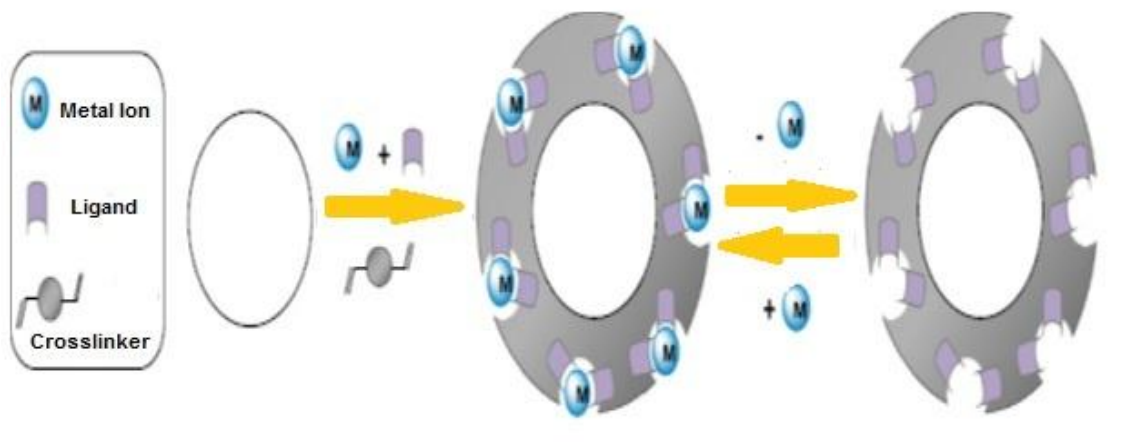


Figure 2.6. Schematic representation of surface imprinting [173].

### 2.2.7.5. The History of Ion Imprinted Polymers

The first ion-imprinted polymers have been introduced by Nishide in 1976 that ion-imprinted polymers were prepared by crosslinking of poly(4-vinylpyridine) with 1, 4-dibromobutane in the presence of a metal ion [176]. But the real development of IIP is more in recent years and a considerable increase of the number of publications dealing with IIPs can be observed in the last 10 years. Some review articles have been published about IIPs [177-178].

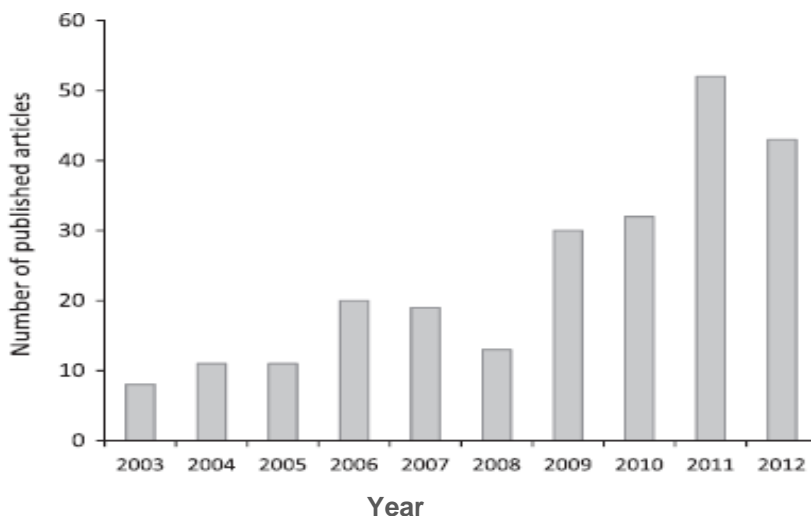


Figure 2.7. Number of published articles about IIP in the last 10 years [178].

### **3. MATERIALS AND METHODS**

#### **3.1. Materials**

2-Hydroxyethyl methacrylate (HEMA), N,N'-methylene bisacrylamide (MBAA), L-cysteine methyl ester, L-histidine methyl ester, L-aspartic acid methyl ester, hydroquinone, triethylamine and nitrates of Cu, Cd, Pb, Fe, Al, Co, Ca, Ni, and Zn were purchased from Sigma (St. Louis, MO, USA). N, N, N, N-tetra-methylethylenediamine (TEMED) and ammonium persulfate (APS) were from BioRad (Hercules, CA, USA). HEMA and TEMED were kept at +4°C. APS was kept in desiccator. The Fe<sub>3</sub>O<sub>4</sub> nanoparticles with diameters less than 5 nm were used in copper imprinted magnetic cryogels and purchased from Sigma. All reagents were used as purchased without any purification. All water used in the experiments was purified using a Barnstead (Dubuque, IA) ROpure LP® reverse osmosis unit. All glassware was extensively washed with dilute nitric acid before use.

#### **3.2. Preparation of Ion-Imprinted Cryogels**

In this thesis, various ion imprinted cryogels were synthesized and examined for their performances to remove metal ions from aqueous solutions. Cryogel membranes which were specific for targeted template ion were prepared via bulk polymerization of 2-hydroxyethyl methacrylate with amino acid based functional monomers. The selection of amino acid, histidine amino acid for complexing Cu(II) ions, cysteine amino acid for complexing Cd(II) ions, and aspartic acid for complexing Pb(II) ions depended on the Pearson acid-base theory which describes the classification of ions according to their Lewis acid-base character. Histidine, cysteine and, aspartic acid have side groups as imidazole, thiol, and dicarboxylic acid, respectively. These groups could specifically interact with respected heavy metal ions. Three heavy metal ions Cu(II), Cd(II), and Pb(II) were chosen as target. After synthesis of functional monomers starting from selected amino acids via substitution reaction between amino acids and methacryloyl chloride, these functional monomers were used for preparing pre-polymerization complexes which would be used in the cryogel production processes. For each cryogel set, the amount of pre-polymerization complexes used in the cryogelation was varied in order to investigate the imprinting

efficiency. Cryogels were prepared in membrane form by applying cryogelation process between two electrophoresis glasses. Then, the cryogels were cut into different shapes i.e. square and circular disks having different diameters. Ion-imprinted magnetic cryogels were also synthesized in order to evaluate the effects of magnetic ingredient [magnetite ( $\text{Fe}_3\text{O}_4$ ) nanopowders] on both cryogelation and adsorption performances of cryogels. The template removal was realized by  $\text{Na}_2(\text{EDTA})$  solution. The increasing number in the cryogel code depended on the increasing amount of imprinted metal ion.

After synthesis steps, the cryogels were characterized by using appropriate instrumental methods. Then, their heavy metal ion adsorption performances were evaluated from singular aqueous heavy metal ion solution while considering effecting factors such as pH, concentration, temperature, and contact time etc. All cryogels were used for competitive heavy metal ion adsorption and specific heavy metal ion enrichment. The structure of thesis was organized in accordance to targeted heavy metal ion and results were reported in this respect. Non-imprinted cryogels were also prepared for comparison and statistical purpose. The results were also analyzed by considering several isotherms and testing several kinetic models to describe the adsorption process and to calculate the thermodynamics variables.

Table 3.1. Summarizing the strategy for cryogel synthesis.

Targeted Ion	Shape	Size or diameter, cm	Functional monomer	Code
Cu(II) imprinted	Disk	1.0	N-methacryloyl-L-histidine (MAH)	Cu-1 Cu-2 Cu-3
Cu*(II) imprinted	Disk	1.0	N-methacryloyl-L-histidine (MAH)	Cu*-1 Cu*-2 Cu*-3 Cu*-4 Cu*-5 Cu*-6 Cu*-7 Cu*-8 Cu*-9
Cd(II) imprinted	Square	1.5 x 1.5	N-methacryloyl-L-cysteine (MAC)	Cd-1 Cd-2 Cd-3
Pb(II) imprinted	Disk	0.5	N-methacryloyl-L-aspartic acid (MAAsp)	Pb-1 Pb-2 Pb-3

\*: Asterisk symbol denotes the magnetic samples.

### 3.2.1. The Cryogels for Cu(II) Ions

#### 3.2.1.1. Synthesis of Functional Monomer

In order to co-ordinate Cu(II) ions, histidine based functional monomer N-methacryloyl-L-histidine (MAH) was synthesized as given: 5.0 g of L-histidine methyl ester and 0.2 g of hydroquinone were dissolved in 100 mL of CH<sub>2</sub>Cl<sub>2</sub>, then this solution was cooled down to 0°C. Triethylamine (12.79) was added to this solution and 5.0 mL of methacryloyl chloride was spilled on the solution slowly. This mixture was stirred magnetically under a nitrogen atmosphere at room



temperature for 2 h. Unreacted methacryloyl chloride was extracted with 10% NaOH solution. The aqueous phase was removed in rotary evaporator and remainder (MAH) was obtained as yellowish solid.

### 3.2.1.2. Preparation of MAH-Cu(II) Pre-complex

Before ion imprinting process, Cu(II) ion (template ion) and MAH functional monomer (ligand) in ratio of 1:1 (mol:mol) were mixed and pre-complex was formed. 22.3 mg (0.1 mmol) of MAH in water (5 mL) was added to 23.3 mg of  $\text{Cu}(\text{NO}_3)_2 \cdot 2.5\text{H}_2\text{O}$  (0.1 mmol) at room temperature. This solution was magnetically stirred for about 3 h and MAH-Cu(II) complex was separated by filtration as a bluish solid. Then, the complex was washed by ethanol: water mixture (75:25, v:v), and dried under vacuum (12 h, 200 mmHg).

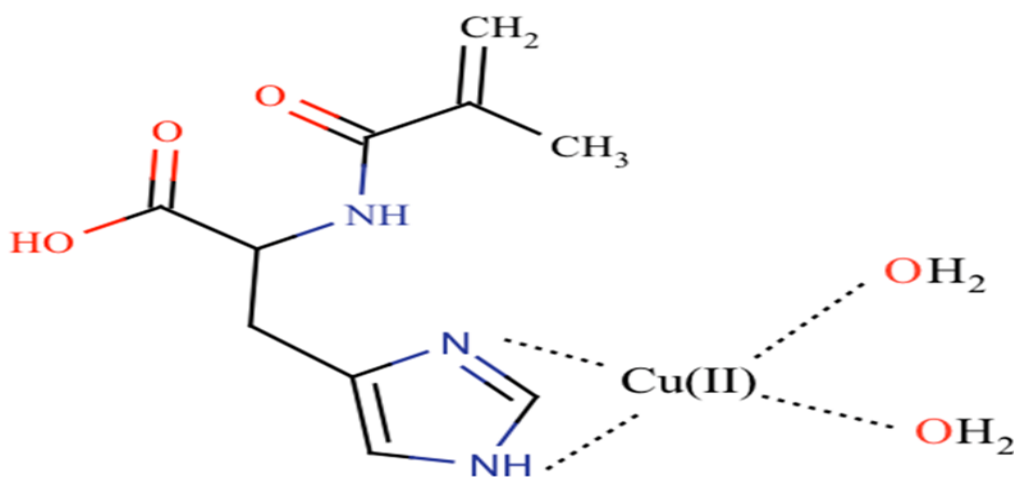


Figure 3.1. Possible formula of MAH-Cu(II) complex.

### 3.2.1.3. Preparation of Cu(II) Ion-Imprinted and Non-Imprinted Non-magnetic Cryogels

Cu(II) ion imprinted cryogels having different compositions were prepared (Table 3.2). 4.7 mL of HEMA (monomer) was dissolved in 5.3 mL of deionized water (phase I). Nitrogen gas was passed through solution for 5 min under vacuum (100 mmHg) to remove dissolved oxygen. Total concentration of monomer was 18.8% (w/v). The second solution was 2.013 mg of methylenebisacrylamide (crosslinker)

dissolved in 20 mL of deionized water (phase II). The first solution (phase I) was added to second one while adding MAH-Cu(II) complex (50 mmol, 100 mmol, and 200 mmol). These cryogels were produced by the free radical polymerization method. APS (100 mg, 1% (w/v) of the total amount of monomer) as initiator was added to solution. Then solution was cooled in an ice bath for 2-3 min. After that, TEMED (100 ml, 1% (w/v) of the total amount of monomer) was added to solution and solution was stirred for one min. This solution was placed between two electrophoresis glasses (25 cm x 25 cm). The teflon plate (thickness 0.2 mm) was used between the glasses and created space between glasses. The three edges of the glasses were closed. Polymerization solution which was poured between glass plates was frozen at -12°C and stayed for 24 h. After 24 hours, water was removed from frozen polymeric structure cryogel at room temperature. The membranes were cut by a perforator in the form of circle with a diameter of 1.0 cm. To remove the unreacted monomers and initiator an extensive cleaning process was applied. Dilute HCl solution and water-ethanol mixtures were used for this purpose. After cleaning process, membrane cryogels were incubated by Na<sub>2</sub>(EDTA) solution for desorption of imprinted Cu(II) metal ions. Desorption processes were continued until removing of all of imprinted Cu(II) ions. Amounts of Cu(II) ions were measured by AAS instrument. The cryogel membranes after cleaning and desorption, were stored in 0.02% sodium azide at +4°C until use.

The same experimental produce was applied for non-imprinted cryogels, just excluding the ion-functional monomer complex in recipe.

Table 3.2. Composition of Cu(II) ion imprinted non-magnetic cryogels

Cryogel Code	MAH-Cu(II) complex (mmol)
Cu-1	0.05
Cu-2	0.1
Cu-3	0.2

HEMA: 4.7 mL (in 5.3 mL of water), Methylene bisacrylamide: 2.013 mg (in 20 mL of water).

#### **3.2.1.4. Preparation of Cu(II) Ion-Imprinted and Non-Imprinted Magnetic Cryogels**

To evaluate magnetism effect on the ion recognition performance of cryogels, magnetic cryogels were also prepared by adding  $\text{Fe}_3\text{O}_4$  particles into polymerization medium. Compositions of Cu(II) ion imprinted magnetic cryogels were also varied (Table 3.3). 4.7 mL of HEMA (monomer) was dissolved in 5.3 mL of deionized water. Nitrogen gas was passed through solution for 5 min under vacuum (100 mmHg) to remove dissolved oxygen. Total concentration of monomer was 18.8% (w/v). For the second aqueous phase, 2.013 mg of methylenebisacrylamide (crosslinker) was dissolved in 20 mL of deionized water. The first solution was added to second phase while adding of MAH-Cu(II) complex in different amounts (50 mmol, 100 mmol, and 200 mmol). The mixture was stirred till homogeneous solution was obtained. Later  $\text{Fe}_3\text{O}_4$  nanoparticles (25, 50, and 100 mg) were also added to polymerization solution. These cryogels were produced by the free radical polymerization. APS (100 mg, 1% (w/v) of the total amount of monomer) as initiator was added to the mixture. Then solution was cooled in an ice bath for 2-3 min. After that, TEMED (100 ml, 1% (w/v) of the total amount of monomer) was added to the mixture and solution was stirred for one minute. This mixture was poured between two electrophoresis glasses (25 cm x 25 cm). The teflon plate (thickness 0.2 mm) was used between the glasses and created space between glasses. The three edges of the glasses were closed. Polymerization solution which was poured between glass plates was frozen at  $-12^\circ\text{C}$  and stayed for 24 h. After 24 h, water was removed from frozen polymeric structure cryogel while thawing at room temperature. The membranes were cut by a perforator in the form of circle with diameter of 1.0 cm. Cleaning and desorption processes were performed as discussed in Section 3.2.1.3. The cryogel membranes after clening and desorbing processes were stored in 0.02% sodium azide at  $+4^\circ\text{C}$ , until use.

The same experimental procedure was applied for non-imprinted magnetic cryogels, just excluding the ion-functional monomer complex in recipe.

Table 3.3. Composition of Cu(II) ion imprinted magnetic cryogels.

Cryogel code	MAH-Cu(II) complex, mmol	Fe <sub>3</sub> O <sub>4</sub> , mg
Cu*-1	0.05	25
Cu*-2	0.10	25
Cu*-3	0.20	25
Cu*-4	0.05	50
Cu*-5	0.10	50
CU*-6	0.20	50
Cu*-7	0.05	100
Cu*-8	0.10	100
Cu*-9	0.20	100

HEMA: 4.7 mL (in 5.3 mL of water), Methylenebisacrylamide: 2.013 mg (in 20 mL of water).

\*: Cu(II) ion imprinted magnetic cryogel.

### 3.2.2. The Cryogels for Cd(II) Ions

#### 3.2.2.1. Synthesis of Functional Monomer

In order to co-ordinate Cd(II) ions, cysteine based functional monomer N-methacryloyl-L-cysteine (MAC) was synthesized as given: 5.0 g L-cysteine hydrochloride and 0.2 g hydroquinone were dissolved in 100 mL of CH<sub>2</sub>Cl<sub>2</sub> then this solution was cooled down to 0°C. Triethylamine (13.0 g) was added to this solution, and 4.0 mL of methacryloyl chloride was spilled on the solution dropwise. This mixture was then stirred magnetically under a nitrogen atmosphere at room temperature for two hours. Unreacted methacryloyl chloride was extracted with 10% NaOH solution. The aqueous phase was removed in rotary evaporator and the remainder (MAC) was dissolved in ethanol.

### 3.2.2.2. Preparation of MAC-Cd(II) Pre-Complex

Before ion imprinting process, Cd(II) ion (template ion) and MAC functional monomer (ligand) in ratio of 1:1 (mol:mol) were mixed and pre-complex was formed. 18.9 mg (0.1 mmol) of MAC in ethanol (5 mL) was added to 30.8 mg of  $\text{Cd}(\text{NO}_3)_2 \cdot 4\text{H}_2\text{O}$  (0.1 mmol) at room temperature. This solution was magnetically stirred for about 3 hours and MAC-Cd(II) complex was separated by filtration. Then, the complex was washed by ethanol: water mixture (75:25, v: v) and dried under vacuum (12 hours, 200 mmHg).

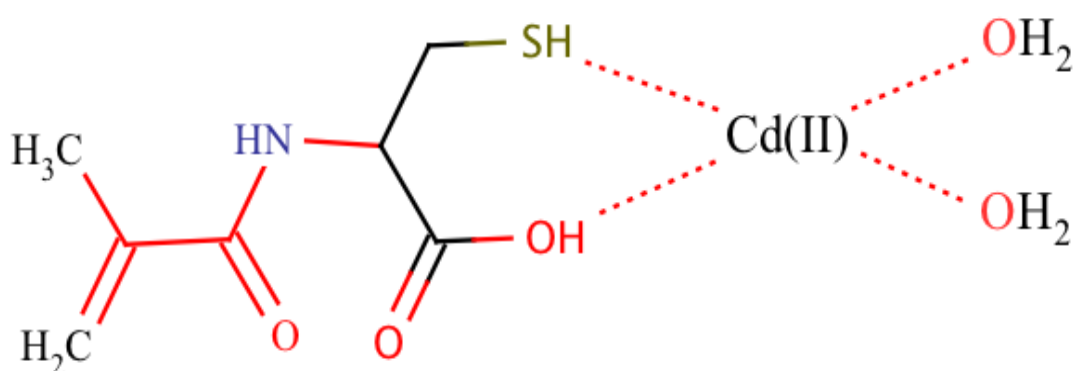


Figure 3.2. Possible formula of MAC-Cd(II) complex.

### 3.2.2.3. Preparation of Cd(II) Ion-Imprinted and Non-Imprinted Cryogels

Cd(II) ion imprinted cryogels having different compositions were synthesized (Table 3.1). 4.7 mL of HEMA (monomer) was dissolved in 5.3 mL of deionized water. Nitrogen gas was passed through solution for 5 min under vacuum 100 mmHg to remove dissolved oxygen. Total concentration of monomer was 18.8% (w/v). The second solution was 2.013 mg of methylenebisacrylamide (crosslinker) dissolved in 20 mL of deionized water. The two solutions were mixed, then following the addition of MAC-Cd(II) complex (0.05 mmol, 0.1 mmol, and 0.2 mmol), it was stirred in an ice-bath until homogeneous solution was obtained. These cryogels were polymerized via free radical polymerization. APS (100 mg, 1% (w/v) of the total amount of monomer) as initiator was included in solution. Then solution was cooled in an ice bath for 2-3 min. After that, TEMED (100 mL,

1% (w/v) of the total amount of monomer) was added to solution and was stirred for one min. This solution was poured between two electrophoresis plates (25 cm x 25 cm). The teflon plate (thickness 0.2 mm) was used between the glasses and created space between them. The three edges of the glasses were closed. Polymerization solution which was included between glass plates was frozen at -12°C and stayed for 24 h. After 24 h, water was removed from frozen polymeric cryogel structure at room temperature. The membranes were cut by a perforator in the form of square which is 1.5 cm on edge. Cleaning and desorption processes were performed as discussed in Section 3.2.1.3. The membrane cryogels were stored in 0.02% sodium azide at +4°C until use.

The same experimental procedure was followed for non-imprinted cryogels, just excluding the MAC-Cd(II) complex in recipe.

Table 3.3. Composition of Cd (II) ion imprinted cryogels.

Cryogel Code	MAC-Cd(II) complex, mmol
Cd-1	0.05
Cd-2	0.1
Cd-3	0.2

HEMA: 4.7 mL (in 5.3 mL of water), Methylen bisacrylamide: 2.03mg (in 20 mL of water)

### 3.2.3. The Cryogels for Pb(II) Ions

#### 3.2.3.1. Synthesis of Functional Monomer

In order to co-ordinate Pb(II) ions, aspartic acid based functional monomer N-methacryloyl-L-aspartic acid (MAAsp) was synthesized as given: 1.0 g of L-aspartic was dissolved in 100 mL of NaOH (1 M), then this solution was slowly added to a solution of methacryloyl benzotriazole (1.03 g) in 25 mL of 1,4-dioxane. This mixture was magnetically stirred for 20 min. After the reaction was completed, 1,4-dioxane was evaporated under vacuum. For removing of benzotriazole, the precipitate was diluted with water and extracted with ethyl acetate (3 x 50 mL). The water phase was neutralized to pH 6.0–7.0 by 10% HCl–

water solution. Then water was removed by rotary-evaporator, and N-methacryloyl-L-aspartic acid (MAAsp) was obtained [179].

### 3.2.3.2. Preparation of MAAsp-Pb(II) Pre-Complex

Before ion imprinting process, Pb(II) ion (template ion) and MAAsp functional monomer (ligand) in ratio 1:1 (mol: mol) were mixed and pre-complex was formed. 53.8 mg (0.1 mmol) of MAAsp (in 5 mL of water) was added to 66.24 mg of  $\text{Pb}(\text{NO}_3)_2 \cdot 2\text{H}_2\text{O}$  (0.1 mmol) at room temperature. This solution was stirred for about 3 hours and MAAsp-Pb(II) complex was separated by filtration. Then, the complex was washed by ethanol: water mixture (75:25, v:v) and dried under vacuum (12 h, 200 mmHg).

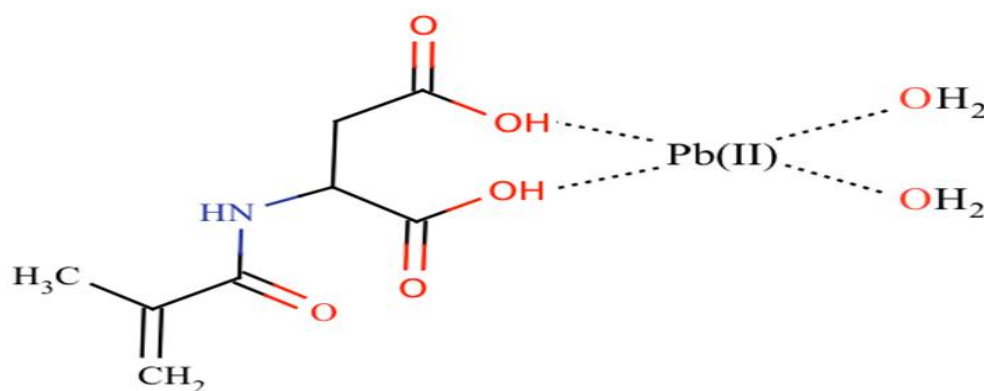


Figure 3.3. Possible formula of MAAsp-Pb(II) complex.

### 3.2.3.3. Preparation of Pb(II) Ion-Imprinted and Non-Imprinted Cryogels

Pb(II) ion imprinted cryogels having different compositions (Table 3.3.) were prepared. 4.7 mL of HEMA (monomer) was dissolved in 5.3 mL of deionized water. Nitrogen gas was passed through solution for 5 min under vacuum (100 mmHg) to remove dissolved oxygen. Total concentration of monomer was 18.8% (w/v). For the second aqueous phase, 2.01 mg of methylenebisacrylamide (crosslinker) was dissolved in 20 mL of deionized water. The first solution was added to second one while adding of MAAsp-Pb(II) complex in different amounts (50 mmol, 100 mmol, and 200 mmol). The mixture was stirred until homogeneous solution was obtained. These cryogels were synthesized via the free radical polymerization. APS (100 mg, 1% (w/v) of the total amount of monomer) as

initiator was added to solution. Then solution was cooled in an ice bath for 2-3 min. After that, TEMED (100 ml, 1% (w/v) of the total amount of monomer) was added to solution and solution was stirred for one min. This solution was poured between two electrophoresis glasses (25 cm x 25 cm). The teflon plate (thickness 0.2 mm) was used between the glasses and created space between glasses. The three edges of the glasses were closed. Polymerization solution which was filled between glass plates was frozen at -12°C and stayed for 24 h. After 24 h, water was removed from frozen polymeric cryogel structure while thawing at room temperature. The membranes were cut by a perforator in the form of circle with a diameter of 0.5 cm. Cleaning and desorption processes were performed as discussed in Section 3.2.1.3. After cleaning process, the cryogel membranes were stored in 0.02% sodium azide at +4°C.

The same synthesis procedure was used for non-imprinted cryogels, just excluding ion-functional monomer complex in recipe.

Table 3.5 Composition of Pb(II) ion imprinted cryogels.

Cryogel Code	MAA <sub>sp</sub> -Pb(II) complexes, mmol
Pb-1	0.05
Pb-2	0.1
Pb-3	0.2

HEMA: 4.7 mL (in 5.3 mL of water), Methylenebisacrylamide: 2.013 mg (in 20 mL of water)

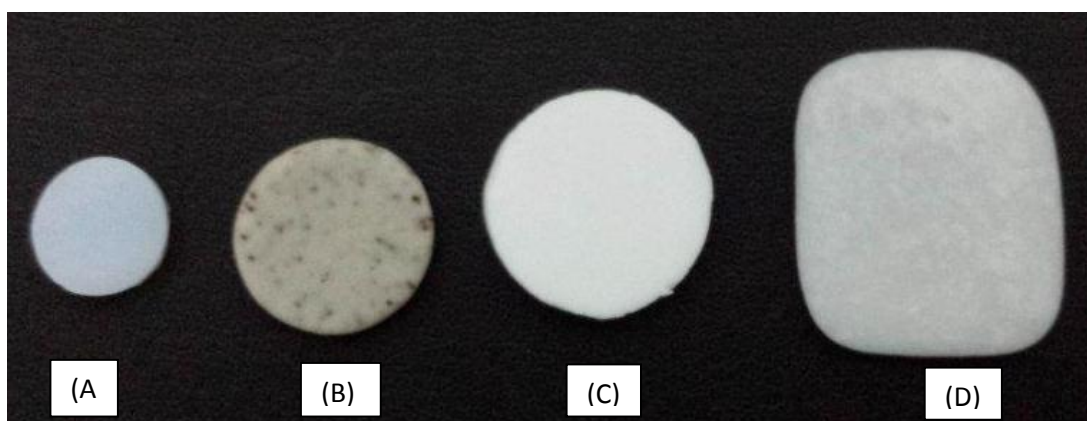


Figure 3.4. Optic photos of ion imprinted cryogels in different shapes; (A): Pb(II), (B): Cu(II), (C): magnetic Cu(II), (D): Cd(II) imprinted cryogels.



### **3.3. Characterization Studies**

In present study, all cryogels were characterized by swelling studies, Fourier transform infrared spectroscopy (FTIR), surface area measurements, scanning electron microscopy (SEM), and energy dispersive X-Ray Analysis (EDX).

#### **3.3.1. Swelling Properties of Cryogel**

The swelling degree of cryogels was determined as follows: the swollen cryogel sample was put in an oven at 54°C for drying. After drying, the mass of the dried sample was determined ( $M_0$ , g). Dried cryogel membrane was put in a beaker which contains 20 mL of water at room temperature. After 2 h, previously determined equilibrium time, this cryogel membrane was wiped out by filter paper to remove surface water and weighed ( $M_s$ ).

The swelling degree of cryogels was defined as:

$$\text{The swelling degree \%} = [(M_s - M_0)/M_0] \times 100\% \quad (3.1)$$

#### **3.3.2. FTIR Studies**

FTIR spectra of ion-imprinted cryogels were obtained by using a FTIR spectrophotometer (Nicolet™ iS™10 FT-IR Spectrometer-USA). The dried, crushed, and powdered samples (about 2 mg) were mixed with KBr (IR-grade 98 mg) , pressed into a pellet and spectrum was recorded .

#### **3.3.3. Surface Morphology**

The surface morphology of the cryogels was examined using scanning electron microscopy (SEM). First, the sample was lyophilized for 12 h. Finally it was coated with gold-palladium (40:60) and examined using a Nova Nanosem 430 scanning electron microscope (FEI Company, USA).

#### **3.3.4. X-Ray Analysis (EDX)**

Elemental composition of cryogels was identified by Energy Dispersive X-Ray Analysis (EDX) method. EDX systems are attachments to Electron Microscopy instruments (Scanning Electron Microscopy (SEM)). The samples were lyophilized for 12 h before examination by EDX.

### 3.3.5. Surface Area Measurements

The specific surface areas of all cryogels were measured according to the Brunauer-Emmett-Teller (BET), multi point analysis method by an AUTOSORP II 6B apparatus from Quantachrome Instruments, USA. Lyophilized cryogel samples were vacuumed to remove oxygen and humidity in pores at 35°C for 6 h, then nitrogen adsorption was studied at room temperature.

### 3.4. Heavy Metal Ion Adsorption from Singular Aqueous Solutions

Cryogels with different properties and compositions were prepared. Parameters that effect adsorption capacities for Cu(II), Cd(II), and Pb(II) imprinted cryogels were studied from aqueous solutions for each ion. Adsorption of these ions was studied in batch mode. Effects of metal ion concentration, pH of the medium and temperature on the adsorption capacity were evaluated. The effect of the initial concentration of metal ions on adsorption capacity was performed by changing the concentration of metal ions between 10-700 ppm. The effect of pH on the adsorption capacity was determined by changing pH of the solution between 3.0 and 6.0 by using nitric acid and sodium hydroxide. The effect of adsorption temperature on the adsorption capacity was determined by changing temperature of the solution between 4.0°C and 42°C. The effect of contact time (5-180 min) on adsorption capacity was also studied. The concentration of metal ions was determined by ICP-AAS method (AAlyst 800, Perkin-Elmer). The amount of adsorbed metal ions per unit mass of cryogels was calculated by the following equation:

$$Q = [(C_0 - C) \cdot V] / m \quad (3.2)$$

where Q is the amount of adsorbed metal ion per gram of cryogel (mg/g);  $C_0$  and C are concentrations of heavy metal ions in solution before and after adsorption, respectively (mg/L); V is the volume of the solution (L) and m is mass of cryogel (g).



Figure 3.5. Atomic absorption spectroscopy instrument.

### 3.5. Selectivity Studies for Metal Ion-Imprinted Cryogels

The selectivity of all ion-imprinted cryogels was studied for specific metal ions and other competitive ions. The selectivity of ion-imprinted cryogels with respect to non-imprinted cryogels was also determined. For this purpose, the selectivity of the Cu(II)-imprinted cryogel for Cu(II) with respect to Cd(II), and Pb(II) ions, the selectivity of the Cu(II)-imprinted magnetic cryogel for Cu(II) with respect to Cd(II), and Pb(II), the selectivity of the Cd(II)-imprinted cryogel for Cd(II) with respect to Cu(II), and Pb(II) and the selectivity of the Pb(II)-imprinted cryogel for Pb(II) with respect to Cu(II), and Cd(II), were examined in batch system.

The distribution coefficients ( $K_d$ ) for other ions with respect to specific ions were calculated by the following equation;

$$K_d = [(C_i - C_f)/C_f] \times V/m \quad (3.3)$$

where  $K_d$  represents the distribution coefficient for the metal ion (L/g);  $C_i$  and  $C_f$  are initial and final concentrations of metal ions (mg/L), respectively,  $V$  is the volume of the solution (L) and  $m$  is the mass of the cryogel (g). The selectivity coefficient ( $k$ ) for the binding of specific ions [Cu(II), Cd(II), and Pb(II)] with competing species (other metal ions) was determined by the following equation:

$$k = K_d (\text{template}) / K_d (\text{competing metal ion}) \quad (3.4)$$

$K_d$  (template) is the distribution coefficient of the template ion [Cu(II), Cd(II), and Pb(II)] and  $K_d$  (competing ion) is the distribution coefficient of the competing ions (other metal ions).

The relative selectivity coefficient ( $k'$ ) which was used to estimate the effect of imprinting on ion selectivity can be defined from the following equation;

$$k' = k_{\text{MIP}} / k_{\text{NIP}} \quad (3.5)$$

where  $k_{\text{MIP}}$  is for MIP cryogel,  $k_{\text{NIP}}$  is for NIP cryogel.

### 3.6. Desorption and Reuse

Desorption of the adsorbed ions from cryogel was studied in batch mode. First adsorption of metal ions from 100 ppm of metal ion solution by specific ion imprinted cryogel was determined, and then the ion was desorbed with 20 mL of 100 mmol EDTA solution. Amount of desorbed metal ions was determined after 1 h, 2 h, 3 h of contact time. Desorption ratio in desorption medium was calculated with the following expression:

$$\text{Desorption ratio (\%)} = (\text{Amount of metal ion in desorption medium}) / (\text{Amount of adsorbed metal ion})$$

In order to show the reusability of cryogel, adsorption-desorption cycle was repeated three times by using the same cryogel.

### 3.7. Competitive Heavy Metal Adsorption/Enrichment

The competitive study of all ion-imprinted cryogels [Cu(II), Cd(II), and Pb(II)] was determined from solution which contains several metal ions, Cd(II), Pb(II), Zn(II), Ca(II), Co(II), Ni(II), and Fe(III). For this purpose, adsorption studies of Cu(II), Cd(II), and Pb(II) imprinted cryogels for Cu(II), Cd(II), and Pb(II) ions were examined with competitive ions Zn(II), Ca(II), Co(II), Ni(II), and Fe(III) ions. The heavy metal ion solution containing all metal ion species was interacted with four ions imprinted cryogels together. Then, adsorbed metal ions were eluted into separate desorption media. The competitive adsorption capacities and heavy metal enrichment efficiencies of ion imprinted cryogels were calculated from data.

## 4. RESULTS AND DISCUSSION

### 4.1. Characterization of Cryogels

#### 4.1.1. Swelling Characterization of Cryogels

Cryogels which were prepared in this study are cross-linked polymers and have highly porous structures. They are insoluble in aqueous medium and swell while adsorbing water molecules into pores. The amount of water that these cryogel can adsorb depend on their cross-linking density, supermacroporous structure and hydrophilic properties of the polymeric matrix. When ratio of cross-linking is low, hydrocarbon network structure stretches easily and swelling ratio of the hydrocarbon becomes large but when ratio of cross-linking is high, hydrocarbon network structure loses its elasticity, decreases resistance against stretching, constricts the pores and decreases the swelling ratio [180].

$$S_R = (W_s - W_d) / W_d \quad (4.1)$$

where,  $S_R$  is the swelling ratio,  $W_s$  is the mass of swollen cryogels and  $W_d$  is the mass of dry cryogels.

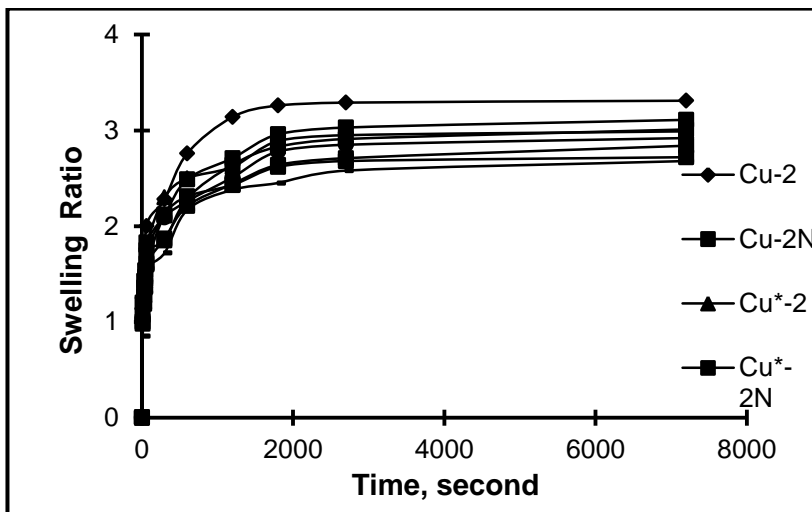


Figure 4.1. Swelling ratio of cryogels (Asterisk superscript is involved for magnetic cryogels). The letter N is incubated for non-imprinted cryogels.

Table 4.1. Swelling ratios of PHEMA cryogels

Time second	Cu-2 w/w%	Cu-2N w/w%	Cu*-2 w/w%	Cu*-2N w/w%	Cd-2 w/w%	Cd-2N w/w%	Pb-2 w/w%	Pb-2N w/w%
0	0	0	0	0	0	0	0	0
10	1.14	1.00	1.32	1.07	1.20	1.03	0.98	0.85
30	1.21	1.36	1.39	1.27	1.43	1.29	1.21	1.13
45	1.36	1.47	1.52	1.45	1.54	1.43	1.37	1.31
60	2.00	1.75	1.81	1.60	1.83	1.75	1.61	1.56
300	2.28	1.85	2.30	2.11	2.12	2.09	1.87	1.72
600	2.76	2.29	2.50	2.31	2.49	2.26	2.21	2.17
1200	3.14	2.64	2.62	2.43	2.71	2.51	2.44	2.38
1800	3.26	2.83	2.89	2.62	2.96	2.78	2.64	2.45
2700	3.29	2.91	2.95	2.68	3.03	2.85	2.71	2.58
7200	3.31	3.01	2.99	2.72	3.11	2.95	2.84	2.69

\* Fe<sub>3</sub>O<sub>4</sub> embedded Cu(II) imprinted magnetic cryogel

In the case of ion-imprinted polymers, the swelling ratio was slightly higher than non-imprinted counterparts due to the additional hydrophilic groups by the bound metal ion-monomer complex.

#### 4.1.2. FTIR Analyses

The FTIR spectra of poly(HEMA-MAH) Cu(II) ion imprinted cryogels are given in Figure 4.2. As shown in Figure 4.2, FTIR spectra of Cu(II) imprinted poly(HEMA-MAH) cryogels have a broad peak at 3200-3600 cm<sup>-1</sup> that consists of several sharp peaks as, the stretching vibration bands of hydrogen bonded alcohol, around 3200 cm<sup>-1</sup>, (-CONH-) around 3300 cm<sup>-1</sup>, and the stretching bonds of vinyl (MAH) around 3400 cm<sup>-1</sup>. Also has characteristic amide I and amide II absorption bands at 1652, and 1532 cm<sup>-1</sup>, respectively, at around 1715 cm<sup>-1</sup> strong carbonyl

stretching vibration, at  $1240\text{ cm}^{-1}$  C-O stretching vibrations, and at  $1152\text{ cm}^{-1}$ , ring vibration were observed.

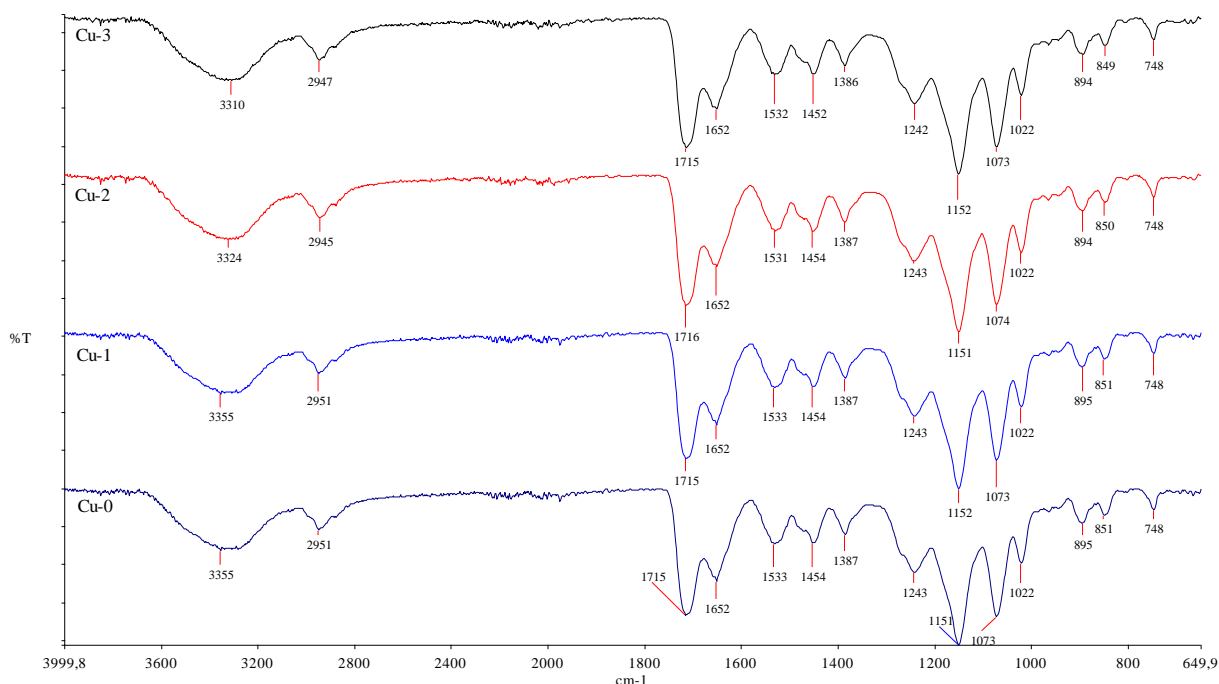


Figure 4.2. FTIR spectra of Cu(II) ion imprinted poly(HEMA-MAH) cryogels.

The FTIR spectra of Cd(II) ion imprinted poly(HEMA-MAC) cryogels are given in Figure 4.3. As shown in the Figure 4.3, FTIR spectra of poly(HEMA-MAC) have a broad peak at  $3200\text{--}3500\text{ cm}^{-1}$  that consists of several sharp peaks as the stretching vibration bands of hydrogen bonded alcohol (HEMA), at around  $3200\text{ cm}^{-1}$ , and (-CONH-) at around  $3300\text{ cm}^{-1}$  (MAC).

The FTIR spectra of Pb(II) ion imprinted poly(HEMA-MAAsp) cryogels are given in Figure 4.4. As shown in the figure, FTIR spectra of poly(HEMA-MAAsp) have a broad peak in  $3200\text{--}3500\text{ cm}^{-1}$ , that consists of several sharp peaks as, the stretching vibration bands of hydrogen bonded alcohol, around  $3200\text{ cm}^{-1}$ , and (-CONH-) around  $3300\text{ cm}^{-1}$  (MAAsp). Also has characteristic amide(I) at  $1653\text{ cm}^{-1}$ , and at  $1716\text{ cm}^{-1}$ , strong carbonyl stretching vibration.

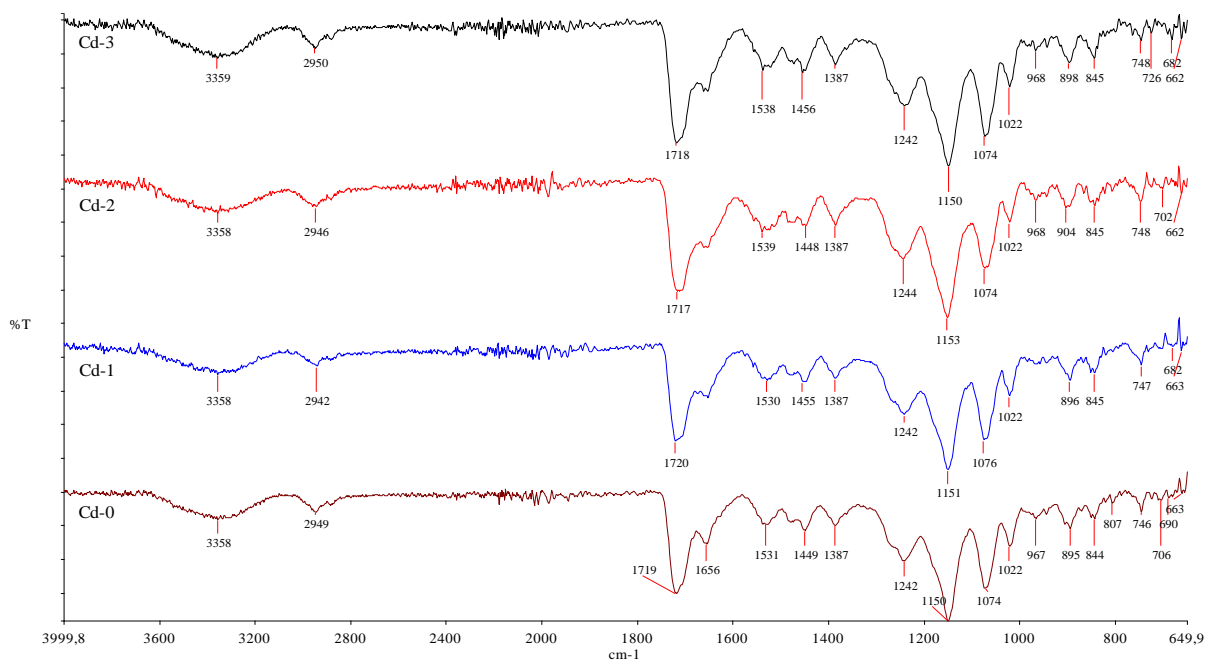


Figure 4.3. FTIR spectra of Cd(II) ion imprinted and non-imprinted poly(HEMA-MAC) cryogels.

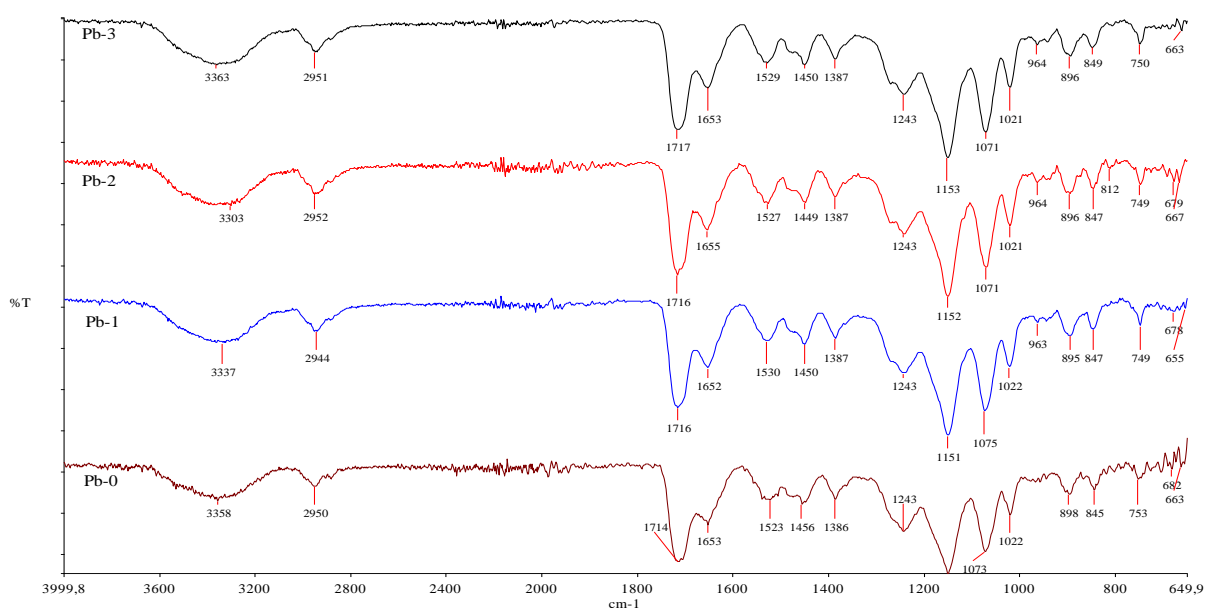


Figure 4.4. FTIR spectra of Pb(II) ion imprinted poly(HEMA-MAAsp) cryogels.

#### 4.1.3. Surface Area Measurements

Surface area is an important parameter in polymers. The specific surface areas of PHEMA based cryogels were determined by a multipoint BET apparatus. Specific surface area, total pore volume and average pore diameter of ion imprinted PHEMA based cryogels are presented in Table 4.2. The sizes of the pores were



determined by BJH and DH methods. The pore diameters changed between 16 Å and 167 Å. Imprinting process increased the surface area of cryogels.

Table 4.2. Surface area measurements (BET) of ion imprinted and non-imprinted cryogels.

Cryogel	Surface area	Total pore volume	Average pore
Code	(m <sup>2</sup> /g)	(cm <sup>3</sup> /g)	Diameter, Å
Cu*-2	106.0	0.05	16.3
Cu*-2N	78.5	0.04	23.9
Cu-2	43.4	0.007	18.8
Cu-2N	18.6	0.011	29.0
Cd-2	92.0	0.05	18.8
Cd-2N	47.0	0.007	33.0
Pb-2	78.5	0.04	23.0
Pb-2N	29.3	0.016	18.0

Specific surface area was determined by multipoint BET and BJH methods.

Total pore volume and average pore diameter were measured by BJH method.

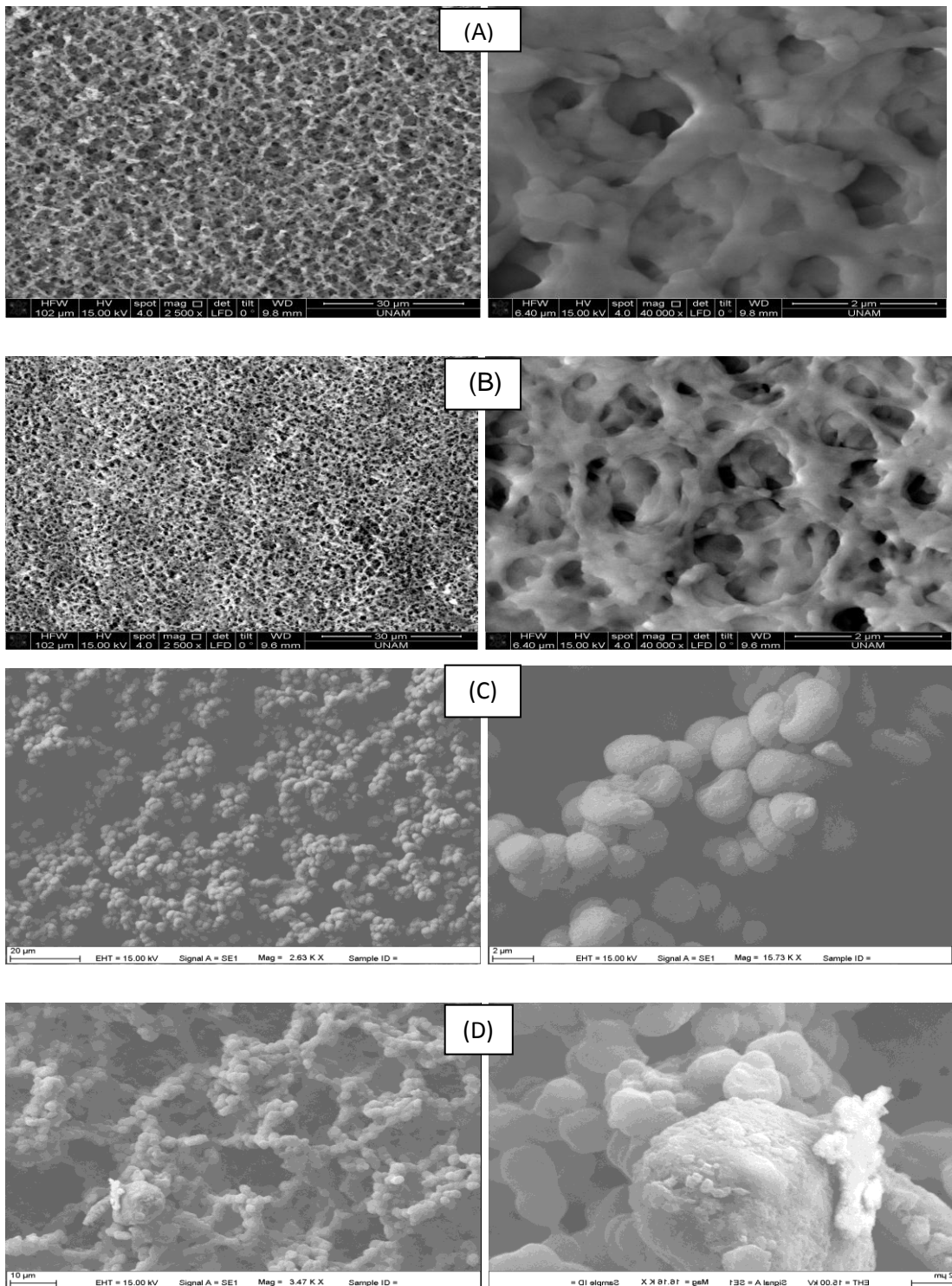


Figure 4.5. SEM photographs of cryogels: (A) Cu(II) ion imprinted; (B) Non-imprinted; (C) Cu(II) ion imprinted magnetic; (D) Non-imprinted magnetic.

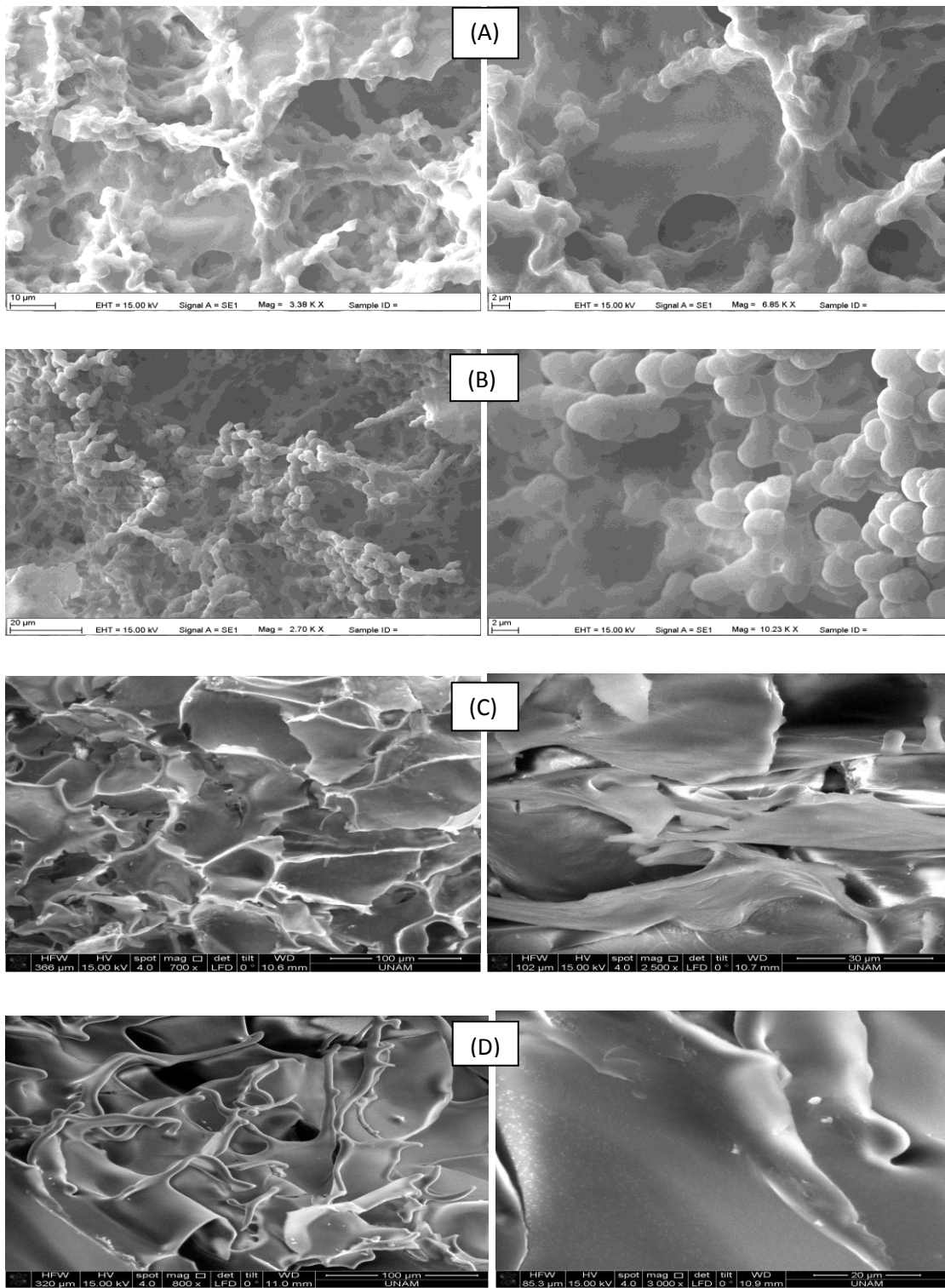


Figure 4.6. SEM photographs of cryogels: (A) Cd(II) ion imprinted; (B) Non-imprinted; (C) Pb(II) ion imprinted; (D) Non-imprinted.

#### 4.1.4. Surface Morphology

The morphology of the ion imprinted and non-imprinted cryogels was examined with scanning electron microscopy (SEM). Figures 4.5 and 4.6 show SEM photographs of ion imprinted and non-imprinted cryogel membranes. These cryogels were composed of interconnected cavities that form a macroporous structure. According to SEM photographs, the size of cavities was roughly determined in the range of 0.4-1.6  $\mu\text{m}$ . Generally, the sizes of cavities of ion imprinted cryogels were larger than non-imprinted cryogels.

#### 4.1.5. X-Ray Analysis (EDX)

Elemental composition of ion imprinted Cu-2, Cd-2 and Pb-2 cryogels was measured by EDX method. The percentages of elements of these cryogels were 4% N, 35% O, 60% C for ion imprinted cryogels and 6% N, 36% O, 56% C for non-imprinted cryogels on a mass basis.

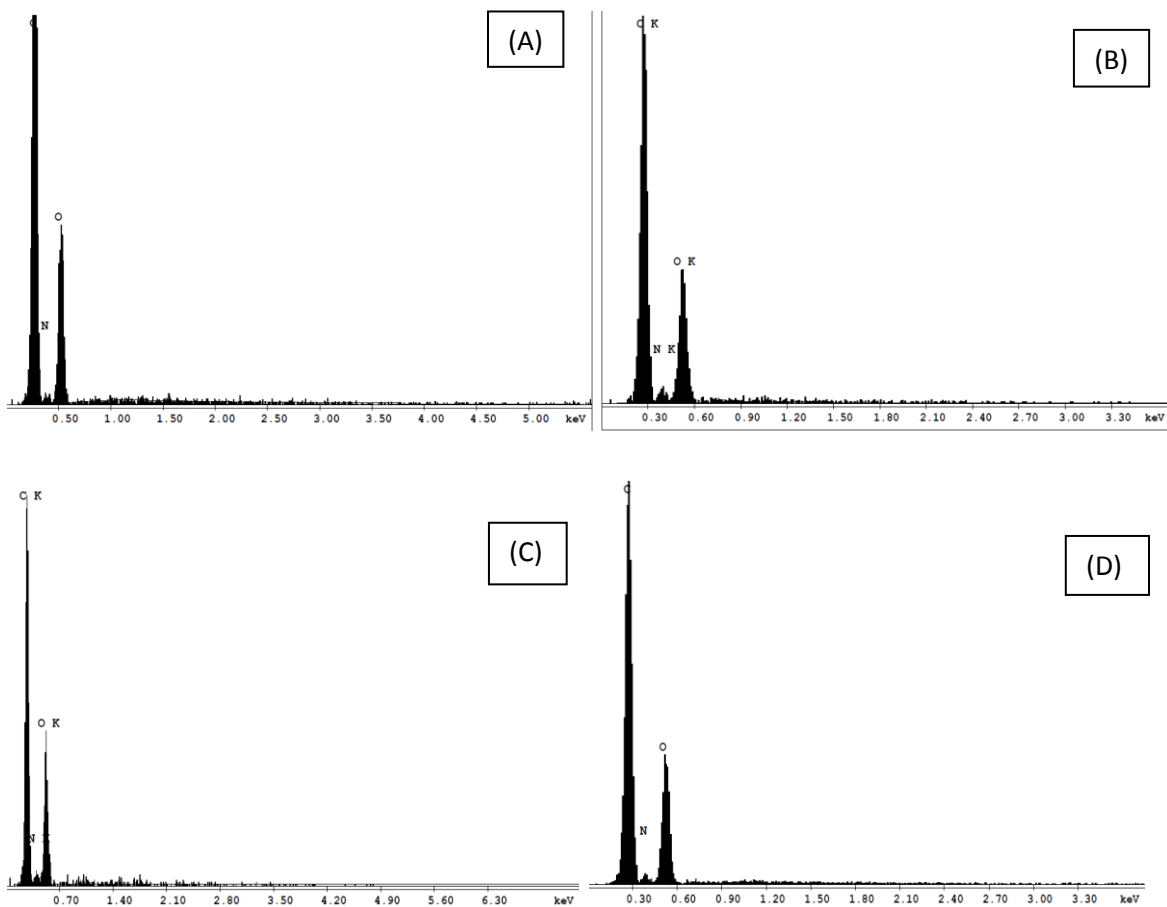


Figure 4.7. EDX spectra of cryogels after desorption of metal ions: (A) Cu(II) imprinted; (B) Cu(II) non-imprinted; (C) Pb(II) imprinted; (D) Pb(II) non-imprinted.

## **4.2. Adsorption Studies with Ion Imprinted Cryogels**

Selective heavy metal removals with molecularly imprinted polymers have been getting very popular in literature recently. The main criteria for this aim are creation of specific cavities by imprinting coordination spheres of targeted metal ions into polymeric networks. By this way, the coordination sphere, ionic radius and chemical affinities of the targeted metal ion have been solidified by crosslinking process during the polymerization applied. Therefore, the polymers could specifically adsorb these metal ions even if multi-metal ion solutions applied. According to these provisions, molecularly imprinted cryogels for selective heavy metal ion removal purposes have been prepared. In this context, three different heavy metal ions [Cu(II), Cd(II), and Pb(II)] have been imprinted into cryogels having different shapes (square, circle with two different diameters). In order to optimize the adsorption conditions for both each heavy metal ion and for each cryogel, the heavy metal ion adsorption studies were performed from singular aqueous solutions of heavy metal ions while varying the effective parameters pH, initial heavy metal ion concentration, temperature, and contact time. In addition, the heavy metal ion removal performances of imprinted and non-imprinted cryogels and magnetic and non-magnetic cryogels have been compared.

### **4.2.1. Effective Parameters on Heavy Metal Adsorption Performances of Molecularly Imprinted Cryogels**

#### **4.2.1.1. Effect of pH**

As mentioned in Materials and Methods Section, amino acid based functional monomers (MAH, MAC, and MAAsp) for coordination of targeted heavy metal ions have been used. As well-known, the complexation reaction between metal ions and functional monomers was influenced by pH of medium. The reason of this behaviour is due to the electrostatic attraction between the surface charge and the dissolved ions in complexation reactions and coordination sphere of the metal ions [181]. Figure 4.8-4.11 show the effect of pH on the adsorption of targeted heavy metal ions [Cu(II), Cd(II), and Pb(II)] by molecularly imprinted cryogel membranes. The adsorption capacities increased with increasing pH values as expected. Optimum pH value was accepted as pH 5.5 for all heavy metal ions. After pH 6.0, the precipitation of heavy metal ions could occur; therefore,

adsorption studies at higher pH values were not conducted. The increase in the adsorption capacities depended on the deprotonation of functional groups found in the amino acid based monomers. Imidazole ring in the MAH monomer, thiol group in MAC and carboxylic acid groups in MAAsp monomers have been deprotonated; so, the increase in pH value enhanced their Lewis base characters. Deprotonation also reduced the possible repulsive interactions between heavy metal ions and protonated (positively charged) groups. The results were reported in accordance with imprinted cryogels and the experimental conditions are given as figure legends. As seen from figures, the amount of pre-polymerization complex included into the polymerization recipe also affected the adsorption capacities, because the amount of imprinted cavities had increased.

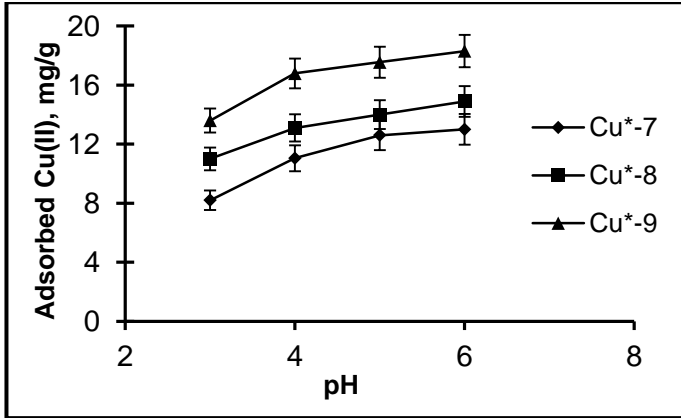
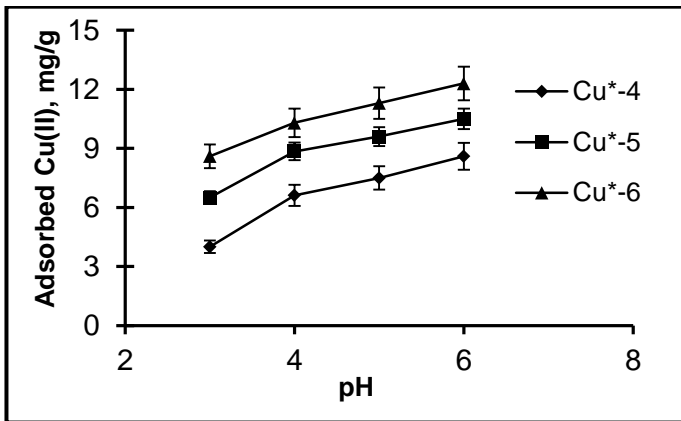
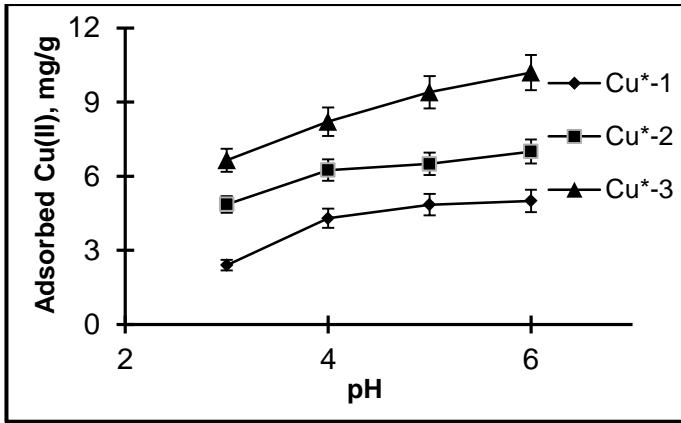


Figure 4.8. The effect of pH on adsorption of Cu(II) by Cu(II) ion imprinted magnetic cryogel membranes. Concentration: 60 mg/L; incubation period: 120 min; and T: 25°C. The capacity values were the averages of three measurements.

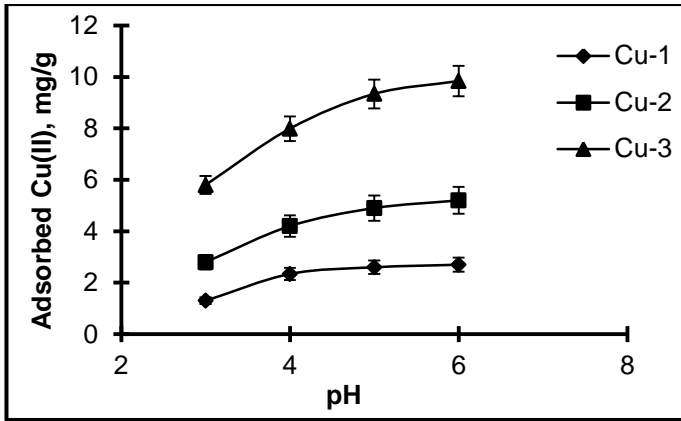


Figure 4.9. The effect of pH on adsorption of Cu(II) by Cu(II)-ion imprinted non-magnetic cryogel membranes; Concentration: 60 ppm; incubation period: 120 min; and T: 25°C. The capacity values were the averages of three measurements.

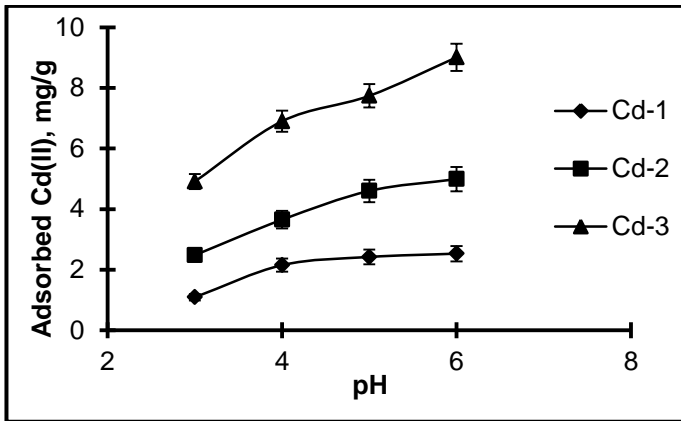


Figure 4.10. The effect of pH on adsorption of Cd(II) by ion imprinted cryogel membranes; Concentration: 60 mg/L; incubation period: 120 min; and T: 25°C. The capacity values were the averages of three measurements.

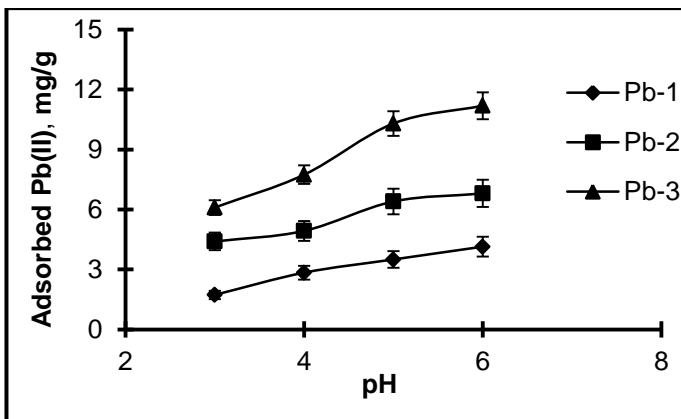


Figure 4.11. The effect of pH on the adsorption of Pb(II) by ion imprinted cryogel membranes; Concentration: 60 mg/L; incubation period: 120 min; T: 25°C. The capacity values were the averages of three measurements.



#### 4.2.1.2. Effect of Initial Concentration

The effect of initial heavy metal ion concentration onto adsorption capacities of cryogels was evaluated for aqueous solutions. The heavy metal ion concentrations were varied between 0-700 mg/L while adjusting pH values to 5.5. Cryogels were interacted with imprinted ions solutions. So, Cu(II) imprinted cryogels were used for Cu(II) adsorption whereas Cd(II) imprinted cryogels were used for Cd(II) adsorption and Pb(II) imprinted cryogels were used for Pb(II) adsorption studies. The results were given in Figures 4.12-15 in accordance with cryogel sub-types. For all cryogels, the adsorption capacities increased with increasing initial heavy metal concentration. The results depend on the driving force for adsorption process that was concentration difference between solution and solid phases. The increase in heavy metal ion concentration causes the increase in the forces driving adsorption process. Initially, the adsorption capacity increased linearly with an increase in initial metal ion concentration. Then, those declined to reach plateau values due to the saturation of active binding sites for targeted heavy metal ions. Figure 4.12 shows the results obtained for magnetic Cu(II) imprinted cryogels. Adsorption capacities of magnetic ion imprinted cryogels for Cu\*-1, Cu\*-2, Cu\*-3, Cu\*-3, Cu\*-4, Cu\*-5, Cu\*-6, Cu\*-7, Cu\*-8, and Cu\*-9 were 35.4, 73.4, 97.9, 59.5, 101.3, 132.7, 82.8, 122.8, and 182.7 mg/g, respectively. Figure 4.13 shows the results obtained for Cu(II) imprinted non-magnetic cryogels. Adsorption capacities of those cryogels for Cu-1, Cu-2, and Cu-3 were 31.3, 58.3, and 77.19 mg/g, respectively. Figure 4.14 shows the results obtained for Cd(II) imprinted cryogels. Adsorption capacities of those cryogels for Cd-1, Cd-2, and Cd-3 were 44.5, 65.3, and 86.7 mg/g, respectively. Figure 4.15 shows the results obtained for Pb(II) imprinted cryogels. Adsorption capacities of those cryogels for Pb-1, Pb-2, and Pb-3 were 41.9, 86.3, and 122.7 mg/g, respectively. Cu(II) adsorption capacities for both magnetic and non-magnetic cryogels were directly effected by amount of pre-polymerization complex [MAH-Cu(II) complexes] and magnetite ( $\text{Fe}_3\text{O}_4$ ) nanoparticles. The increase in their amounts caused the increase for the adsorption capacities. The similar results for Cd(II) and Pb(II) imprinted cryogels were obtained. By increasing the amount of MAC-Cd(II) complex imprinted from 0.05 mmol to 0.20 mmol, the adsorption capacities increased from 44.5 mg/g to 86.7 mg/g. Similarly, the adsorption capacities for

Pb(II) ions increased from 41.9 mg/g to 122.7 mg/g with respect to an increase in pre-polymerization complex [MAAsp-Pb(II)] from 0.05 mmol to 0.20 mmol. Increasing the amount of pre-polymerization complex in synthesis, the amount of imprinted target ion increased causing an increase in number of imprinted cavities. Therefore, the increasing number of recognition sites caused the higher adsorption capacity as expected.

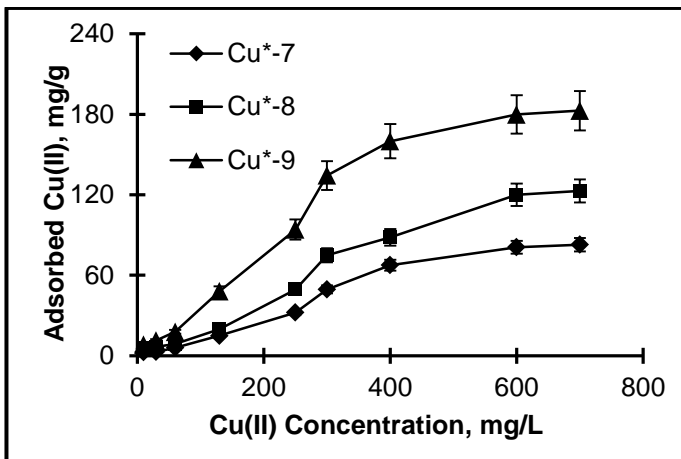
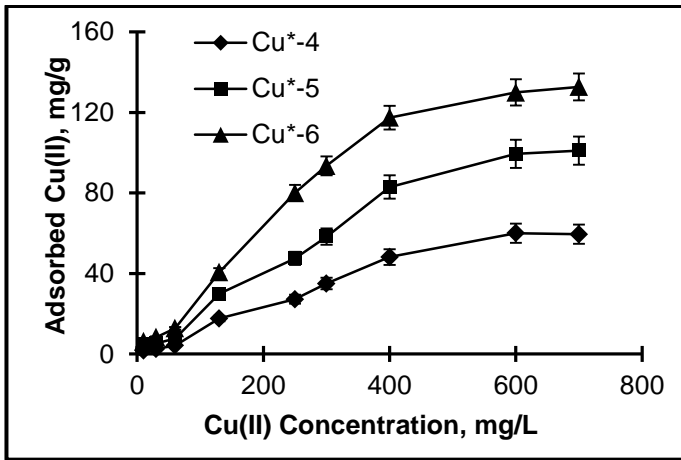
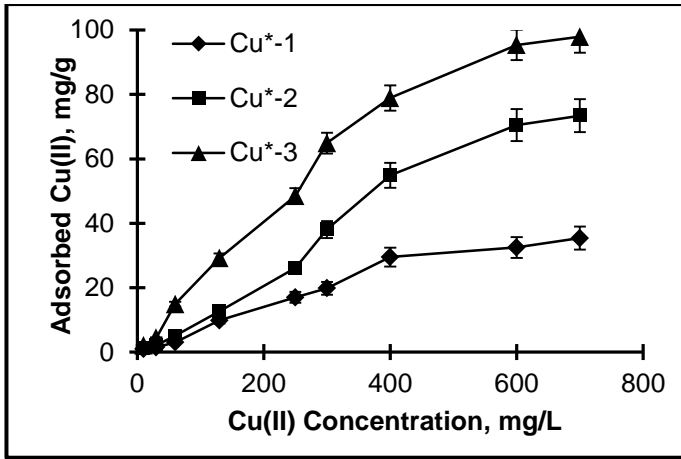


Figure 4.12. The effect of initial concentration on adsorption of Cu(II) by ion-imprinted magnetic cryogel membranes; pH: 5.5; incubation period: 120 min and T: 25°C. The capacity values were the averages of three measurements.

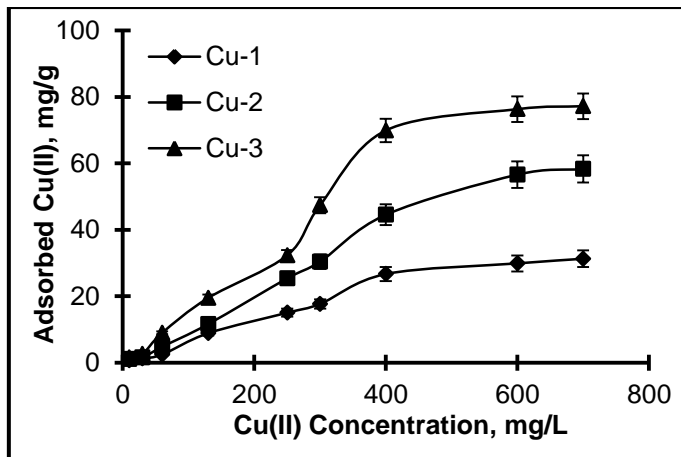


Figure 4.13. The effect of initial concentration on adsorption of Cu(II) by ion imprinted non-magnetic cryogel membranes; pH: 5.5; incubation period: 120 min and T: 25°C. The capacity values were the averages of three measurements.

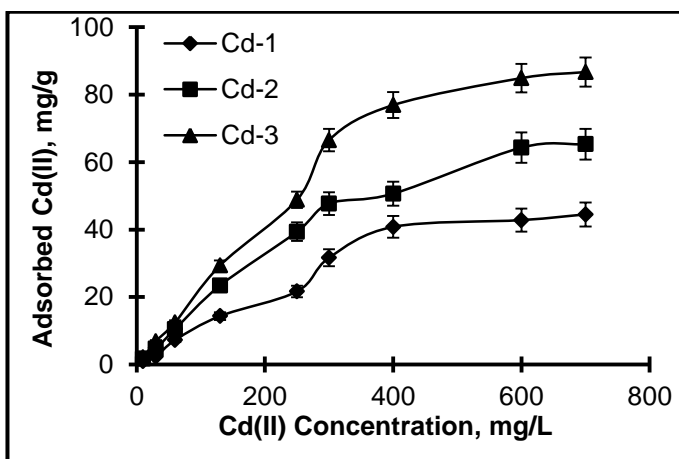


Figure 4.14. The effect of initial concentration on the adsorption of Cd(II) by ion-imprinted cryogel membranes; pH: 5.5; incubation period: 120 min; and T: 25°C. The capacity values were the averages of three measurements.

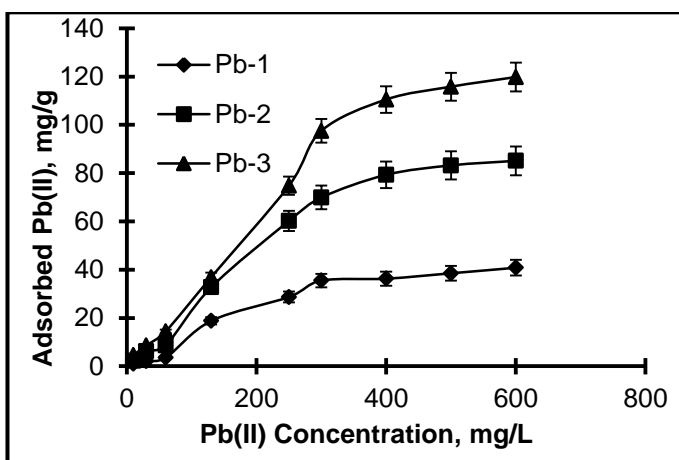


Figure 4.15. The effect of initial concentration in adsorption of Pb(II) by ion-imprinted cryogel membranes, pH: 5.5; incubation period: 120 min; and T: 25°C. The capacity values were the averages of three measurements.

#### **4.2.1.3. Effect of Temperature**

In order to calculate thermodynamic variables and to describe the adsorption process, the effect of temperature on heavy metal ion adsorption was also evaluated. Temperature of the original heavy metal ion solution was varied in the range of 5°C - 40°C. The results showed that the adsorption capacities decreased with an increase in the temperature for all cryogel sub-types. The results depend on the nature of the interaction between functional monomers (MAH, MAC, and MAAsp) and template heavy metal ions [Cu(II), Cd(II), and Pb(II)]. As mentioned in the experimental section, the functional monomers were polymerizable derivatives of some amino acids such as histidine, cysteine, and aspartic acid. So, they formed co-ordinated covalent bonds with target metal ions during pre-polymer complex formation process. These bonds (dative bonds) have electrostatic nature and getting weaker by increasing temperature because of disturbing coordination spheres of heavy metal ions. Figures 4.16-4.18 show the adsorption capacities of Cu(II) imprinted magnetic cryogels with respect to both temperature and initial Cu(II) ion concentration. As shown from these figures, the adsorption capacities decreased with increasing temperature for all different initial Cu(II) ion concentrations.

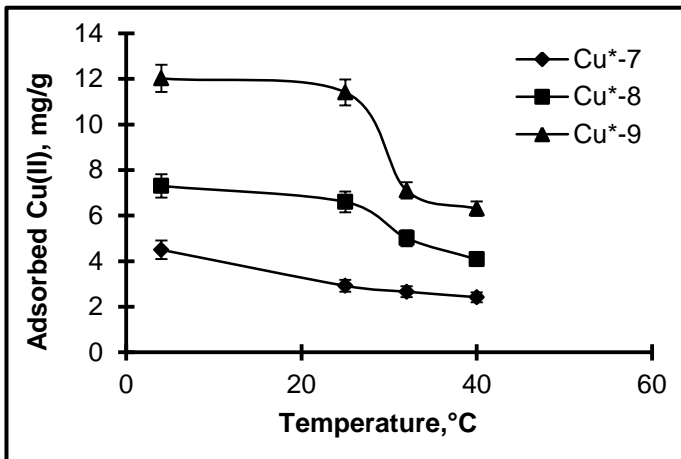
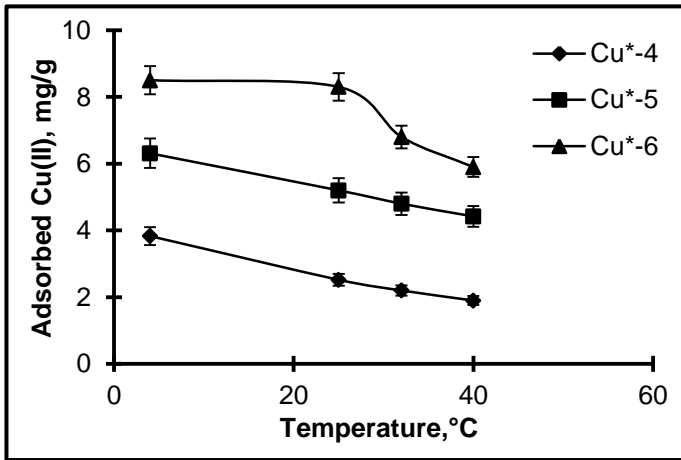
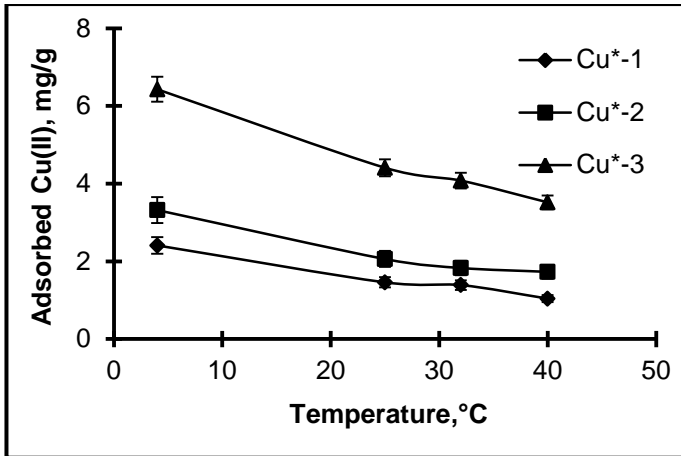


Figure 4.16. The effect of temperature on adsorption of Cu(II) by ion-imprinted magnetic cryogel membranes; Concentration: 30 ppm; pH: 5.5 and incubation period: 120 min. The capacity values were the averages of three measurements.

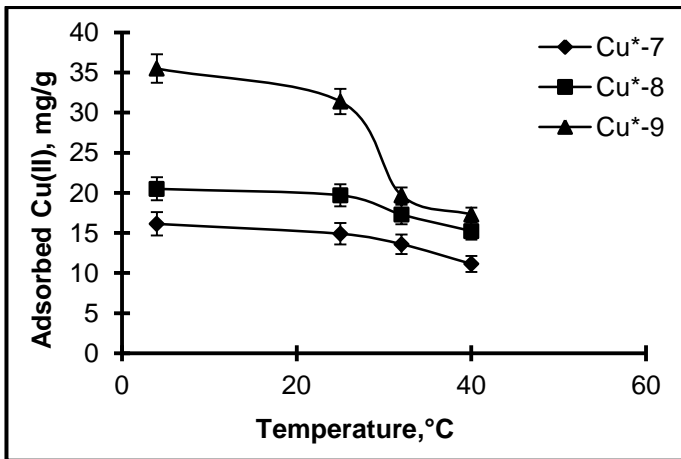
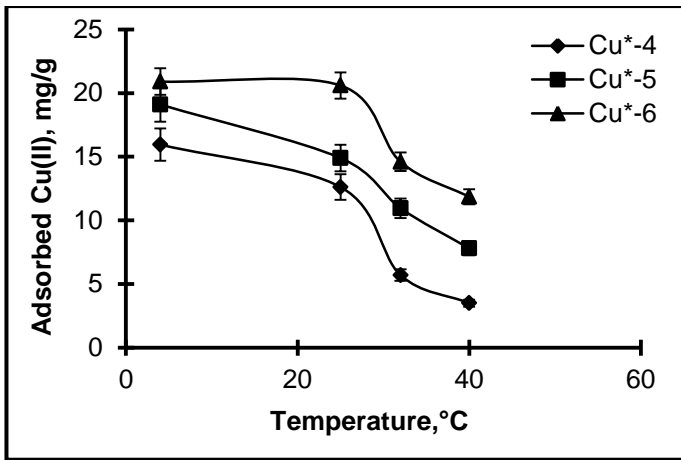
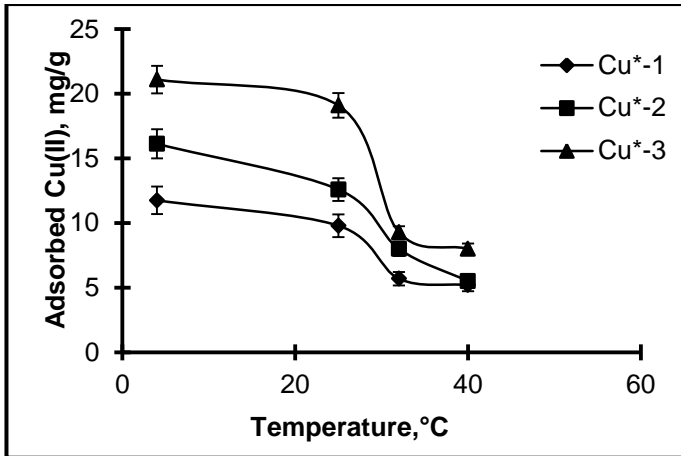


Figure 4.17. The effect of temperature on adsorption of Cu(II) by ion-imprinted magnetic cryogel membranes; Concentration: 130 ppm; pH: 5.5 and incubation period: 120 min. The capacity values were the averages of three measurements.

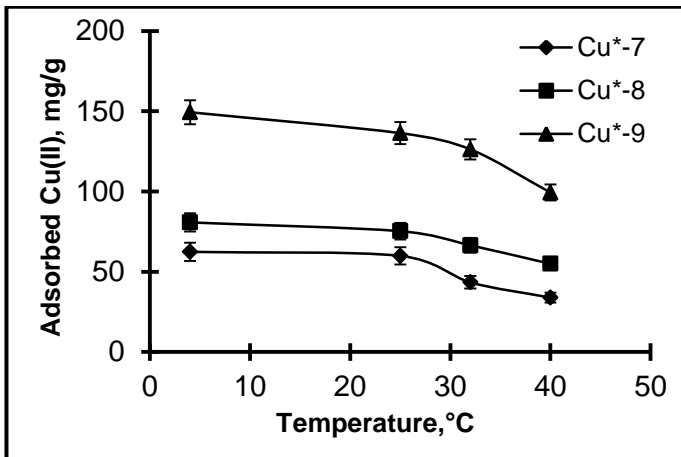
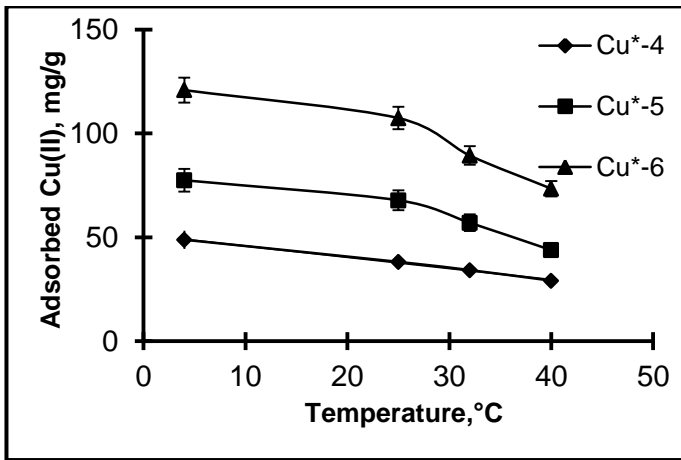
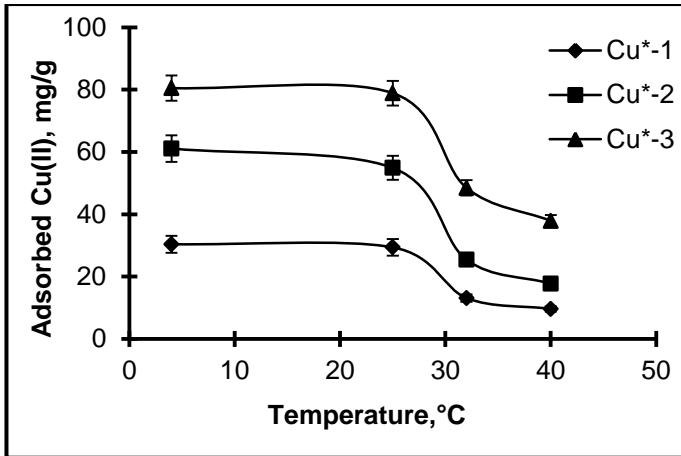


Figure 4.18. The effect of temperature on adsorption of Cu(II) by ion-imprinted magnetic cryogel membranes; Concentration: 400 ppm; pH: 5.5 and incubation period: 120 min. The capacity values were the averages of three measurements.



For magnetic cryogels the temperature dependence, Cu(II) adsorption capacity dependency on the temperature was given in Figure 4.19. As shown from figures, maximum adsorption capacity, 77.5 mg/g for Cu(II) ion was obtained at 4°C and for 400 mg/L concentration. The results for Cd(II) and Pb(II) imprinted cryogels were given in Figures 4.20 and 4.21, respectively. As shown from these figures, the maximum adsorption capacities were obtained at the lowest temperature (4°C) and highest initial heavy metal ion concentration (400 mg/L) as expected. These values for Cd(II) and Pb(II) imprinted cryogels were 92.8 mg/g and 106.1 mg/g, respectively.

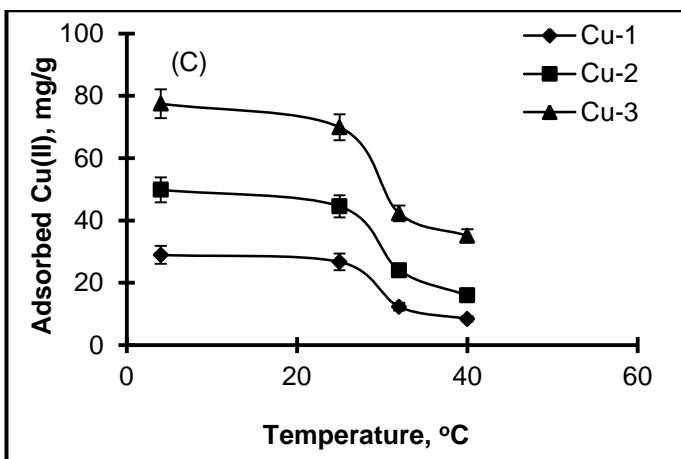
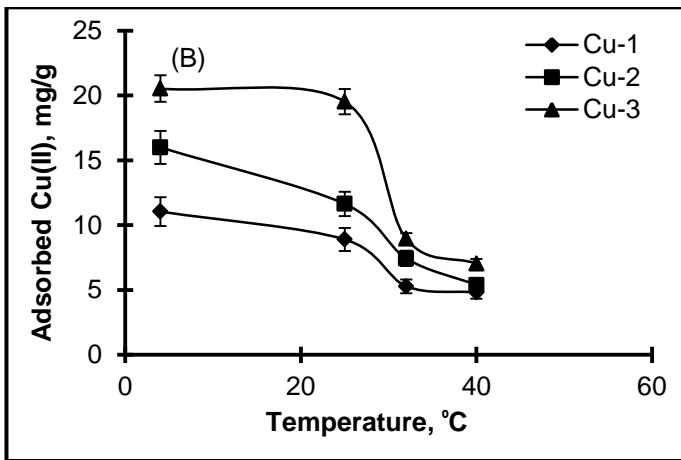
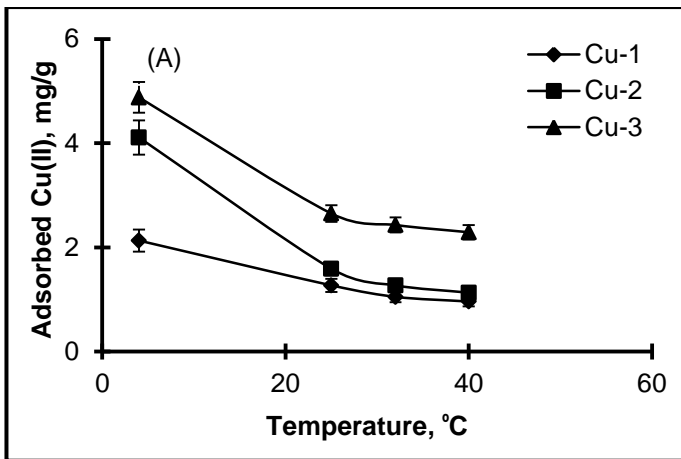


Figure 4.19. Effect of temperature on the adsorption of Cu(II) by Cu(II) ion imprinted non-magnetic cryogel membranes; pH: 5.5; incubation period: 120 min; and concentration (A): 30 ppm, (B): 130 ppm and (C): 400 ppm. The capacity values were the averages of three measurements.

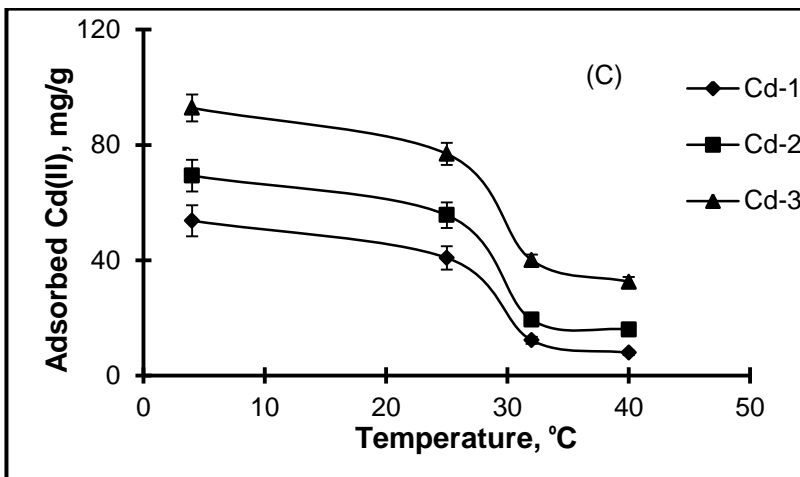
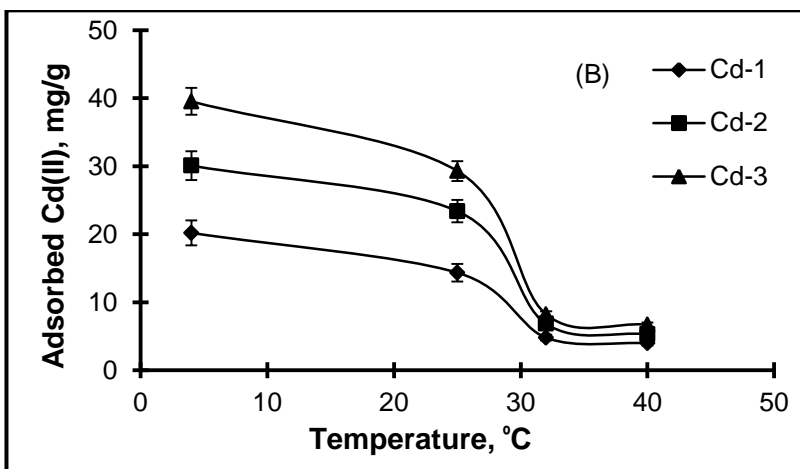
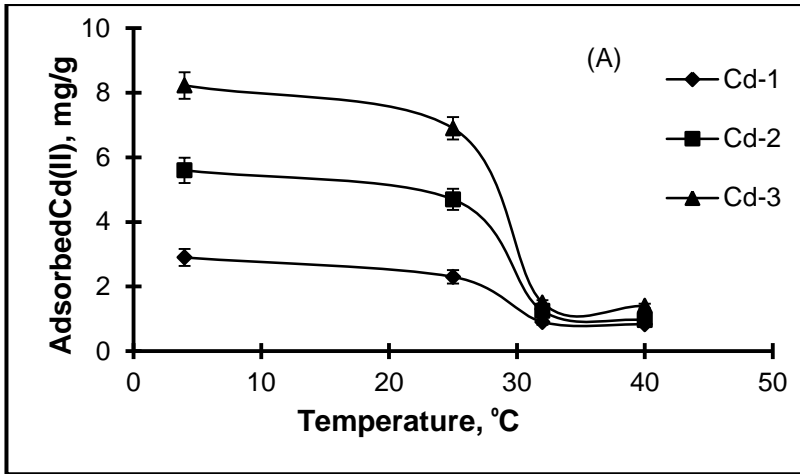


Figure 4.20. The effect of temperature on the adsorption of Cd(II) by ion imprinted cryogel membranes; pH: 5.5; incubation period: 120 min; and concentration (A): 30 ppm; (B): 130 ppm; (C): 400 ppm. The capacity values were the averages of three measurements.

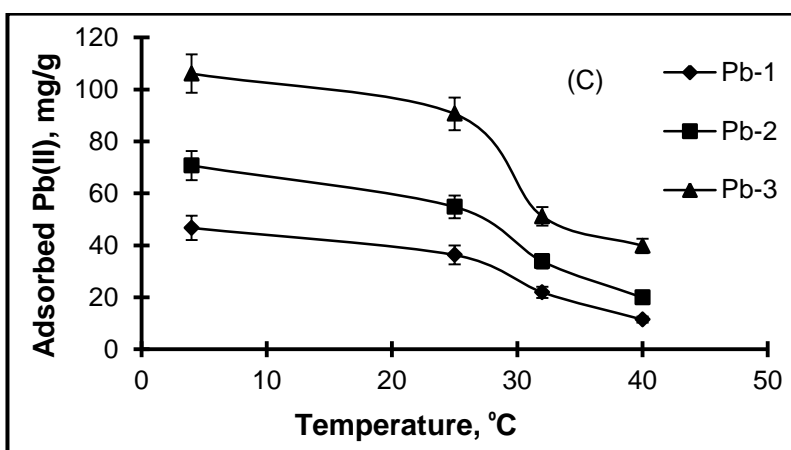
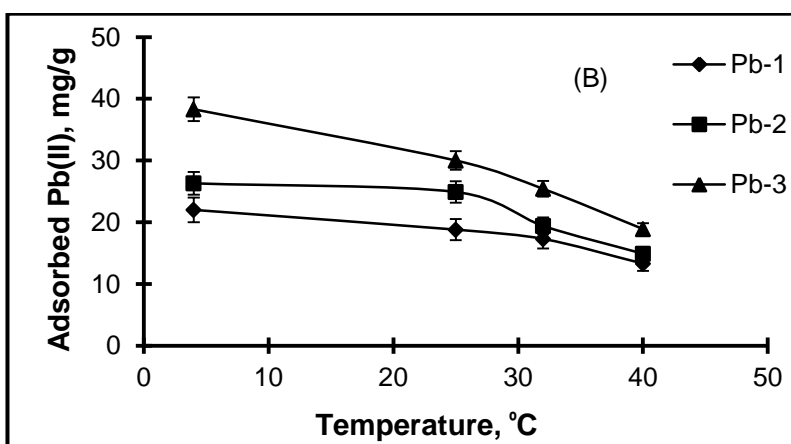
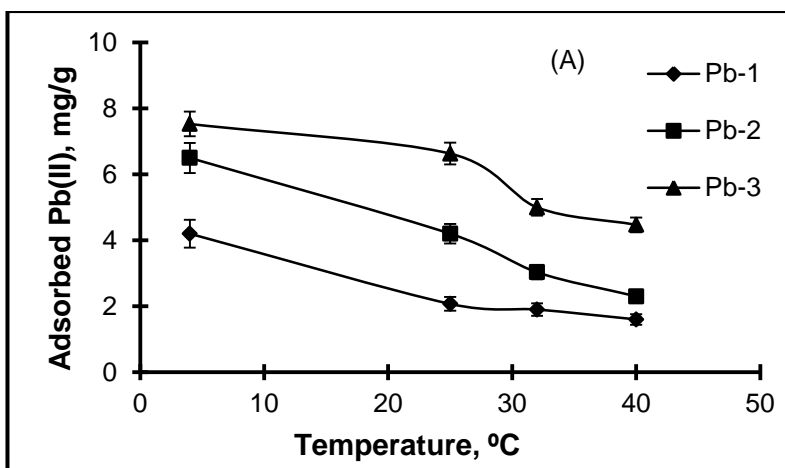


Figure 4.21. The effect of temperature on the adsorption of Pb(II) by ion imprinted cryogel membranes; pH: 5.5; incubation period: 120 min; and concentration (A): 30 ppm; (B): 130 ppm; (C): 400 ppm. The capacity values were the averages of three measurements.

#### 4.2.1.4. Effect of Contact Time

Cryogels have supermacroporous structure which enhances diffusion of solvent into pores and makes easier adsorption process. Also, this property makes possible to study with viscous solutions such as wastewater including heavy metal ions. In the light of these provisions, effect of contact time on adsorption capacity for heavy metal ion solutions with ion imprinted cryogels was examined. The samples were collected from adsorption media in appropriate time intervals to determine instant adsorption capacity. The results for all cryogels sub-types were similar. At the beginning of adsorption period, the adsorption capacities increased drastically with respect to time. Within this period, the adsorption capacities were directly proportional to contact time. Then, the adsorption capacities started to decline up to 45 min and reached to a constant value at about 90 min. Beyond 90 min., the adsorption capacities did not change significantly. The time required to reach equilibrium for the heavy metal adsorption processes depends on different parameters including stirring rate, amount of adsorbent, initial heavy metal ion concentration, structural properties of sorbent (size, porosity, surface area, etc.), the properties of metal ions, initial concentration of metal ions, pH, temperature, affinity of the metal ion to the functional groups in the structure of the sorbent, the number of active centers which metal ions can be connected and the presence of other ions which compete this metal ion. In addition, three main steps for adsorption were movement of analyte molecules through the pores, diffusion of them into pores, and interaction with recognition site (ion imprinted cavities and functional groups of functional monomers). The equilibrium time is required for completion of these steps. As conclusion, the heavy metal adsorption onto ion imprinted cryogels is the one of the kinetic controlled processes as expected and equilibrium adsorption could be achieved in about 60 min which was relatively fast for adsorption. The results for Cu(II) imprinted magnetic and non-magnetic, Cd(II) imprinted, and Pb(II) imprinted cryogels were given in Figures 4.22-4.25, respectively. The experimental conditions are given as figure legends. Adsorption capacities depend on the pre-polymerization

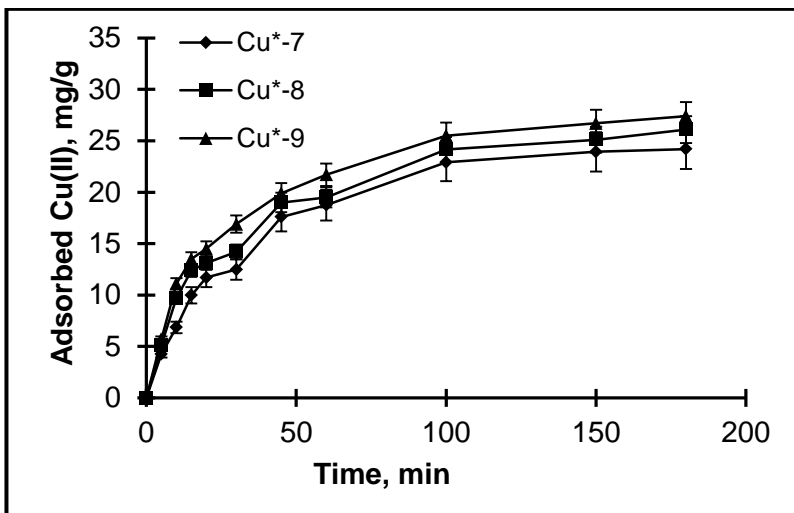
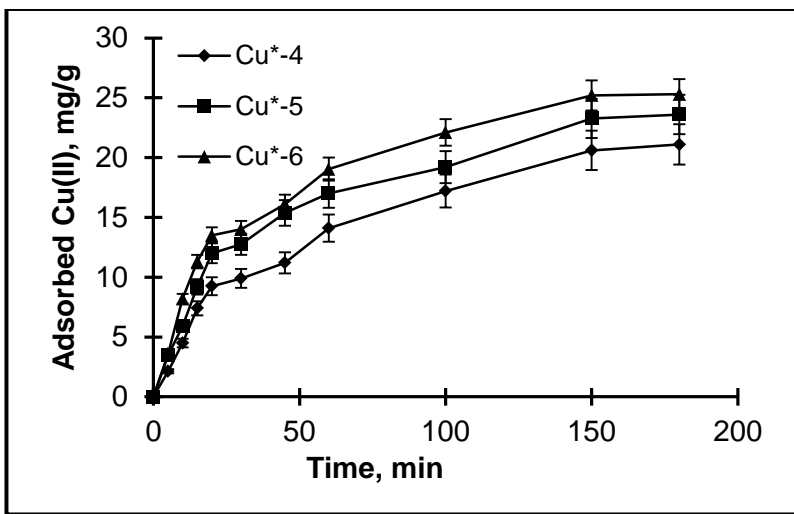
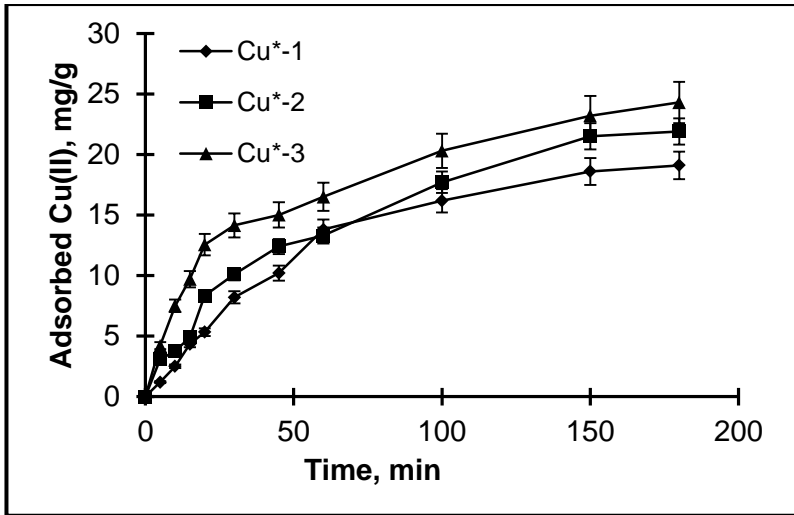


Figure 4.22. The effect of contact time on adsorption of Cu(II) by ion-imprinted magnetic cryogel membranes; Concentration: 60 ppm; pH: 5.5; and T: 25°C. The capacity values were the averages of three measurements.

complexes imprinted as discussed before and varied with time similarly for all cryogel sub-types.

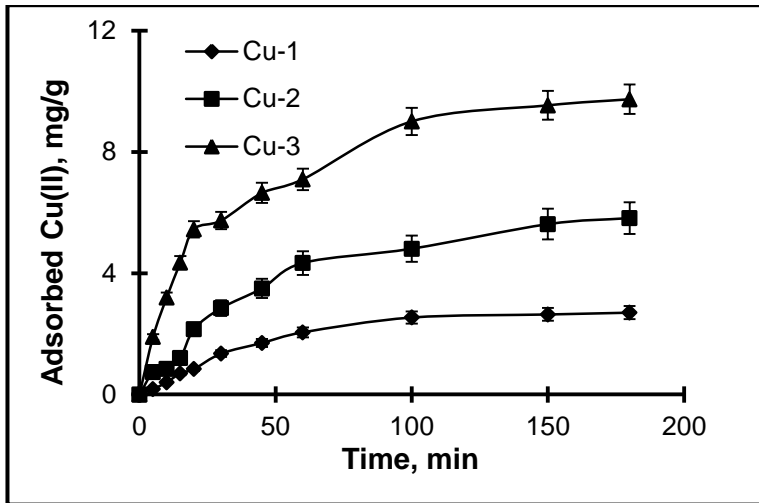


Figure 4.23. The effect of contact time on adsorption of Cu(II) by ion imprinted non-magnetic cryogel membranes; Concentration: 60 ppm; pH: 5.5 and T: 25°C. The capacity values were the averages of three measurements.

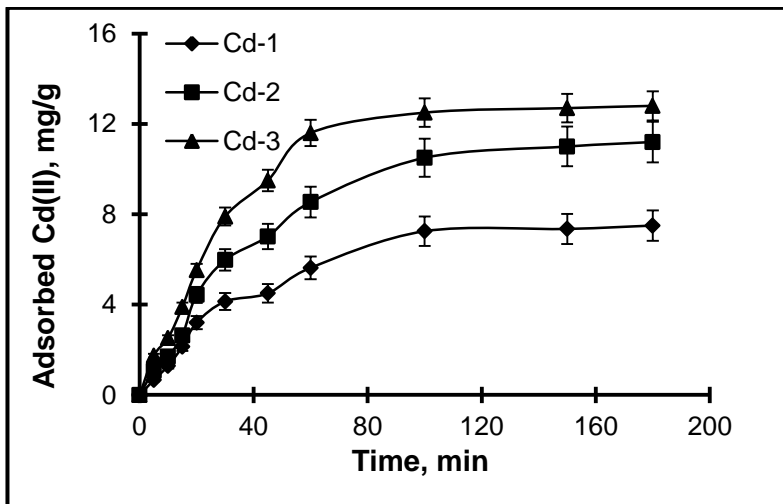


Figure 4.24. The effect of contact time on the adsorption of Cd(II) by ion imprinted cryogel membranes; Concentration: 60 ppm; pH: 5.5 and T: 25°C. The capacity values were the averages of three measurements.

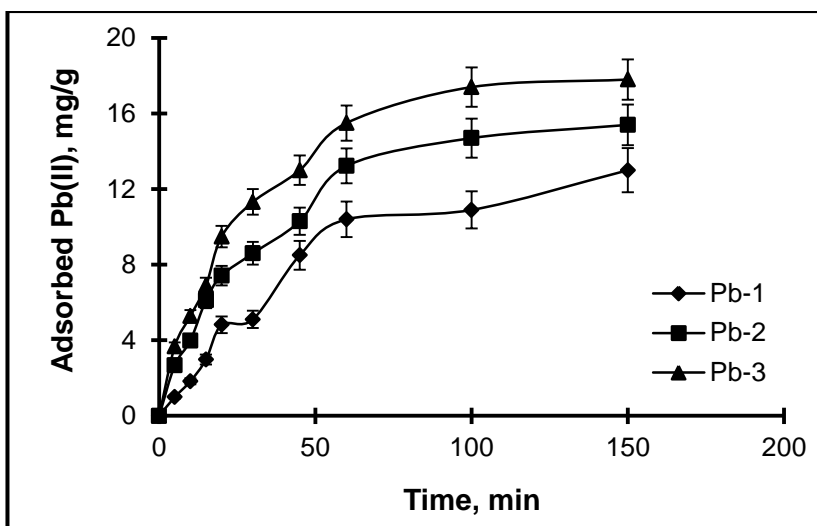


Figure 4.25. The effect of contact time for adsorption of Pb(II) by ion imprinted cryogels; Concentration: 60 ppm; pH: 5.5; incubation period: 120 min; and T: 25°C. The capacity values were the averages of three measurements.

#### 4.2.1.5. Adsorption Isotherms

Adsorption continues until achieving a balance between concentration of accumulated adsorbate on the surface of adsorbent and concentration of adsorbate in solution. Adsorption is usually described by isotherms. Adsorption isotherm is a curve that defines the amount of adsorbate on the adsorbent as a function of its concentration at constant temperature. The most common isotherms for describing adsorption process are Freundlich and Langmuir isotherms [25,26]. The adsorption mechanism can be defined by physicochemical parameters, thermodynamic assumptions, surface properties and the degree of affinity of the adsorbents [182]. Over the years another equilibrium isotherm models such as, Tempkin, Brunauer–Emmett–Teller, Redlich–Peterson, Dubinin–Radushkevich and Flory–Huggins have been formulated.



#### 4.2.1.5.1. Langmuir Isotherm

Langmuir isotherm is based on three assumptions:

- Adsorption is monolayer (the adsorbed layer is one molecule in thickness).
- Adsorption sites are homogeneous, which each molecule possesses constant enthalpies and sorption activation energy, these values are equal for all adsorbed molecules and all sites possess equal affinity for the adsorbate.
- Adsorption of a molecule in a specific site is independent of the other molecules [25].

The Langmuir equation is expressed as:

$$Q = Q_{\max} \cdot b \cdot C_{\text{eq}} / (1 + b C_{\text{eq}}) \quad (4.1)$$

where

$Q_{\max}$  (mg/g) is the theoretical maximum amount of the adsorbate per unit weight of the adsorbent to form a complete monolayer on the surface

$b$  (mL/mg): Langmuir constant related to the affinity of the binding sites

$C_{\text{eq}}$ (mg/mL): amount of adsorbate which remains in solution after adsorption

$Q$ (mg/g): The amount of adsorbate which is adsorbed on the adsorbent

The linear form of Langmuir isotherm is as follows:

$$1/Q = 1/(Q_{\max} \cdot b \cdot C_{\text{eq}}) + 1/Q_{\max} \quad (4.2)$$

The plot of  $1/Q$  versus  $1/C_{\text{eq}}$  gives  $1/Q_{\max}$  as intercept and  $1/(Q_{\max} \cdot b)$  as slope [183].

The essential characteristics of Langmuir isotherm can be expressed by a dimensionless constant called separation factor or equilibrium parameter,  $R_L$ , defined by Weber and Chakkravortias [184]:

$$R_L = 1 / (1 + b \cdot C_{\text{eq}}) \quad (4.3)$$

where  $b$  (L/mg) refers to the Langmuir constant and  $C_{\text{eq}}$  is referred to the adsorbate equilibrium concentration (mg/L).  $R_L$  value indicates the adsorption

nature and this is unfavorable when ( $R_L > 1$ ), linear ( $R_L = 1$ ), favorable ( $0 < R_L < 1$ ) or irreversible ( $R_L = 0$ ).

#### 4.2.1.5.2. Freundlich Isotherm

This model is the earliest model which is based on sorption on a heterogeneous layer of a surface. Binding sites have different affinities to adsorbates; therefore first the sites which form stronger binding sites and then the other sites with lower affinity are occupied. This empirical model can be applied to multilayer adsorption and not restricted to be monolayer [26].

Freundlich model can be expressed by the following equation [182-185]

$$Q_{eq} = K_F \cdot C_{eq}^{1/n} \quad (4.4)$$

where

$K_F$ : Freundlich adsorption coefficient

$C_{eq}$  (mg/L): Amount of adsorbate which remains in solution after adsorption

$Q_{eq}$  (mg/g): The amount of adsorbate which is adsorbed on the adsorbent

$n$ : The characteristic coefficient of the Freundlich isotherm

Linear form of Freundlich isotherm is as follows:

$$\ln Q_{eq} = \ln K_F + (1/n) \cdot \ln C_{eq} \quad (4.5)$$

The plot of  $\ln Q_{eq}$  versus  $\ln C_{eq}$  gives  $\ln K_F$  as intercept and  $1/n$  as slope.

$K_F$  and  $1/n$  are Freundlich coefficients which indicate adsorption capacity and intensity, respectively.  $1/n$  is factor of heterogeneity and values are in the range of 0-1. When  $0 < 1/n < 1$ , the adsorption is favorable; when  $1/n = 1$ , the adsorption is irreversible; and when  $1/n > 1$ , the adsorption is unfavorable. Adsorption becomes more heterogeneous as its value gets closer to zero. A value for  $1/n$  above one indicates a cooperative adsorption.

Langmuir and Freundlich isotherms were applied for four cryogel sub-types and the curves were given in Figures 4.28-4.33 and the calculated parameters were summarized in Tables 4.3-4.6. The results for Cu(II) imprinted magnetic cryogels

were shown in Figures 4.26 and 4.27. The results were shown in Figures 4.28 and 4.29 for Cu(II) imprinted non-magnetic cryogels, for Cd(II) imprinted cryogels in Figures 4.30 and 4.31, and in Figures 4.32 and 4.33 for Pb(II) imprinted cryogels. The parameters calculated from those curves were summarized in Tables 4.3-4.6 for Cu(II) imprinted magnetic, Cu(II) imprinted non-magnetic, Cd(II) imprinted, and Pb(II) imprinted cryogels respectively. As seen from those figures, the adsorption processes well-fitted to Langmuir isotherm with respect to correlation coefficient ( $R^2$ ) values. That means heavy metal ion adsorption onto ion imprinted cryogels was monolayer coverage, the recognition sites (ion imprinted cavities) were homogeneously distributed and energetically equivalent. In addition, target metal ions did not choose the cavities randomly and not interact with other metal ions remained in the solution phase as expected.  $R_L$  values calculated for all cryogel sub-types were between 0 and 1 indicating the favorability of the heavy metal ion adsorption onto imprinted cryogels. The closeness between experimental adsorption capacities and those calculated from Langmuir models shows the correlation of results with Langmuir model and indicates that adsorption process occurred without any diffusion restrictions and steric hindrances. The  $1/n$  values calculated from Freundlich isotherms also support these results because their values were highly close to 1, meaning that the homogeneous monolayer coverage occurred. As conclusion, Langmuir isotherm was a better model than Freundlich isotherm to describe the heavy metal ion adsorption onto all ion imprinted cryogels.

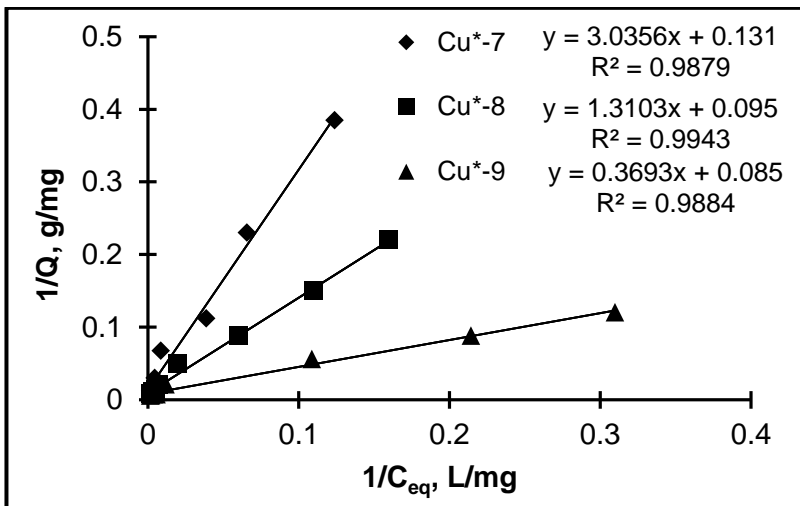
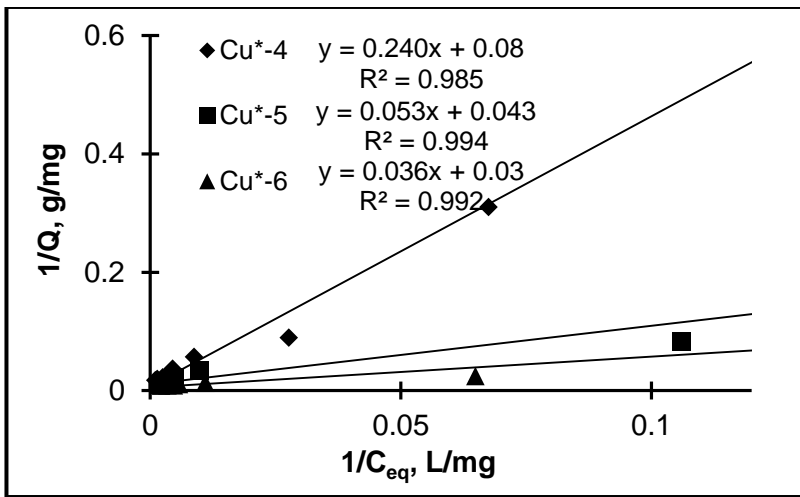
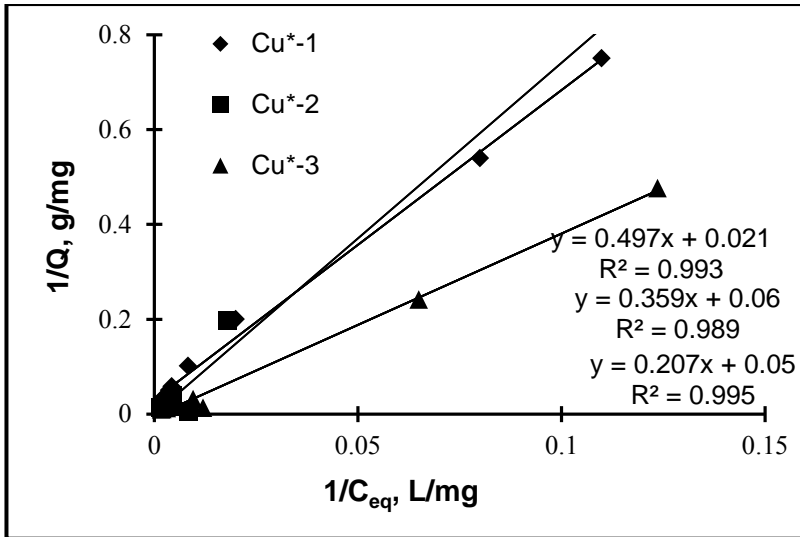


Figure 4.26. Langmuir isotherm model for adsorption of Cu(II) by ion imprinted magnetic cryogel membranes.

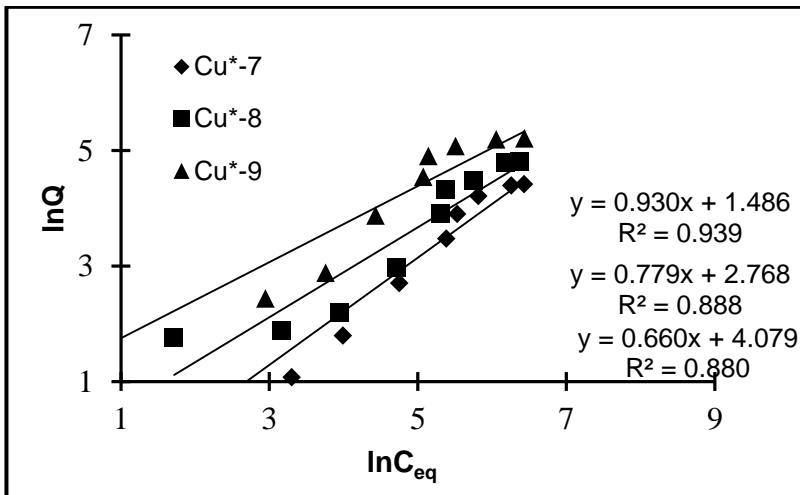
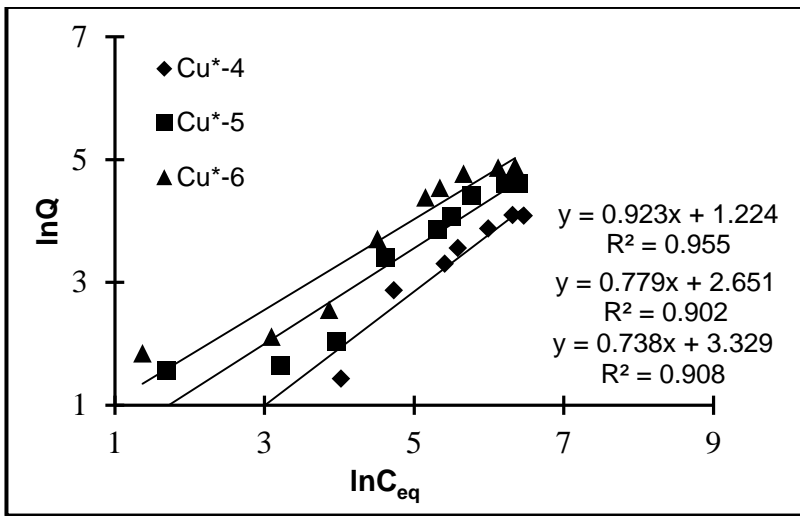
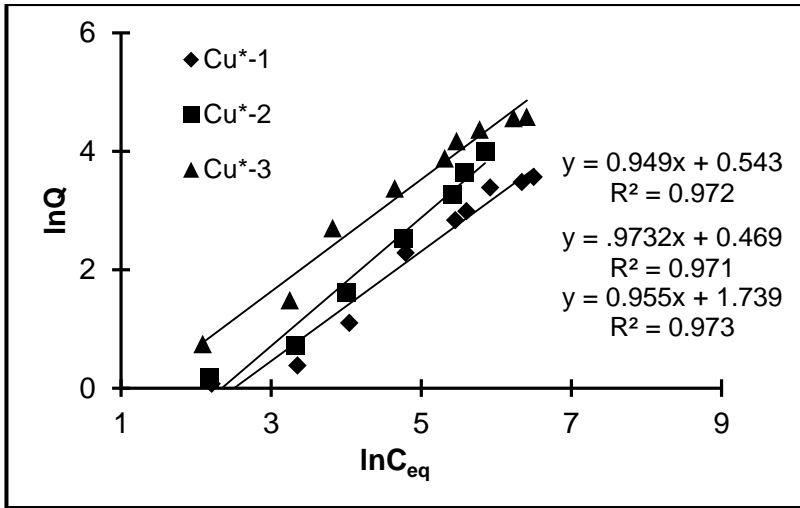


Figure 4.27. Freundlich isotherm model for adsorption of Cu(II) by ion imprinted magnetic cryogel membranes.

Table 4.3. Langmuir and Freundlich models parameters for adsorption of Cu(II) by ion imprinted magnetic cryogels.

Cryogel Codes	$Q_{exp}$ , mg/g	Langmuir			Freundlich			
		$Q_{max}$ , mg/g	b, L/mg $\times 10^{-4}$	$R^2$	$R_L$	$K_F$	1/n	$R^2$
Cu*-1	35.4	38.3	4.9	0.993	0.75	1.72	0.95	0.949
Cu*-2	73.7	81.8	2.1	0.989	0.88	1.56	0.97	0.972
Cu*-3	97.9	106.3	1	0.996	0.94	5.69	0.95	0.973
Cu*-4	59.5	68.7	1.92	0.985	0.89	3.4	0.923	0.955
Cu*-5	105.0	109.7	2.3	0.994	0.98	14.17	0.78	0.902
Cu*-6	132.7	139.1	1.1	0.992	0.99	27.91	0.74	0.908
Cu*-7	82.8	91.2	0.9	0.990	0.95	4.41	0.93	0.939
Cu*-8	122.8	134.7	0.2	0.987	0.98	15.92	0.79	0.888
Cu*-9	178.7	189.6	0.04	0.971	0.99	59.08	0.66	0.880

exp, experimental

Table 4.4. Langmuir and Freundlich models parameters for adsorption of Cu(II) by ion imprinted non-magnetic cryogels.

Cryogel Codes	$Q_{exp}$ , mg/g	Langmuir			Freundlich			
		$Q_{max}$ , mg/g	b, L/mg $\times 10^{-4}$	$R^2$	$R_L$	$K_F$	1/n	$R^2$
Cu-1	31.3	46.7	10	0.992	0.6	2.63	0.936	0.970
Cu-2	58.2	65	3.4	0.989	0.8	2.81	0.938	0.944
Cu-3	77.19	87.6	1.4	0.994	0.9	3.06	0.925	0.959

exp, experimental

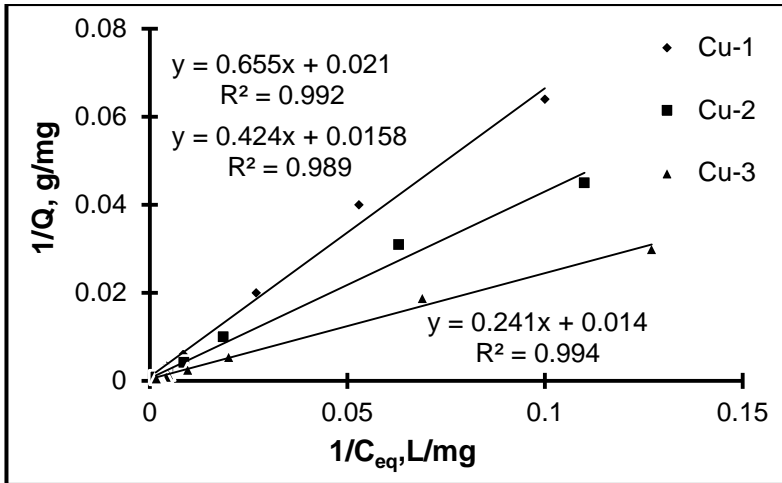


Figure 4.28. Langmuir isotherm model for adsorption of Cu(II) by ion-imprinted non-magnetic cryogel membranes.

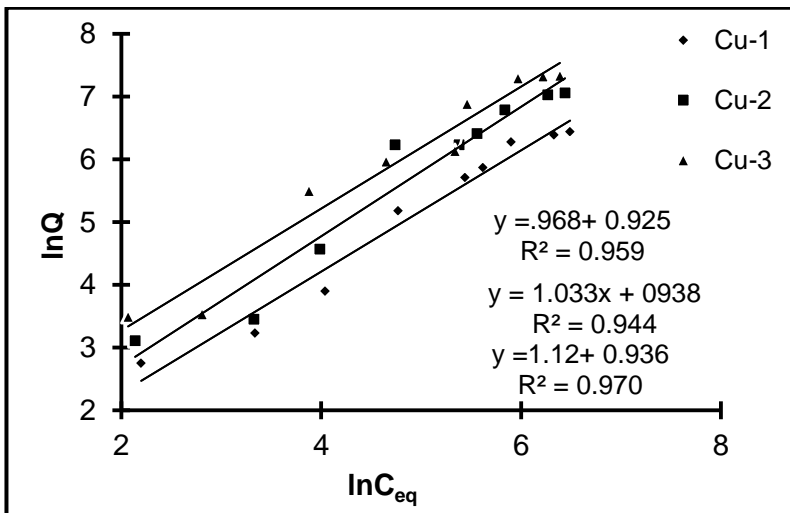


Figure 4.29. Freundlich isotherm model for adsorption of Cu(II) by ion-imprinted non-magnetic cryogel membranes.

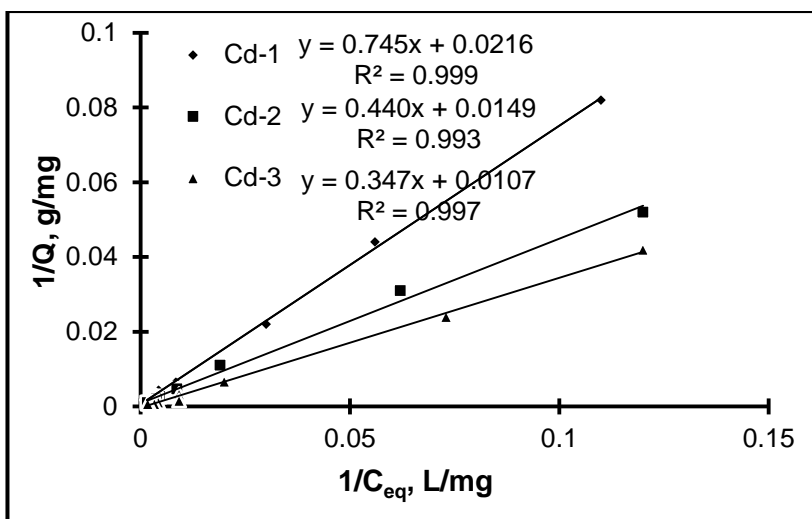


Figure 4.30. Langmuir isotherm model for adsorption of Cd(II) by ion imprinted cryogel membranes.

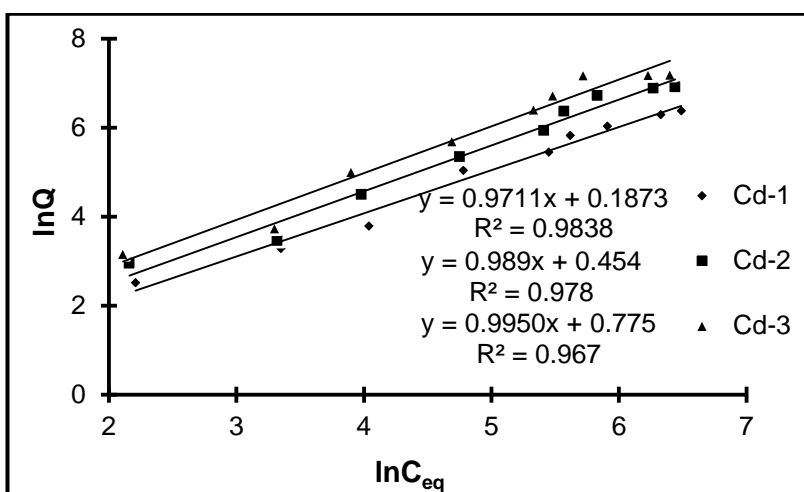


Figure 4.31. Freundlich isotherm model for adsorption of Cd(II) by ion-imprinted cryogel membranes.

Table 4.5. Langmuir and Freundlich model parameters for adsorption of Cd(II) by ion imprinted cryogel membranes.

Cryogel Codes	$Q_{exp}$ , mg/g	Langmuir			Freundlich			
		$Q_{max}$ , mg/g	$b$ , L/mg $\times 10^{-4}$	$R^2$	$R_L$	$K_F$	$1/n$	$R^2$
Cd-1	44.5	46.3	12	0.999	0.65	1.21	0.971	0.983
Cd-2	67.4	67.4	4	0.993	0.8	1.6	0.989	0.978
Cd-3	86.7	91.2	2.4	0.997	0.9	2.2	0.995	0.976

exp, experimental



Table 4.6. Langmuir and Freundlich models parameters for adsorption of Pb(II) by ion imprinted cryogel membranes.

Cryogel Codes	$Q_{exp}$ , mg/g	Langmuir			Freundlich			
		$Q_{max}$ , mg/g	$b$ , L/mg $\times 10^{-4}$	$R^2$	$R_L$	$K_F$	$1/n$	$R^2$
Pb-1	41.9	50.01	4.4	0.992	0.74	3.8	0.915	0.903
Pb-2	86.3	101.8	2.6	0.992	0.76	7.6	0.878	0.878
Pb-3	122.7	145.4	1.6	0.990	0.93	12.3	0.952	0.950

exp, experimental

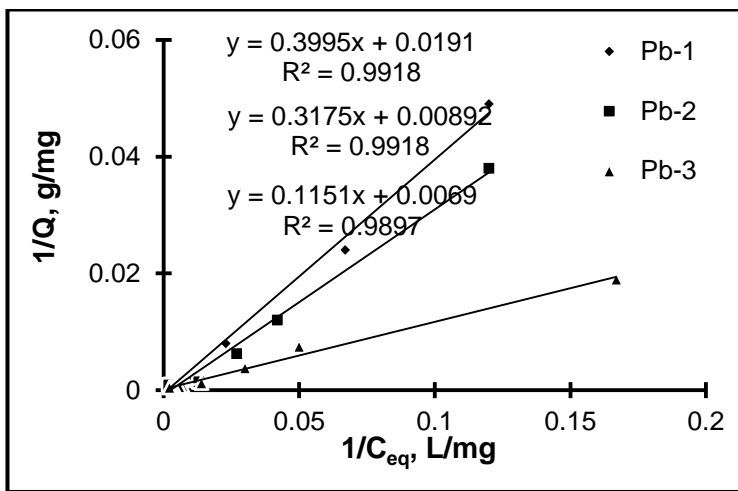


Figure 4.32. Langmuir isotherm model for adsorption of Pb(II) by ion imprinted cryogel membranes.

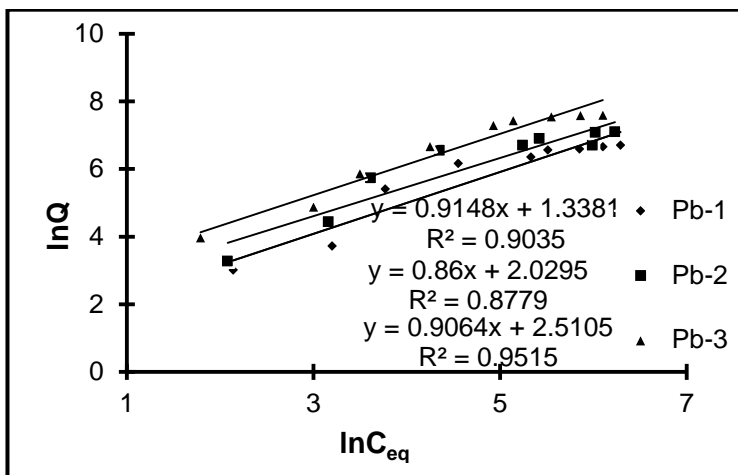
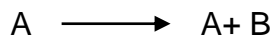


Figure 4.33. Freundlich isotherm model for adsorption of Pb(II) by ion-imprinted cryogel membranes.

#### 4.2.1.6. Adsorption Thermodynamics

In order to determine thermodynamic variables for the adsorption process, adsorption studies involving variation of initial metal ion concentration and temperature were evaluated. The Langmuir isotherm model was applied for each setup and  $K_L$  values were calculated to be used for Van't Hoff model. The mathematical backgrounds for this part were given as follows. Adsorption and desorption of molecule from surface binding sites can be considered as a chemical reaction.  $K$  is the equilibrium constant for chemical equilibrium and for



this constant is as follows

$$K = (a_A \cdot a_B) / a_{AB}; C^0 = 1.0 \text{ mol/L}; P^0 = 1 \text{ bar} \rightleftharpoons K = ([A] \cdot [B]) / [AB] \quad (4.6)$$

where

$a_A$ ,  $a_B$  and  $a_{AB}$  are activities of A, B, and AB respectively, [A], [B], and [AB] are symbols of concentration for liquids and pressure for molecules of gases.

$K$  (equilibrium constant) and  $\Delta_r G^0$  (Gibbs free energy change) are related together by;

$$\Delta_r G^0 = -RT \ln K$$

The equilibrium constant for surface adsorption of gas molecules is;

$$K_{ad} = (S^0 P) / S_1 \quad (4.7)$$

Where

$S^0$  is the amount of free binding sites,  $S_1$  is the amount of adsorbed adsorbate and  $P$  is the pressure of gas molecules [186].

$$\theta = S_1 / S \quad (4.8)$$

$$S = S^0 + S_1 \quad (4.9)$$

$\theta$  is the amount of surface coverage.

$$\theta = P / (K_{ad} + P); \theta = K_L P / (1 + K_L P); K_{ad} = \exp (-\Delta_{ad} G^0 / RT)$$

$K_L$  and  $K_{ad}$  are related together;

$$K_L = 1/K_{ad} \quad (4.10)$$

When replace  $\Delta_r G^\circ$  by  $\Delta G^\circ$ ;

$$\Delta G^\circ = -RT \ln K_{ad} \quad (4.11)$$

$$-RT \ln K_{ad} = \Delta H^\circ - T\Delta S^\circ$$

$$\ln K_L = \Delta H^\circ / (RT) - \Delta S^\circ / R \quad (4.12)$$

As mentioned before, concentration variations were performed at four different temperatures and Langmuir isotherm was applied for each data setup.  $\ln K_L$  vs  $1/T$  plots gave a slope as  $\Delta H^\circ$  and an interception of y-axis as  $\Delta S^\circ$  values. Gibbs free energy values for these processes were also calculated from appropriate equations. In liquid-solid systems adsorption process is, desorption of previously adsorbed solvent molecules and adsorption of adsorbate molecules. The negative value of  $\Delta G^\circ$  confirms the feasibility of process and spontaneous nature of adsorption, the positive value of  $\Delta S^\circ$  indicates that there was an increase in the randomness of heavy metal adsorption at the cryogel-solution interface and the negative values of  $\Delta H^\circ$  implies the exothermic nature of the adsorption.

Table 4.7. Langmuir model parameters for adsorption of Cu(II) by Cu(II) ion imprinted magnetic cryogels at 4°C and 25°C.

Cryogel Codes	Temperature, °C	R <sup>2</sup>	Q <sub>max</sub> , mg/g	Q <sub>exp</sub> , mg/g	Langmuir constant, b (1/K <sub>L</sub> )
Cu*-1	4	0.998	32.4	30.4	0.001
Cu*-2	4	0.999	64.3	61.1	0.001
Cu*-3	4	0.993	87.3	80.5	0.0001
Cu*-4	4	1.000	49.5	48.7	0.0003
Cu*-5	4	0.985	81.0	77.5	0.0001
Cu*-6	4	0.993	122.1	120.9	0.00004
Cu*-7	4	0.995	66.8	62.4	0.0002
Cu*-8	4	0.979	86.2	87.5	0.00009
Cu*-9	4	0.969	156.3	149.4	0.00002
Cu*-1	25	1.000	30.5	29.4	0.002
Cu*-2	25	0.997	58.1	54.9	0.0013
Cu*-3	25	0.999	86.4	78.9	0.0002
Cu*-4	25	0.999	39.6	38.15	0.0006
Cu*-5	25	0.975	69.2	67.8	0.00016
Cu*-6	25	0.989	111.1	107.8	0.00006
Cu*-7	25	1.000	62.3	59.9	0.0004
Cu*-8	25	0.986	78.1	75.3	0.0001
Cu*-9	25	0.976	139.4	136.4	0.00003
exp, experimental					

Table 4.8. Langmuir model parameters for adsorption of Cu(II) by Cu(II) ion imprinted magnetic cryogels at 32°C and 40°C.

Cryogel Codes	Temperature, °C	R <sup>2</sup>	Q <sub>max</sub> , mg/g	Q <sub>exp</sub> , mg/g	Langmuir constant, b (1/K <sub>L</sub> )
Cu*-1	32	0.999	14.8	13.12	0.003
Cu*-2	32	1.000	27.5	25.45	0.0018
Cu*-3	32	0.994	49.8	48.5	0.0003
Cu*-4	32	0.995	37.2	34.2	0.0009
Cu*-5	32	0.987	59.3	57.1	0.0002
Cu*-6	32	0.997	92.0	89.4	0.00009
Cu*-7	32	0.990	46.0	43.1	0.0006
Cu*-8	32	0.993	69.1	66.5	0.00017
Cu*-9	32	0.965	130.5	126.3	0.00008
Cu*-1	40	0.980	10.2	9.65	0.005
Cu*-2	40	0.993	19.3	17.75	0.0019
Cu*-3	40	0.992	39.4	37.9	0.0004
Cu*-4	40	0.988	31.3	29.1	0.0013
Cu*-5	40	0.992	50	43.8	0.00027
Cu*-6	40	0.996	76.9	73.4	0.00012
Cu*-7	40	0.999	35.7	33.9	0.0008
Cu*-8	40	0.997	63.8	54.95	0.0003
Cu*-9	40	0.965	103.5	99.4	0.00009
exp, experimental					

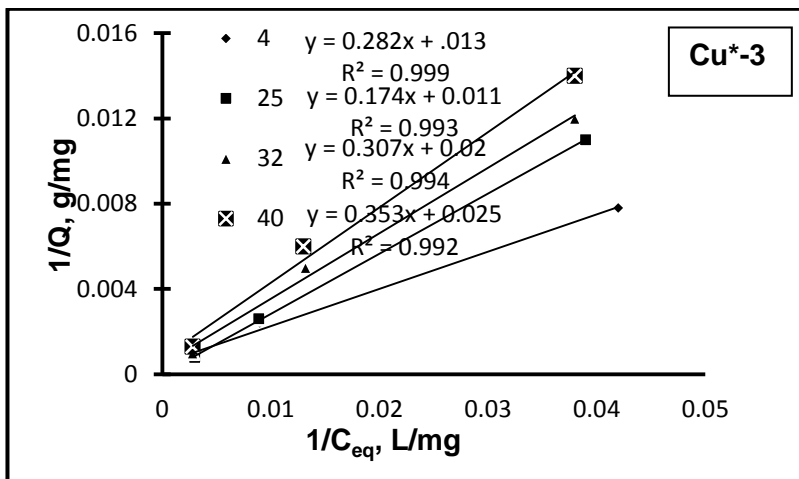
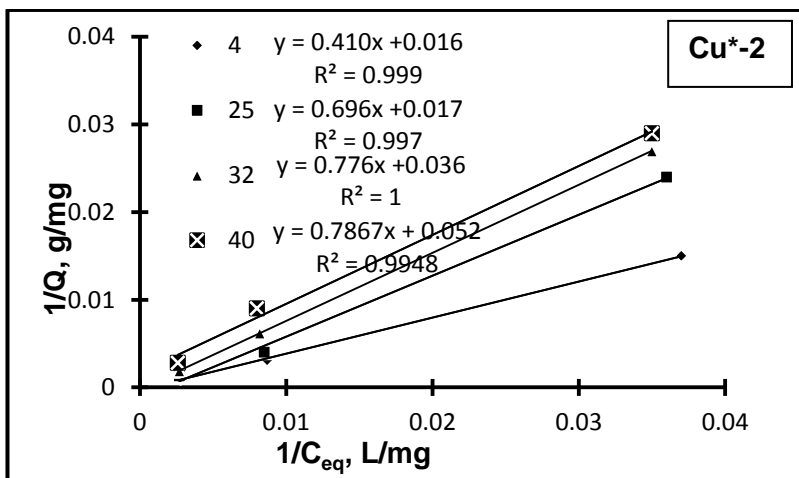
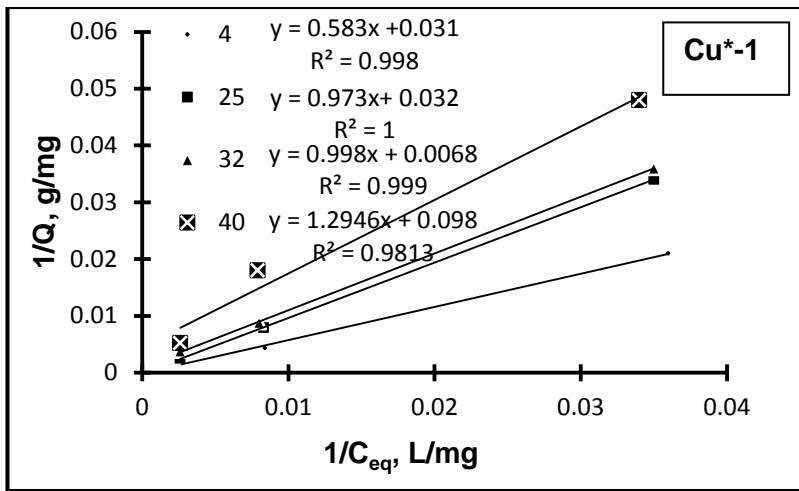


Figure 4.34. Langmuir isotherms of ion imprinted magnetic cryogels (Cu\*-1, Cu\*-2, Cu\*-3) at different temperatures (4, 25, 32, 40°C).

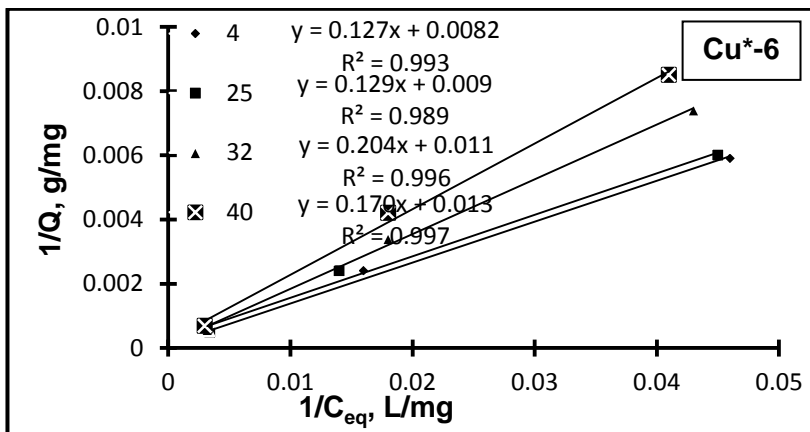
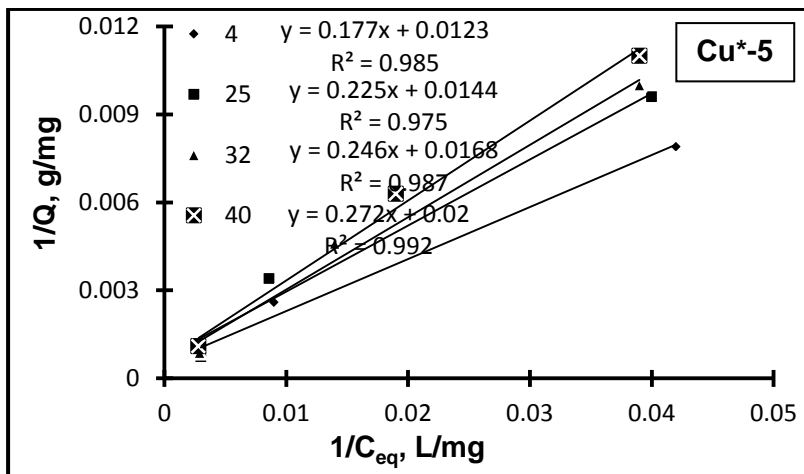
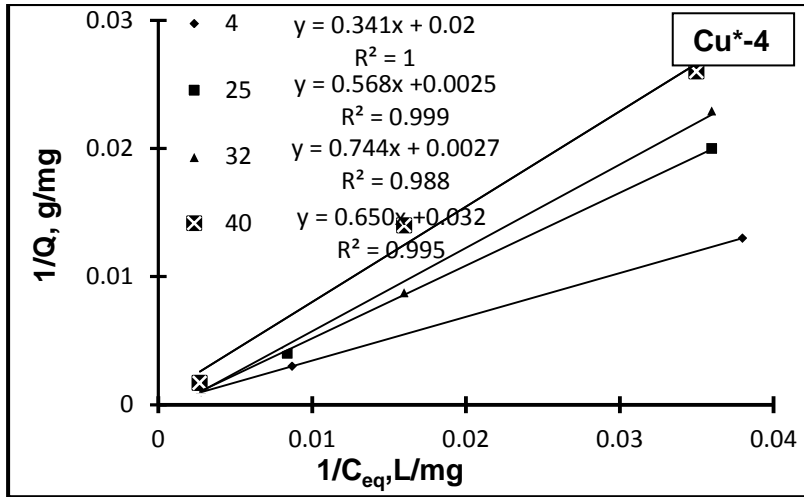


Figure 4.35. Langmuir isotherms of ion imprinted magnetic cryogels (Cu\*-4, Cu\*-5, Cu\*-6) at different temperatures (4, 25, 32, 40°C).

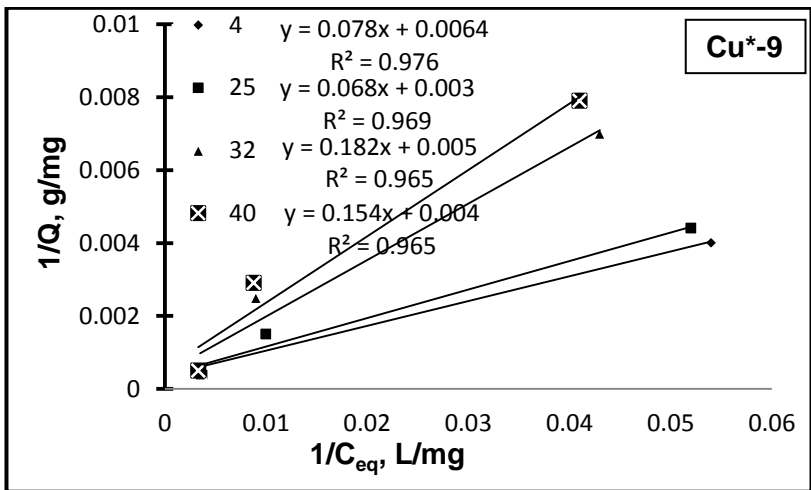
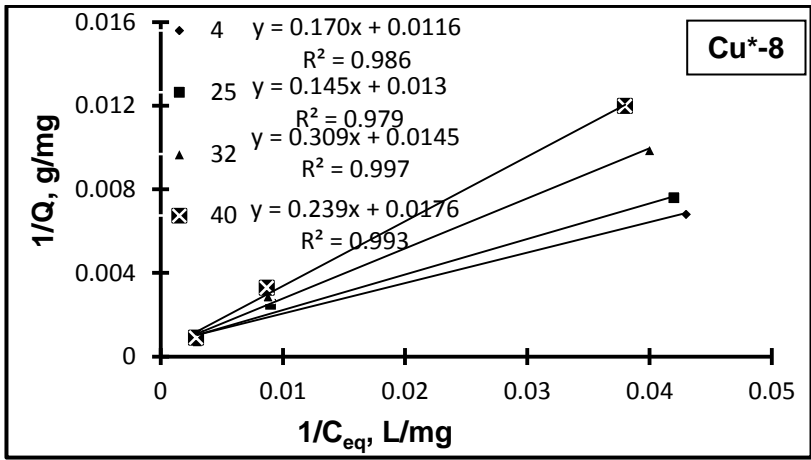
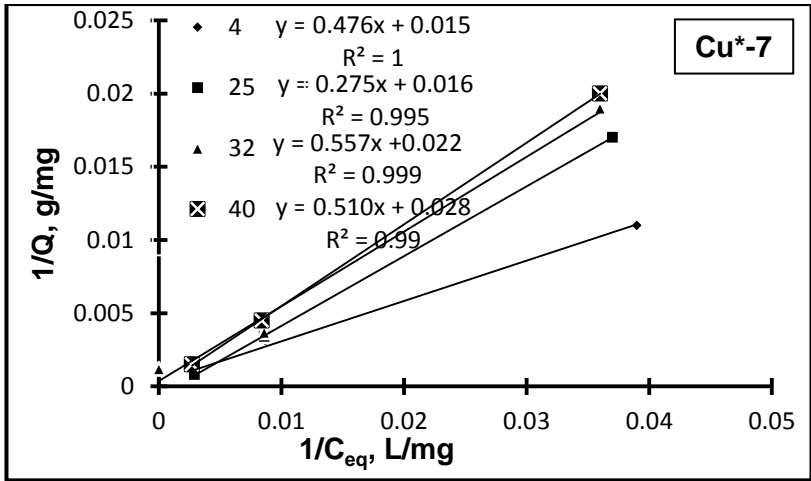


Figure 4.36. Langmuir isotherms of ion imprinted magnetic cryogels (Cu\*-7, Cu\*-8, Cu\*-9) at different temperatures (4, 25, 32, 40°C).



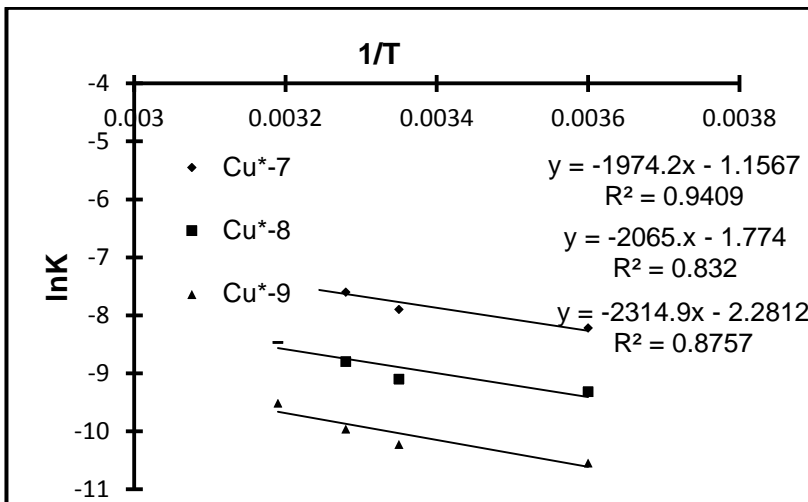
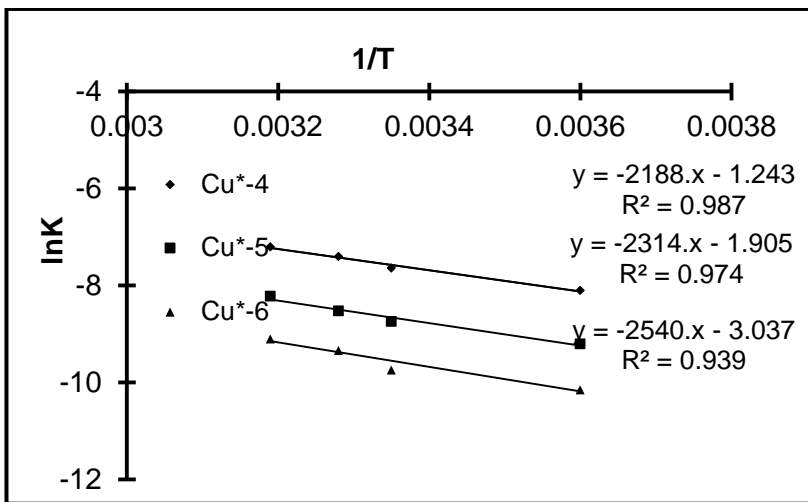
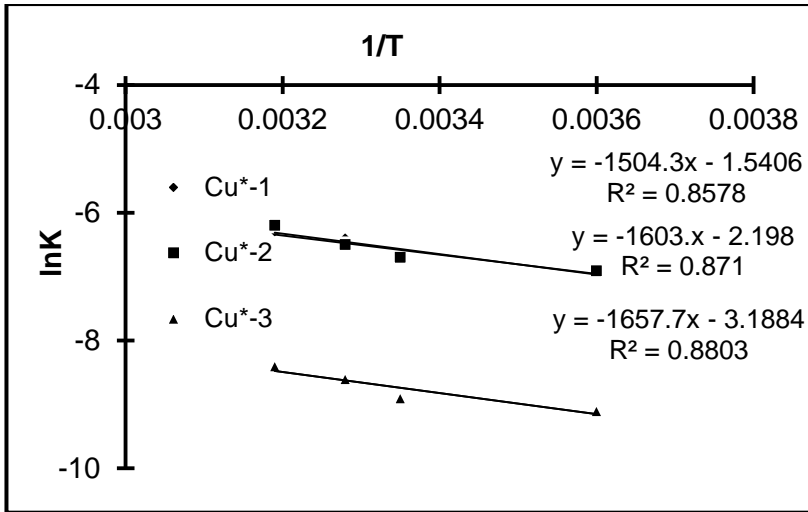


Figure 4.37. Van't Hoff plots for adsorption of Cu(II) on the ion imprinted magnetic cryogels.

Table 4.9. Thermodynamic parameters for adsorption of Cu(II) by ion imprinted magnetic cryogels.

Cryogel Codes	$\Delta G^\circ @ 25^\circ\text{C}$ kJ/mol	$\Delta H^\circ @ 25^\circ\text{C}$ kJ/mol	$\Delta S^\circ @ 25^\circ\text{C}$ J/mol.K
Cu*-1	-15.4	-12.5	12.8
Cu*-2	-16.8	-13.3	18.3
Cu*-3	-21.1	-13.8	26.5
Cu*-4	-18.4	-18.2	10.3
Cu*-5	-21.7	-19.2	15.8
Cu*-6	-24.1	-21.1	25.5
Cu*-7	-19.4	-16.4	9.6
Cu*-8	-22.8	-17.2	14.7
Cu*-9	-25.8	-19.2	20.0

Table 4.10. Langmuir model parameters for adsorption of Cu(II) by ion imprinted non-magnetic cryogels at different temperatures.

Cryogel Codes	Temperature, °C	$R^2$	$Q_{\max}$ , mg/g	$Q_{\text{exp}}$ , mg/g	Langmuir constant, $b(1/ K_L)$
Cu-1	4	0.997	32.9	28.95	0.001
Cu-2	4	0.99	55.5	49.85	0.0003
Cu-3	4	0.998	82.5	77.5	0.00018
Cu-1	25	0.996	28.6	26.7	0.0016
Cu-2	25	0.999	49.2	44.53	0.0004
Cu-3	25	0.999	76.5	69.9	0.0002
Cu-1	32	0.999	15.7	12.3	0.0028
Cu-2	32	0.998	26.3	24.03	0.0008
Cu-3	32	0.994	45.1	43.2	0.0006
Cu-1	40	0.999	11.4	8.4	0.003
Cu-2	40	0.999	17.5	15.9	0.001
Cu-3	40	0.987	39.2	35.1	0.0007
exp, experimental					

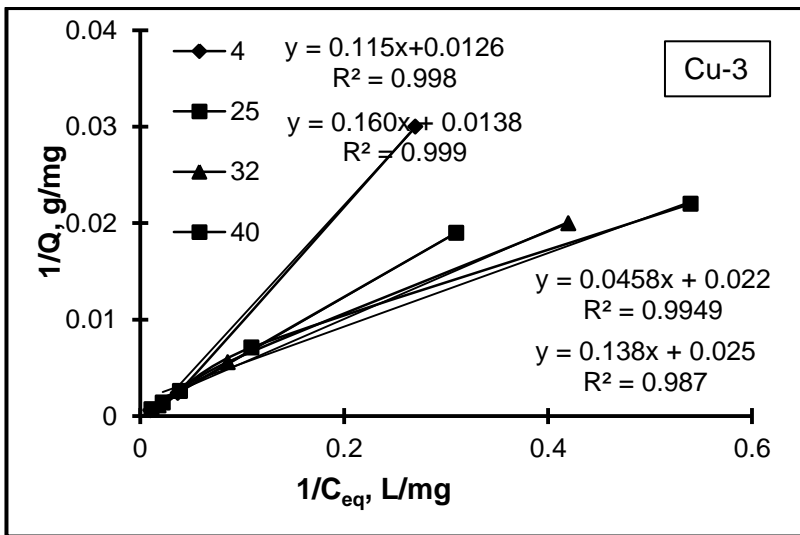
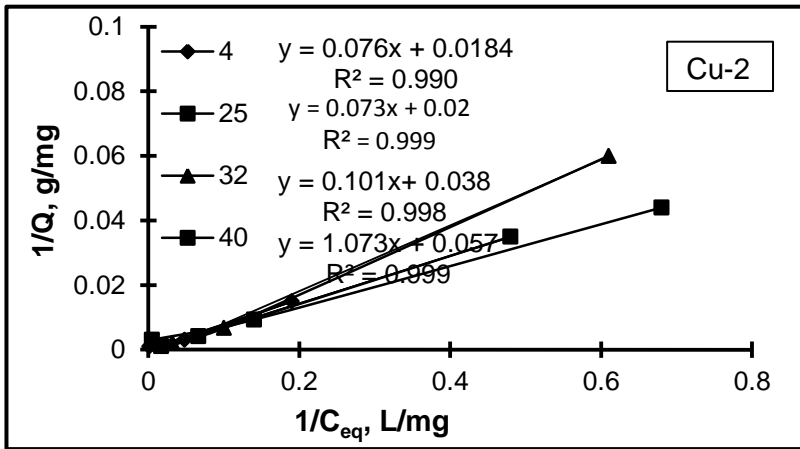
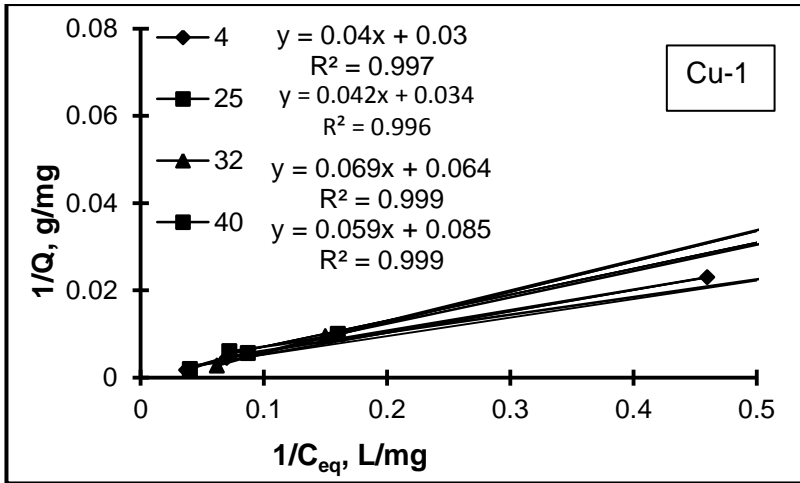


Figure 4.38. Langmuir isotherms for adsorption of Cu(II) by ion imprinted non-magnetic cryogel membranes at different temperatures.

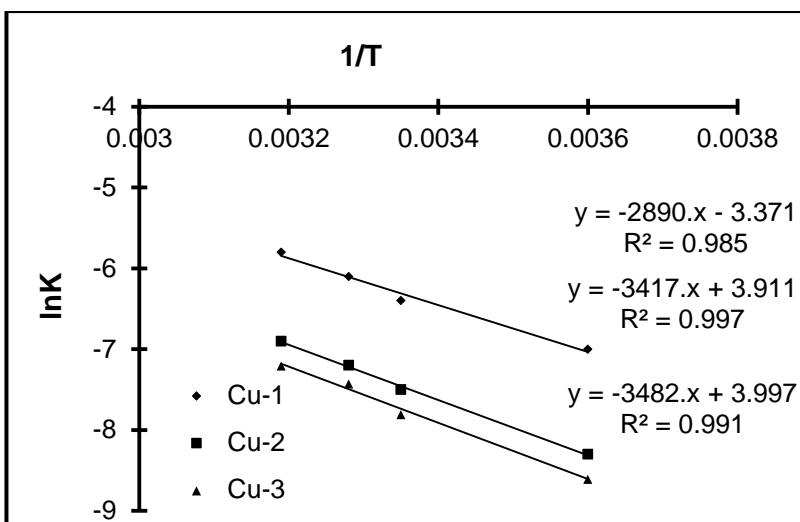


Figure 4.39. Van't Hoff plot for the adsorption of Cu(II) by imprinted non-magnetic cryogel membranes.

Table 4.11. Thermodynamic parameters for adsorption of Cu(II) by ion imprinted non-magnetic cryogels.

Cryogel Codes	$\Delta G^\circ @ 25^\circ\text{C}$ kJ/mol	$\Delta H^\circ @ 25^\circ\text{C}$ kJ/mol	$\Delta S^\circ @ 25^\circ\text{C}$ J/mol.K
Cu-1	-15.2	-24.9	28.0
Cu-2	-19.6	-28.4	32.5
Cu-3	-20.1	-28.9	33.3

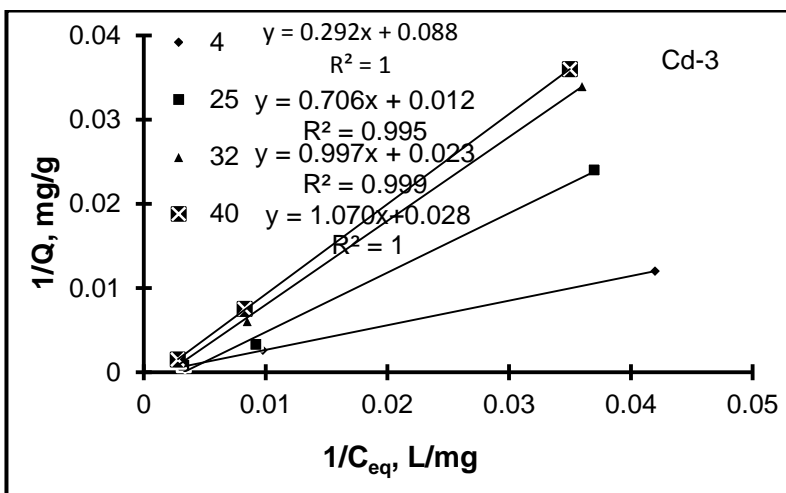
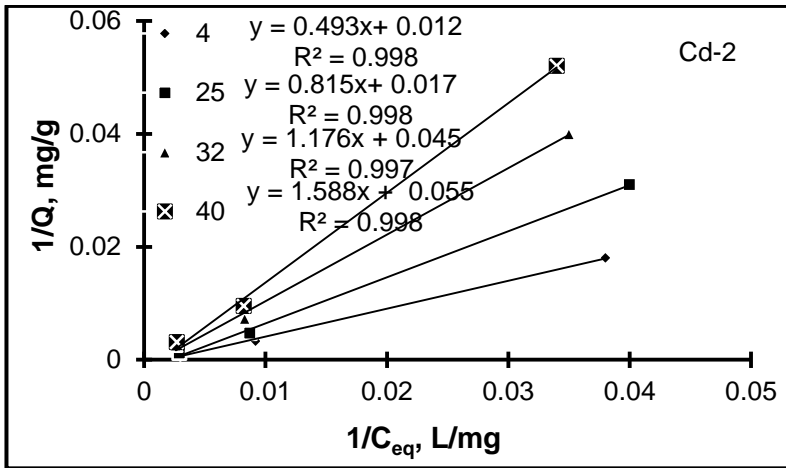
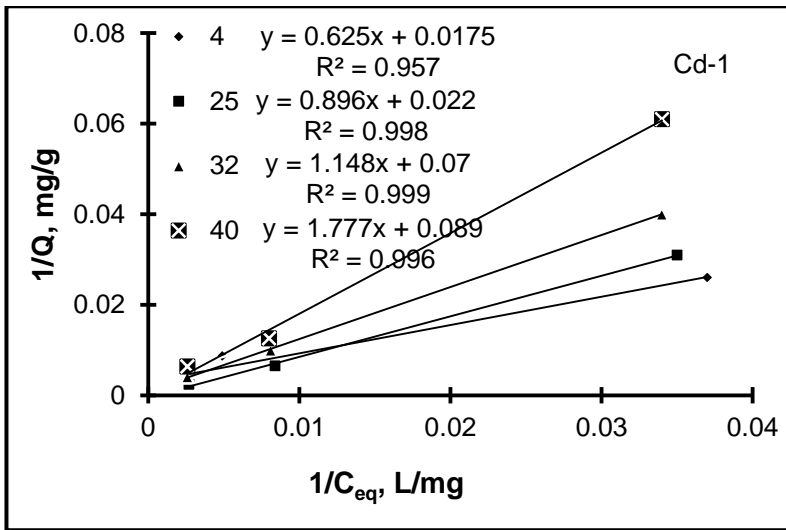


Figure 4.40. Langmuir isotherms for adsorption of Cd(II) by ion imprinted cryogels at different temperatures (4, 25, 32, 40°C).

Table 4.12. Langmuir model parameters for adsorption of Cd(II) by ion imprinted cryogels at different temperatures.

Cryogel Codes	Temperature, °C	R <sup>2</sup>	Q <sub>max</sub> , mg/g	Q <sub>exp</sub> , mg/g	Langmuir constant, b(1/K <sub>L</sub> )
Cd-1	4	0.957	57.2	53.7	0.0021
Cd-2	4	0.998	83.3	69.4	0.001
Cd-3	4	1.000	102.8	92.8	0.00065
Cd-1	25	0.998	44.6	40.8	0.0024
Cd-2	25	0.998	58.8	55.6	0.0012
Cd-3	25	0.995	82.3	76.9	0.00074
Cd-1	32	0.990	14.3	12.2	0.0039
Cd-2	32	0.997	22.2	19.3	0.0024
Cd-3	32	0.999	43.5	40	0.0012
Cd-1	40	0.996	11.2	7.84	0.0015
Cd-2	40	0.998	18.2	15.8	0.0031
Cd-3	40	1.000	36.4	32.5	0.037

exp, experimental

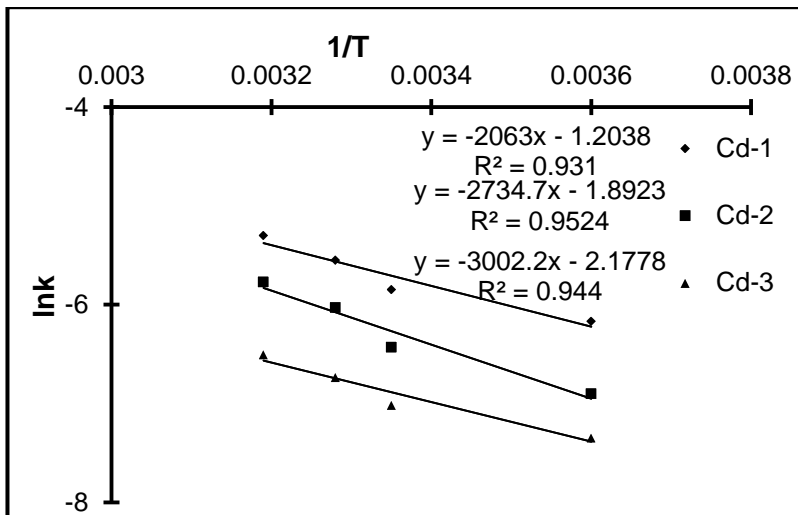


Figure 4.41. Van't Hoff plot for the adsorption of Cd(II) by imprinted cryogel membranes.

Table 4.13. Thermodynamic parameters for adsorption of Cd(II) by ion imprinted cryogels.

Cryogel Codes	$\Delta G^\circ @ 25^\circ\text{C}$ kJ/mol	$\Delta H^\circ @ 25^\circ\text{C}$ kJ/mol	$\Delta S^\circ @ 25^\circ\text{C}$ J/mol.K
Cd-1	-14.95	-16.68	10.01
Cd-2	-16.25	-22.4	15.73
Cd-3	-17.86	-24.96	18.11

Table 4.14. Langmuir model parameters for adsorption of Pb(II) by ion imprinted cryogels at different temperatures.

Cryogel Codes	Temperature, °C	$R^2$	$Q_{\text{max}}$ , mg/g	$Q_{\text{exp}}$ , mg/g	Langmuir constant, $b$ (1/ $K_L$ )
Pb-1	4	0.995	48.1	46.7	0.001
Pb-2	4	0.977	76.1	70.7	0.0007
Pb-3	4	0.996	111.2	106.1	0.00045
Pb-1	25	0.993	37.1	36.3	0.013
Pb-2	25	0.989	56.1	54.8	0.0009
Pb-3	25	0.999	94.2	90.6	0.0005
Pb-1	32	0.980	22.4	21.9	0.002
Pb-2	32	0.987	35.2	33.8	0.0014
Pb-3	32	0.993	51.15	53.1	0.0009
Pb-1	40	0.997	12.5	11.4	0.004
Pb-2	40	0.982	20.3	19.9	0.0025
Pb-3	40	0.999	41.1	39.8	0.0012
exp, experimental					

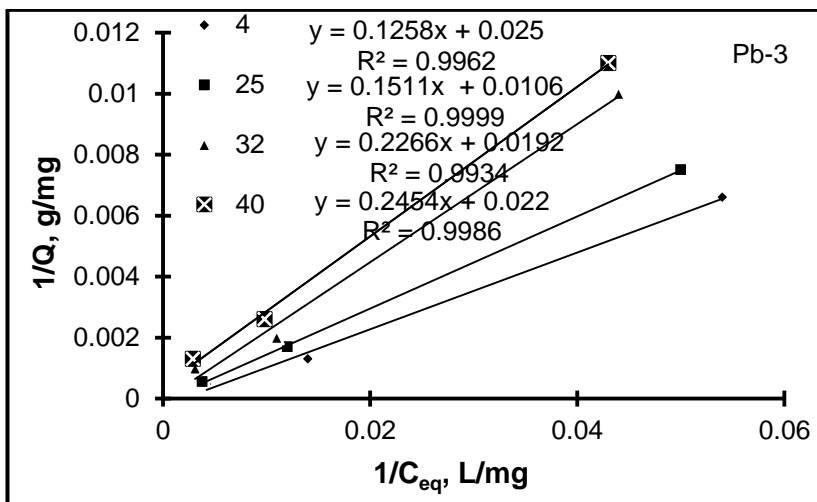
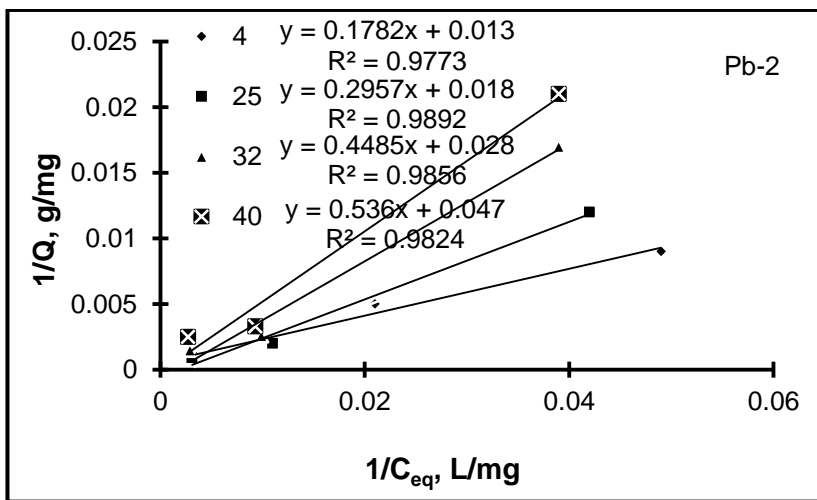
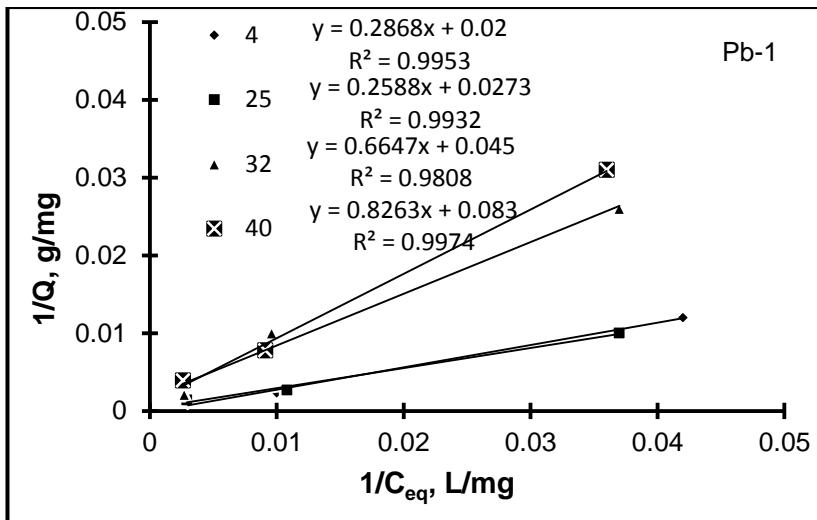


Figure 4.42. Langmuir isotherms for adsorption of Pb(II) by ion imprinted cryogels at different temperatures.



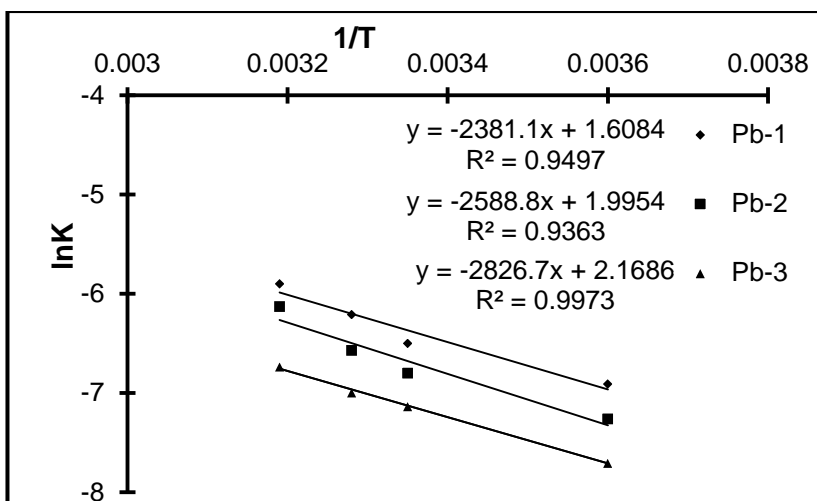


Figure 4.43. Van't Hoff plots for the adsorption of Pb(II) by ion imprinted cryogels.

Table 4.15. Thermodynamic parameters for adsorption of Cd(II) by ion imprinted cryogels.

Cryogel Codes	$\Delta G^\circ @ 25^\circ\text{C}$ kJ/mol	$\Delta H^\circ @ 25^\circ\text{C}$ kJ/mol	$\Delta S^\circ @ 25^\circ\text{C}$ J/mol.K
Pb-1	-16.64	-19.80	13.37
Pb-2	-17.40	-21.72	16.59
Pb-3	-18.74	-23.50	18.03

#### 4.2.1.7. Adsorption Kinetics

Pseudo first-order and pseudo second-order kinetic models were mostly used kinetic equations to describe the adsorption systems and to evaluate controlling parameters for adsorption processes. These models were applied for all cryogel sub-types for describing of the adsorption mechanism and analyzing of mechanism as a series of simple steps. Rate equations are differential equations and integrated according to concentrations as a function of time [183].

Kinetic models, first-order and second-order models can be used to understand adsorption process mechanisms when measured concentration is accepted equal to adsorbent surface concentration. The Lagergren pseudo-first-order model is the most used model for the adsorption of solute from liquid solution [187].

$$dq_t/dt = k_1(q_{eq} - q_t) \quad (4.13)$$

where

$k_1$  : the pseudo- first-order rate constant (1/min),

$q_t$  and  $q_{eq}$  : adsorbed amounts at time  $t$  and at equilibrium (mg/g),

Integrating the equation for the boundary conditions  $q = 0$  to  $q = q_t$  at  $t = 0$  to  $t = t$  is simplified as,

$$\log[q_{eq}/(q_{eq}-q_t)] = (k_1 t)/2.303$$

$$\log(q_{eq}-q_t) = \log(q_{eq}) - (k_1 t)/2.303 \quad (4.14)$$

The first-order rate constant  $k_1$  can be obtained from the slope of plot,  $\log (q_{eq} - q_t)$  vs time (Figure 4.20). The correlation coefficient ( $R^2$ ) shows the suitability of model for adsorption.

Adsorption kinetics explained by the pseudo-second- order model was given by Ho and McKay [188]

$$dq_t/dt = k_2(q_{eq}-q_t)^2 \quad (4.15)$$

Integrating the equation for the boundary conditions,  $q = 0$  to  $q = q_t$  at  $t = 0$  to  $t = t$  is simplified as,

$$1/(q_{eq}-q_t) = (1/q_{eq}) + k_2 t$$

$$(t/q_t) = (1/k_2 q_{eq}^2) + (1/q_{eq}) t \quad (4.16)$$

where  $k_2$  (1/mg.min) is the second-order rate constant which can be determined from the plot of  $t/q_t$  vs  $t$  (Figure 4.21).

For all cryogel groups, correlation coefficients ( $R^2$ ) values for pseudo-second order kinetic equation were higher than those for pseudo-first order kinetic equation. Thus, the second-order model was more suitable to predict the kinetics of adsorption of heavy metal ions onto the ion imprinted cryogels. The calculated  $q_{max}$  values by second-order model agree very well with the experimental values. The results mean that adsorption process was controlled by chemical recognition of ions instead of diffusion controlled one. As well-known, the second order kinetic is described by chemically controlled reaction without any diffusion restrictions. In this study, the excellent properties of cryogels and ion-imprinting process were combined. By this way, different ion imprinted cryogels for three different heavy metal ions [Cu(II), Cd(II), and Pb(II) ions] were prepared. The supermacroporous structures let the feeding solutions flow through polymeric network without any

diffusion limitations even if they had high concentrations and viscosities. Heavy metal ions easily flow through cryogels and diffuse into macropores of the cryogels and interact with recognition sites (ion imprinted cavities) without any problem. So, the controlling step should be last step, chemical interactions between functional monomers and heavy metal ions. As conclusion, the adsorption process between heavy metal ions and ion imprinted cryogels was chemisorption controlled process and chemical adsorption was the rate limiting step.

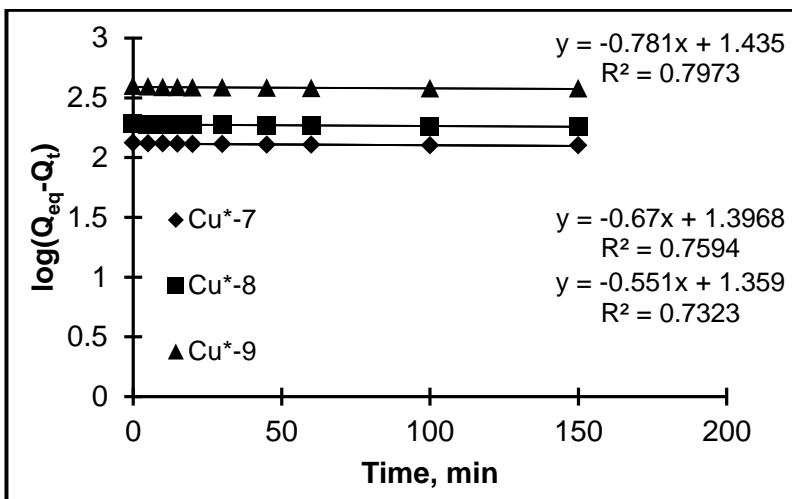
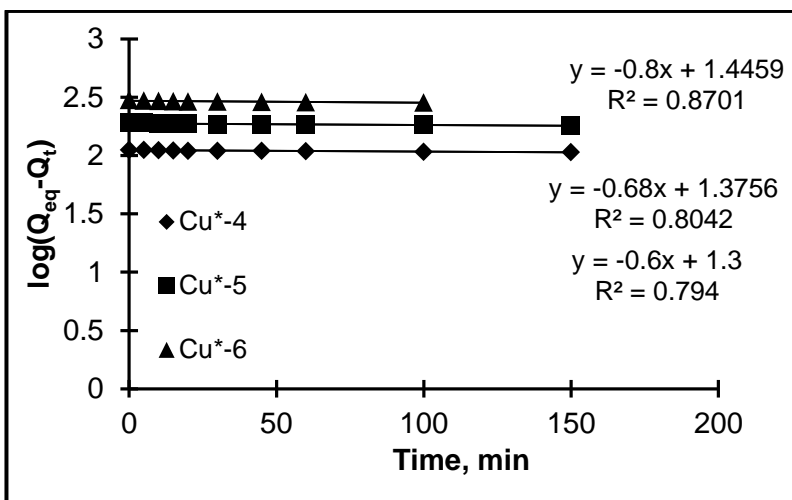
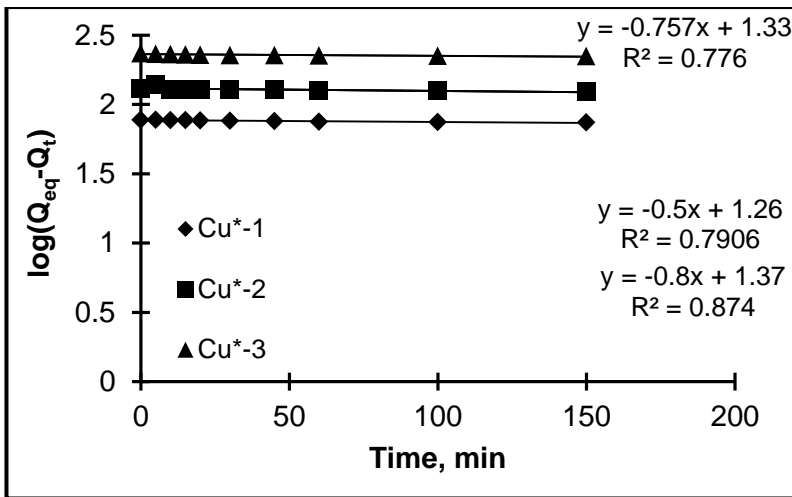


Figure 4.44. Pseudo first-order kinetic model for adsorption of Cu(II) by ion imprinted magnetic cryogel membranes.

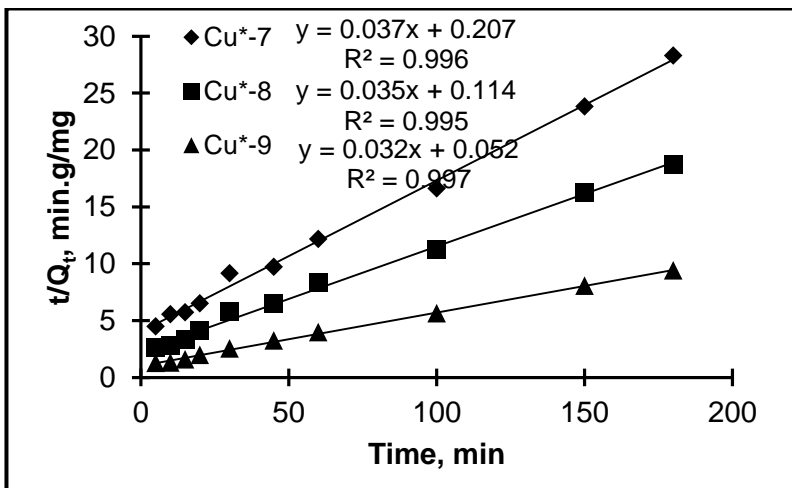
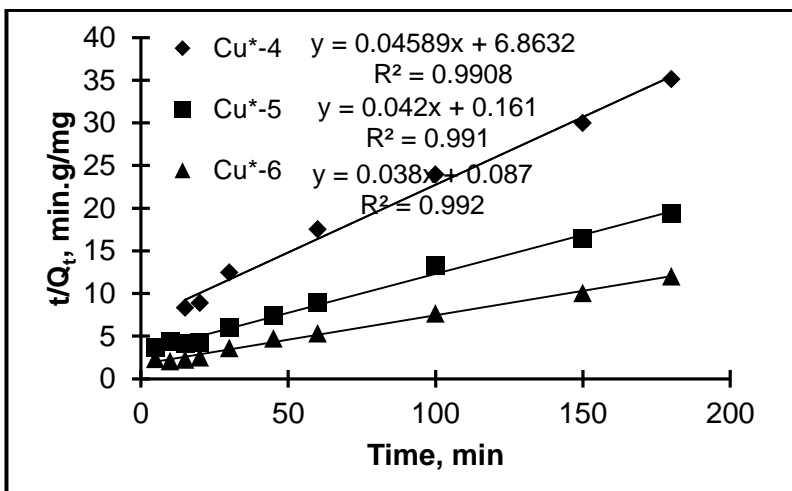
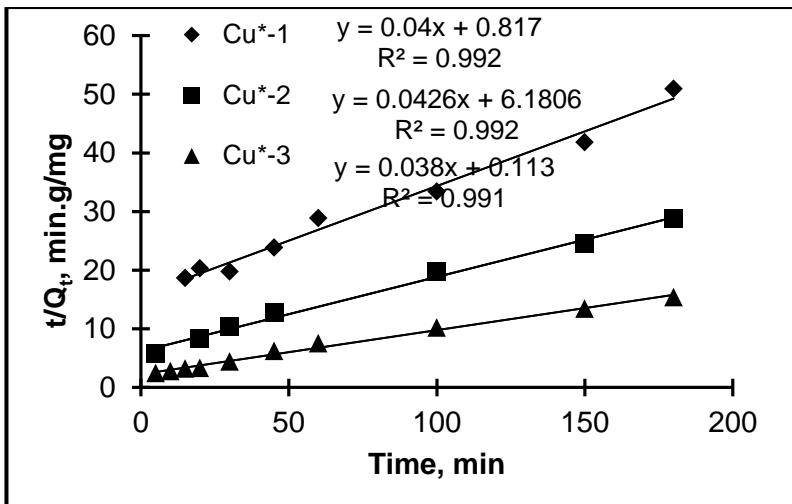


Figure 4.45. Pseudo second-order kinetic model for adsorption of Cu(II) by ion imprinted magnetic cryogel membranes.

Table 4.16. Pseudo first-order and second-order kinetic models parameters for adsorption of Cu(II) by ion imprinted magnetic cryogel membranes.

Cryogel Codes	$Q_{exp}$ , mg/g	First-order			Second-order		
		$Q_{max}$ , mg/g	$k_1 \times 10^{-2}$ , 1/min	$R^2$	$Q_{max}$ , mg/g	$k_2 \times 10^{-5}$ , g/mg.min	$R^2$
Cu*-1	19.1	18.5	1.24	0.874	21.6	8.8	0.992
Cu*-2	21.9	21.3	1.73	0.776	24.3	9.1	0.991
Cu*-3	24.3	23.4	1.91	0.790	26.1	12.7	0.992
Cu*-4	21.1	19.95	1.38	0.870	22.6	13.2	0.990
Cu*-5	23.6	23.4	1.89	0.804	23.9	12.6	0.991
Cu*-6	25.6	23.8	1.84	0.794	26.9	9.6	0.992
Cu*-7	24.2	22.4	2.02	0.797	25.8	26.4	0.996
Cu*-8	26.1	24.5	2.16	0.759	27.5	18.5	0.995
Cu*-9	27.1	26.7	1.84	0.732	29.1	10.1	0.997

exp: experimental

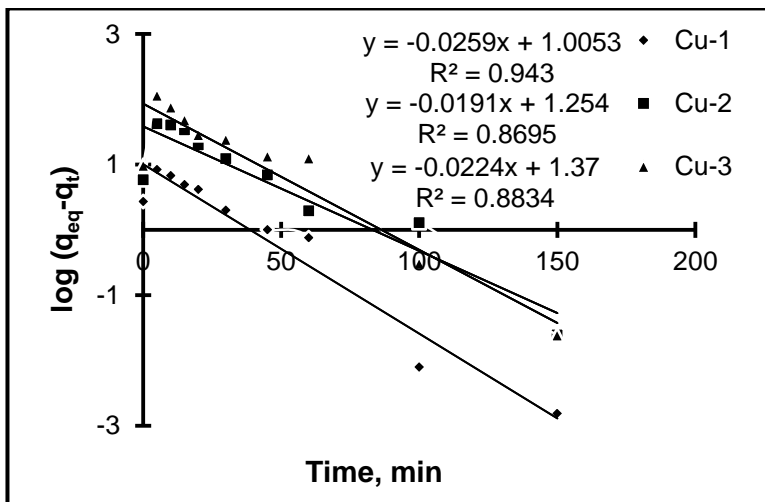


Figure 4.46. Pseudo first-order kinetic model plots for adsorption of Cu(II) by ion imprinted non-magnetic cryogels.

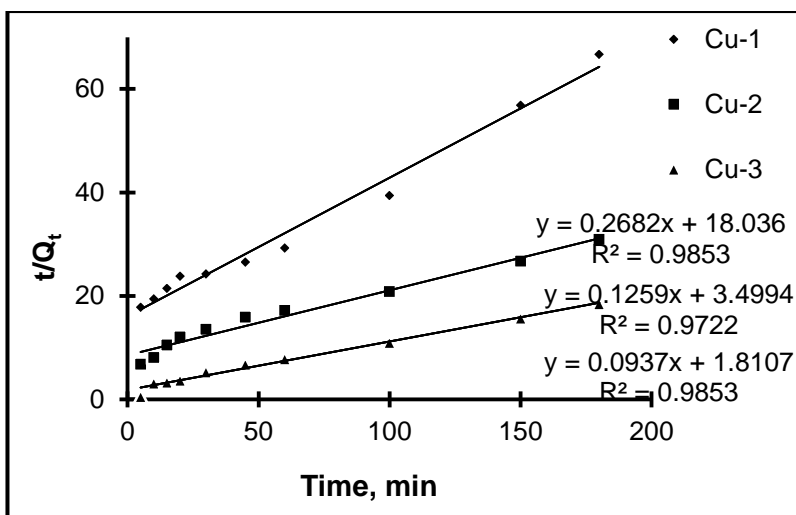


Figure 4.47. Pseudo second-order kinetic model plot for adsorption of Cu(II) by ion imprinted non-magnetic cryogels.

Table 4.17. Pseudo first-order and second-order kinetic models parameters for adsorption of Cu(II) by ion imprinted non-magnetic cryogel membranes.

Cryogel Codes	$Q_{exp}$ , mg/g	First-order			Second-order		
		$Q_{max}$ , mg/g	$k_1 \times 10^{-2}$ , 1/min	$R^2$	$Q_{max}$ , mg/g	$k_2 \times 10^{-5}$ , g/mg.min	$R^2$
Cu-1	2.7	10.1	3.9	0.943	3.6	4.06	0.985
Cu-2	5.82	18.1	4.4	0.869	7.9	4.2	0.972
Cu-3	9.47	24.5	5.5	0.883	10.7	4.8	0.985

exp: experimental

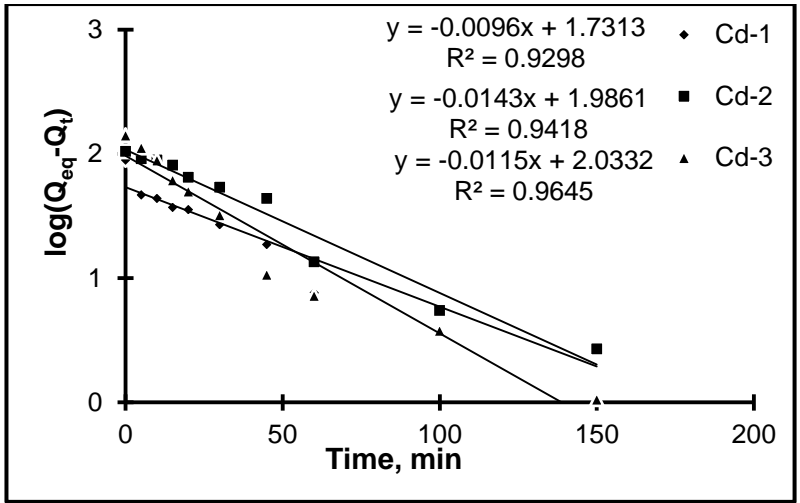


Figure 4.48. Pseudo first-order kinetic model for adsorption of Cd(II) by ion imprinted cryogel membranes.

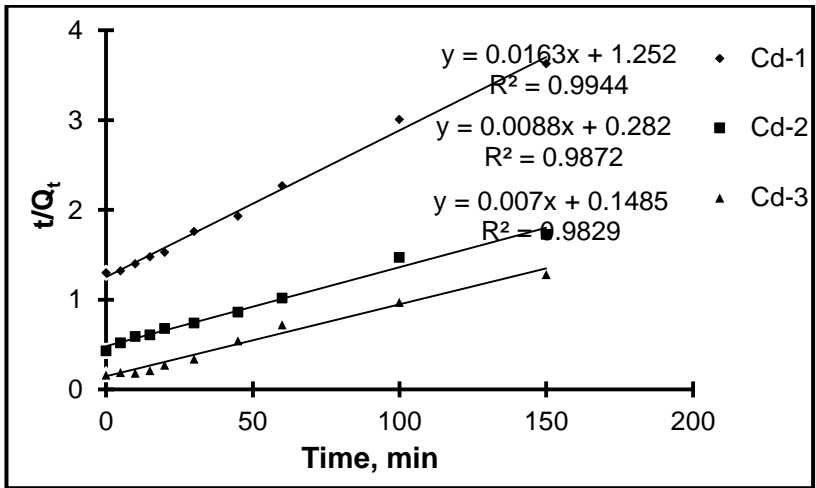


Figure 4.49. Pseudo second-order kinetic model for adsorption of Cd(II) by ion imprinted cryogels.



Table 4.18. Pseudo first-order and second-order kinetic models parameters for adsorption of Cd(II) by ion imprinted non-magnetic cryogel membranes.

Cryogel Codes	$Q_{exp}$ , mg/g	First-order			Second-order		
		$Q_{max}$ , mg/g	$k_1 \times 10^{-2}$ , 1/min	$R^2$	$Q_{max}$ , mg/g	$k_2 \times 10^{-5}$ , g/mg.min	$R^2$
Cd-1	7.5	6.9	2.2	0.929	8.3	3.2	0.994
Cd-2	11.2	10.8	3.3	0.942	13.5	3.4	0.987
Cd-3	12.8	10.6	3.4	0.965	13.9	4.6	0.983

exp: experimental

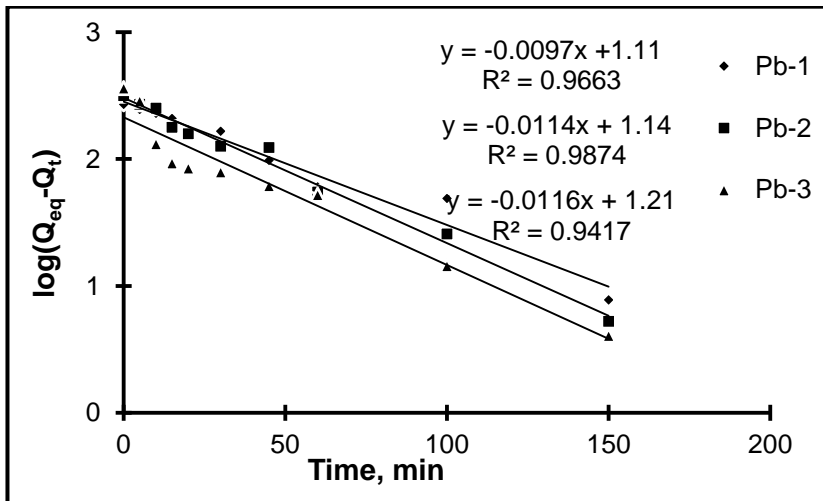


Figure 4.50. Pseudo first-order kinetic model for adsorption of Pb(II) by ion imprinted cryogel membranes.

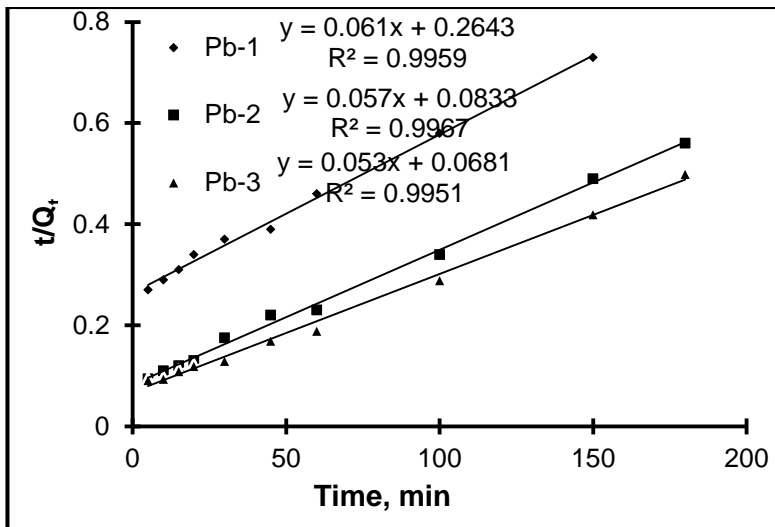


Figure 4.51. Pseudo second-order kinetic model for adsorption of Pb(II) by ion imprinted cryogel membranes.

Table 4.19. Pseudo first-order and second-order kinetic models parameters for adsorption of Pb(II) by ion imprinted non-magnetic cryogel membranes.

Cryogel Codes	$Q_{exp}$ , mg/g	First-order			Second-order		
		$Q_{max}$ , mg/g	$k_1 \times 10^{-2}$ , 1/min	$R^2$	$Q_{max}$ , mg/g	$k_2 \times 10^{-5}$ , g/mg.min	$R^2$
Pb-1	13.4	12.8	2.2	0.966	14.58	3.1	0.996
Pb-2	15.99	13.9	2.6	0.987	17.8	3.7	0.997
Pb-3	17.94	16.3	2.7	0.942	18.6	4.2	0.995

exp: experimental

#### 4.2.2. Magnetic vs Non-Magnetic Cu(II)-Imprinted Cryogels

Magnetite ( $Fe_3O_4$ ) nanoparticles embedding into cryogel network gave magnetic character for the cryogels and caused an increase in surface area and porosity of the polymeric structure [174]. As expected, adsorption of Cu(II) by ion imprinted magnetic cryogels was higher than that of ion imprinted non-magnetic cryogels (Figure 4.51). In addition, the amount of magnetite nanoparticles affected the adsorption capacities. The increase of magnetite content from 25 mg to 100 mg caused an increase for adsorption capacity from 35.4 mg/g to 97.9 mg/g. Also, the increment by magnetite nanoparticle addition increased the capacity in 113%, 126%, and 127% for 25 mg of  $Fe_3O_4$  incorporated, 50 mg of  $Fe_3O_4$  incorporated, and 100 mg of  $Fe_3O_4$  incorporated cryogels, respectively. The results indicated

that magnetite nanoparticles also enhanced the adsorption process due to an increase in surface area, porosity, and the favorable distribution of imprinted cavities.

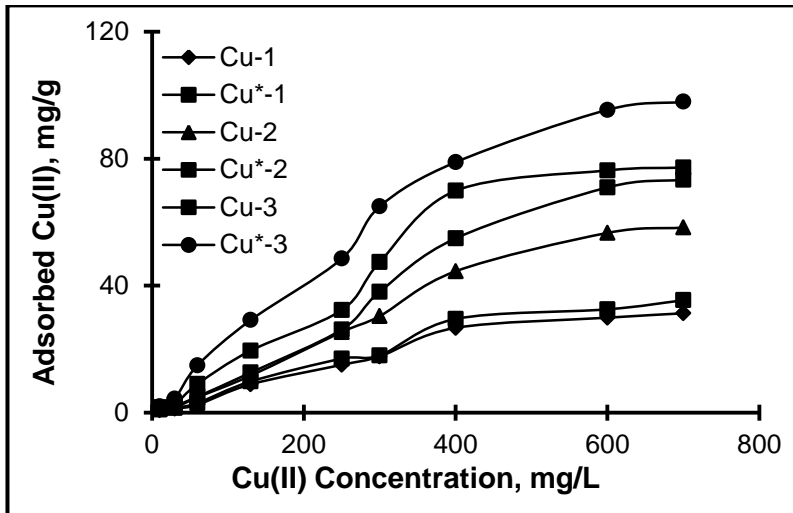


Figure 4.52. Comparison of adsorption capacities of ion imprinted magnetic and non-magnetic cryogels; pH: 5.5; incubation period: 120 min and T: 25°C.

### 4.2.3. Selectivity Studies

#### 4.2.3.1. Ion Imprinted vs Non-Imprinted Cryogels

##### 4.2.3.1.1. Cu(II) Ion-Imprinted Magnetic vs Non-Imprinted Cryogels

Non-imprinted cryogel membranes were also prepared for comparison purpose. These cryogel membranes were incubated with  $\text{Cu}(\text{NO}_3)_2$  solutions having different concentrations under the optimum conditions determined for magnetic Cu(II) ion imprinted cryogels. Adsorption capacities of non-imprinted and ion imprinted cryogel membranes are compared (Figure 4.52). Adsorption capacity of ion imprinted magnetic cryogels is higher than that of non-imprinted magnetic cryogels. Distribution coefficient of Cu(II) ions for ion imprinted magnetic cryogels,  $K_d$  was 0.083 whereas that of Cu(II) ions for non-imprinted magnetic cryogels,  $K_d$  was 0.024. Relative selectivity coefficient,  $k'$  was calculated as 3.46.

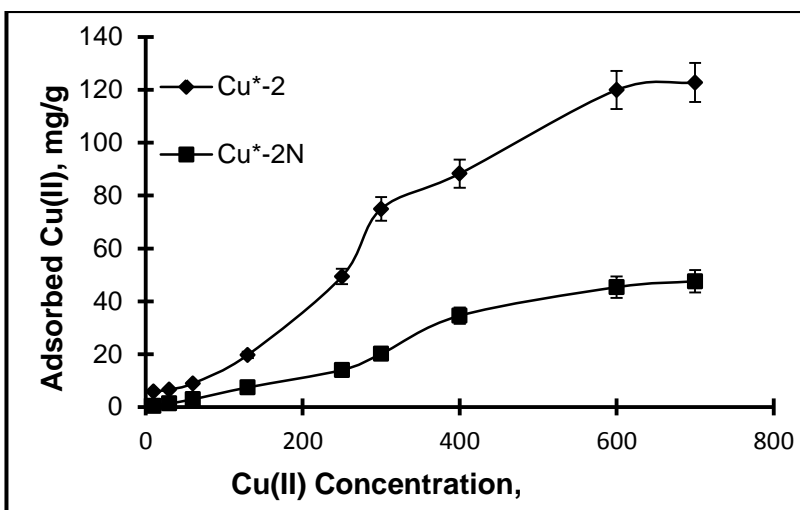


Figure 4.53. Comparison of adsorption capacities of magnetic Cu(II) ion-imprinted vs non-imprinted cryogels; pH: 5.5; T: 25°C; and incubation period: 120 min.

#### 4.2.3.1.2. Cu(II) Ion-Imprinted vs Non-Imprinted Cryogels

Non-imprinted cryogel membranes were also prepared for comparison. Again these cryogels were incubated with  $\text{Cu}(\text{NO}_3)_2$  solutions of different concentrations under the same optimum conditions determined for Cu(II) ion-imprinted cryogels. Adsorption capacity of non-imprinted and ion imprinted cryogel membranes are compared (Figure 4.53). Adsorption capacity of ion imprinted cryogels was higher than that of non-imprinted magnetic cryogels. Ion coordination was responsible for the formation of imprinted cavities on surface of cryogels and made MAH monomer as more accessible for ion recognition and adsorption. Distribution coefficient of Cu(II) ions for ion imprinted magnetic cryogels,  $K_d$  was 0.037 whereas that of Cu(II) ions for non-imprinted magnetic cryogels,  $K_d$  was 0.014. Relative selectivity coefficient,  $k'$  was calculated as 2.64.

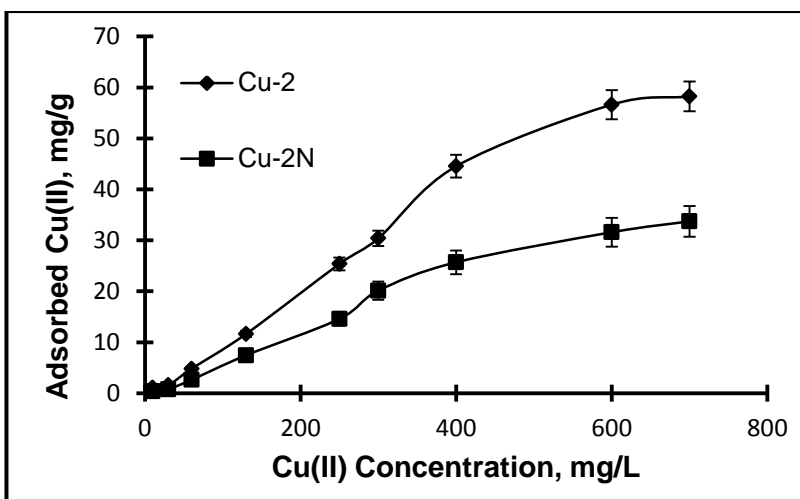


Figure 4.54. Comparison of adsorption capacities of Cu(II) ion imprinted vs non-imprinted cryogels; pH: 5.5; T: 25°C; and incubation period: 120 min.

#### 4.2.3.1.3. Cd(II) Ion-Imprinted vs Non-Imprinted Cryogels

Non-imprinted cryogel membranes were also prepared for comparison. These cryogels were incubated with  $\text{Cd}(\text{NO}_3)_2$  solutions having different concentrations under the optimum conditions determined for Cd(II) ion imprinted cryogels. Adsorption capacities of non-imprinted and ion imprinted cryogel membranes are given in Figure 4.54. Adsorption capacity of ion imprinted cryogels was higher than that of non-imprinted cryogels. Distribution coefficient of Cd(II) ions for ion imprinted cryogels,  $K_d$  was 0.043 whereas that of Cd(II) ions for non-imprinted magnetic cryogels,  $K_d$  was 0.016. Relative selectivity coefficient,  $k'$  was calculated as 2.69.

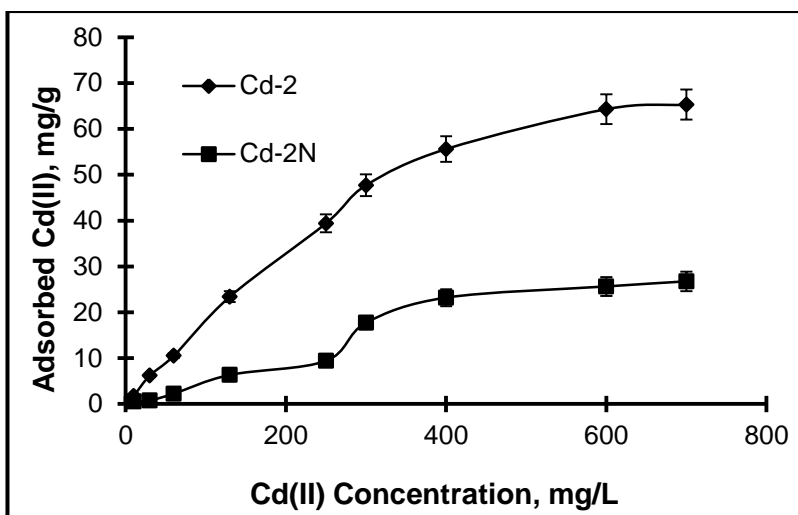


Figure 4.55. Comparison of adsorption capacities of Cd(II) ion-imprinted and non-imprinted cryogels; pH: 5.5; incubation period: 120 min; and T; 25°C.

#### 4.2.3.1.4. Pb(II) Ion-Imprinted with Non-Imprinted Cryogels

Non-imprinted cryogel membranes were also prepared for comparison. These cryogels were incubated with  $\text{Pb}(\text{NO}_3)_2$  solutions having different concentrations under the same optimum conditions determined for Pb(II) ion imprinted magnetic cryogel (with 0.1 mmol of Pb(II)-MAAsp pre-complex). Adsorption capacities of non-imprinted and ion imprinted cryogel membranes are compared in Figure 4.55. Adsorption capacity of ion imprinted cryogels was higher than that of non-imprinted cryogels. Distribution coefficient of Pb(II) ions for ion imprinted magnetic cryogels,  $K_d$  was 0.040 whereas that of Pb(II) ions for non-imprinted magnetic cryogels,  $K_d$  was 0.019. Relative selectivity coefficient,  $k'$  was calculated as 2.10.

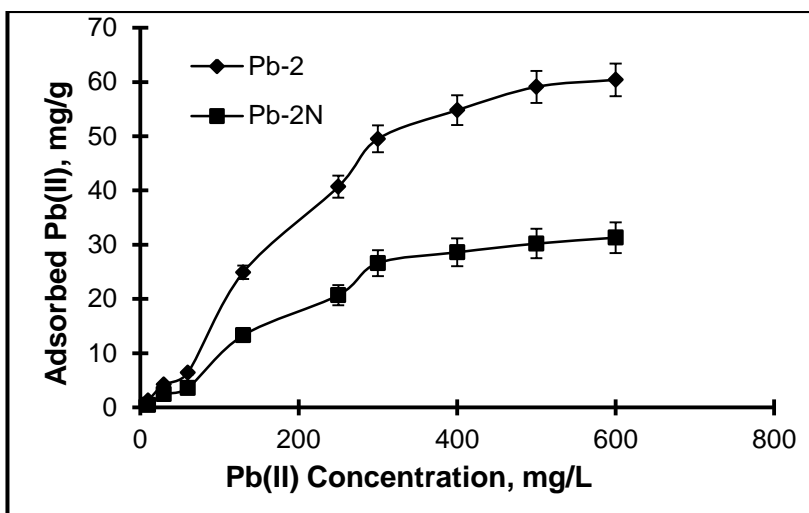


Figure 4.56. Comparison of adsorption capacities of Pb(II) ion imprinted with non-imprinted cryogels; T: 25°C; pH: 5.5; incubation: 120 min.

Ion imprinting process caused an increase in adsorption capacities for all heavy metal ions. By ion imprinting process, the recognition abilities for Cu(II) imprinted magnetic cryogels, Cu(II) imprinted non-magnetic cryogels, Cd(II) imprinted cryogels, and Pb(II) imprinted cryogels were enhanced about 3.46, 2.64, 2.69, and 2.10 folds, respectively. The results may depend on more homogeneous distribution of functional monomer during ion imprinting process because of pre-polymerization complexes. Also, presence of heavy metal ions may cause differences in the polymerization process at interface of unfrozen and frozen phases.

Table 4.20. Comparison of selectivities of ion imprinted with non-imprinted cryogels.

	Distribution coefficient, $K_d$		Relative selectivity coefficient
	Ion imprinted	Non-imprinted	$k'$
Cu <sup>2+</sup> -2 vs Cu <sup>2+</sup> -2N	0.083	0.024	3.46
Cu-2 vs Cu-2N	0.037	0.014	2.64
Cd-2 vs Cd-2N	0.043	0.016	2.69
Pb-2 vs Pb-2N	0.040	0.019	2.10

#### 4.2.3.2. Competitive Adsorption by Ion-Imprinted Cryogels

##### 4.2.3.2.1. Adsorption of Cu(II), Cd(II), Pb(II), and Zn(II) by Cu(II) Ion-Imprinted Magnetic Cryogel

A solution containing 100 ppm of each of four Cu(II), Cd(II), Pb(II), and Zn(II) ions at a constant pH (5.5) and at 25°C was incubated with Cu(II) imprinted magnetic cryogel membrane in batch system. Adsorption capacity values are given in Table 4.22. The adsorbed amount of Cu(II) ions was higher than those of other ions. When the resulting value was compared with the single ion containing system (non competitive system) this adsorption amount was lower than that of it, meaning that antagonistic effect was observed for this adsorption system. As seen from the table, Cu(II) ion imprinted magnetic cryogels show relative selectivity coefficients as 5.27, 15.8, and 2.63 for Cu(II)/Cd(II), Cu(II)/Pb(II), and Cu(II)/Zn(II) pairs, respectively. The results indicated that ion imprinting process caused the selective recognition ability for Cu(II) imprinted magnetic cryogels. Cu(II) imprinted cryogels showed selectivity for Pb(II) ions around 15.8 folds. It was probably due to the Lewis acid character difference between Cu(II) ion and Pb(II) ion. But, the difference between Cu(II) and Zn(II) was 2.63 folds although they had similar Lewis acid character against nitrogen atoms in functional monomer, MAH. So, the ion imprinting process really caused specific recognition ability against competitor ions as a competitive manner.

Table 4.21. Competitive adsorption of heavy metal ions by Cu(II) magnetic ion imprinted cryogel from multi-metal ions solution.

Ion	Adsorption Capacity, mg/g	$K_d$ , mL/mg	$k'$
Cu(II)	16.43	0.079	-
Cd(II)	3.80	0.015	5.27
Pb(II)	1.26	0.005	15.8
Zn(II)	6.94	0.030	2.63

Concentration of each metal ion, 100 ppm; pH 5.5; and temperature 25°C. Non-competitive adsorption capacity for template Cu(II) ion: 36.9 mg/g.



#### 4.2.3.2.2. Adsorption of Cu(II), Cd(II), Pb(II), and Zn(II) by Cu(II) Ion-Imprinted Non-Magnetic Cryogel

A solution containing 100 ppm of each of four Cu(II), Cd(II), Pb(II), and Zn(II) ions at a constant pH (5.5) and at 25°C was also incubated with Cu(II) imprinted non-magnetic cryogel membrane in batch system. Adsorption capacity values, distribution and relative selectivity coefficients are given in Table 4.23. The adsorbed amount of Cu(II) ions was higher than those of other ions. When this value was compared with the single ion containing system (non competitive system) the value was lower than that of single system as discussed before. The competitive adsorption capacities of Cu(II) ion imprinted cryogels for Cu(II), Cd(II), Pb(II), and Zn(II) ions under competitive manner were 11.20 mg/g, 3.35 mg/g, 1.16 mg/g, and 5.74 mg/g, respectively. As expected from adsorption capacity difference for magnetic and non-magnetic cryogels, the relative selectivity coefficients slightly decreased. But, the Cu(II) ion imprinted cryogels still showed higher adsorption tendency against template [Cu(II)] ions and relative selectivity coefficient was higher than 1 which indicated the selectivity of these cryogels. Here, it should be noted that the adsorption capacity obtained from singular heavy metal ion solution decreased under competitive conditions meaning that heavy metal ions have antagonistic effects on other heavy metal ions.

Table 4.22. Competitive adsorption of heavy metal ions by Cu(II) non-magnetic ion imprinted cryogel from multi-metal ions solution.

Ion	Adsorption Capacity, mg/g	$K_d$ , mL/mg	$k'$
Cu(II)	11.20	0.052	-
Cd(II)	3.35	0.014	3.7
Pb(II)	1.16	0.0047	11.06
Zn(II)	5.74	0.025	2.08
Concentration of each metal ion, 100 ppm; pH 5.5; and temperature 25°C. Non-competitive adsorption capacity for template Cu(II) ion: 15.02 mg/g.			

#### 4.2.3.2.3. Adsorption of Cd(II), Cu(II), Pb(II), and Zn(II) by Cd(II) Ion-Imprinted Cryogel

Competitive heavy metal ion solution containing 100 ppm of each of four Cu(II), Cd(II), Pb(II), and Zn(II) ions at a constant pH (5.5) and at 25°C was also incubated with Cd(II) imprinted cryogel membranes in batch system. Adsorption capacity values, distribution and relative selectivity coefficients are given in Table 4.24. The adsorbed amount of Cd(II) ions was higher than those of other ions; but, lower than that of singular Cd(II) solution. The competitive adsorption capacities of Cd(II) ion imprinted cryogels for Cd(II), Cu(II), Pb(II), and Zn(II) ions under competitive manner were 13.91 mg/g, 2.40 mg/g, 2.20 mg/g, and 2.62 mg/g, respectively. The relative selectivity coefficients for Cd(II)/Cu(II), Cd(II)/Pb(II), and Cd(II)/Zn(II) pairs were calculated as 6.90, 7.67, and 6.27, respectively. These results indicated the high selectivity and specificity between Cd(II) imprinted cryogels and template [Cd(II)] ions due to ion imprinting process. Similarly, antagonistic effect of competitor heavy metal ions was also determined for Cd(II) imprinted cryogels as well. The highest relative selectivity coefficient was obtained for Cd(II)/Pb(II) pairs because of ionic radii and Lewis acid character differences as expected.

Table 4.23. Competitive adsorption of heavy metal ions by Cd(II) ion imprinted cryogel from multi-metal ions solution.

Ion	Adsorption Capacity, mg/g	$K_d$ , mL/mg	$k'$
Cd(II)	13.91	0.069	-
Cu(II)	2.40	0.010	6.90
Pb(II)	2.20	0.009	7.67
Zn(II)	2.62	0.011	6.27

Concentration of each metal ion, 100 ppm; pH 5.5; and temperature 25°C. Non-competitive adsorption capacity for template Cd(II) ion: 22.68 mg/g.

#### 4.2.3.2.4. Adsorption of Pb(II), Cu(II), Cd(II), and Zn(II) by Pb(II) Ion-Imprinted Cryogel

Competitive heavy metal ions solution containing 100 ppm of each of four Cu(II), Cd(II), Pb(II), and Zn(II) ions at a constant pH (5.5) and at 25°C was also interacted with Pb(II) imprinted cryogel membrane in batch system. Adsorption capacity values are given in Table 4.25. The adsorbed amount for Pb(II) ions was higher than those of other ions. When this value was compared with the single ion containing system (non competitive system), the value was lower than that of the single system. The competitive adsorption capacities of Pb(II) ion imprinted cryogels for Pb(II), Cu(II), Cd(II), and Zn(II) ions under competitive manner were 17.94 mg/g, 2.78 mg/g, 2.10 mg/g, and 2.40 mg/g, respectively. The relative selectivity coefficients for Pb(II)/Cu(II), Pb(II)/Cd(II), and Pb(II)/Zn(II) pairs were calculated as 6.00, 11.63, and 9.60, respectively. The highest relative selectivity coefficient was determined for Pb(II)/Cd(II) pair because of the highest difference of ionic radii and Lewis acid characters for Pb(II) and Cd(II) ions as discussed before.

Table 4.24. Competitive adsorption of heavy metal ions by Pb(II) ion imprinted cryogel from multi-metal ions solution.

Ion	Adsorption Capacity, mg/g	$K_d$ , mL/mg	$k'$
Pb(II)	17.94	0.096	-
Cu(II)	2.78	0.016	6.00
Cd(II)	2.10	0.0087	11.03
Zn(II)	2.40	0.010	9.60

Concentration of each metal ion, 100 ppm; pH 5.5; and temperature 25°C. Non-competitive adsorption capacity for template Pb(II) ion: 28.38 mg/g.

#### 4.2.4. Simultaneous Competitive Adsorption on Ion Imprinted Cryogels

Generally water and wastewater samples in the nature contain several heavy metal ions, therefore competitive adsorptions of Cu(II), Cd(II), Pb(II), and Zn(II) ions were also studied by each of ion imprinted cryogel membranes [Cu(II), Cd(II), Pb(II)], simultaneously. The total adsorption capacity for each heavy metal ion was calculated from initial and final solution concentrations whereas the specific adsorption capacity for each ion imprinted cryogels was calculated from elution solutions. A competitive heavy metal ion solution containing 100 ppm of each of Cu(II), Cd(II), Pb(II), Zn(II), Ni(II), Ca(II) Co(II), and Fe (III) ions at a constant pH (5.5) and at 25°C was simultaneously incubated with Cu(II), Cd(II), and Pb(II) imprinted cryogel membranes in batch system. Total and specific adsorption capacity values are summarized in Table 4.26. The adsorbed amounts for Cu(II), Cd(II) and Pb(II) ions were higher than those of other ions but when these values were compared with the single systems for these ions (non competitive systems) the values were lower than those of single systems. The results indicated that heavy metal ions have antagonistic effects on the template ions due to the competition between template and others.

Table 4.25. Simultaneous competitive adsorption of heavy metal ions by Pb(II), Cu(II), and Cd(II) ion imprinted cryogels from multi metal ions solution.

Ions	Adsorption capacity, mg/g			
	Total	Cu-2	Cd-2	Pb-2
Pb(II)	18.35	2.30	2.94	12.4
Cd(II)	13.74	1.80	9.30	1.50
Cu(II)	11.58	8.70	1.60	1.10
Zn(II)	3.10	0.60	1.40	0.30
Co(II)	1.96	0.90	0.40	0.30
Ca(II)	2.20	0.60	1.10	0.07
Ni(II)	1.74	0.30	0.70	0.50
Fe(III)	1.38	0.40	0.10	0.60
Total	54.05	15.6	17.54	16.77

#### 4.4. Desorption and Reuse

Reuse of polymeric membranes because of improving process economics is important [189]. First each of ion imprinted cryogels was incubated with 20 mL of nitrate solution of imprinted ion (100 ppm) for 2 h separately. Then heavy metals adsorbed onto these membranes were desorbed with 100 mmol of Na<sub>2</sub>(EDTA) solution and desorbed amounts of cryogels were measured after 3 h. These adsorption-desorption cycles were repeated for three times. After 3<sup>rd</sup> cycle, the adsorption capacities for all ion imprinted cryogels did not significantly decrease. These results indicated that the proposed cryogels were cost-friendly adsorbents and the applied desorption process was appropriate and did not cause any structural and functional problem for these ion imprinted cryogels.

Table 4.26. Adsorption/desorption/regeneration cycles for ion imprinted cryogels.

Cycle No	Cu-2		Cu*-2		Cd-2		Pb-2	
	Ads, mg/g	Des, %	Ads, mg/g	Des, %	Ads, mg/g	Des, %	Ads, mg/g	Des, %
1	13.5	97.8	15.6	99.2	11.0	97.4	20.8	96.5
2	13.3	96.2	15.6	98.5	10.8	98.3	20.4	98.2
3	13.2	97.6	15.4	98.8	10.5	97.6	20.2	96.9

Ads: adsorption capacity; Des: desorption ratio. Concentration of each metal ion: 50 ppm; pH: 5.5; and temperature: 25°C.

#### 4.5. Comparison with Literature

Different materials have been used as adsorbents for adsorption of heavy metals from wastewater. Adsorption capacities of several adsorbents which were used in other studies are compared with this study (Table 4.28)

Table 4.27. Comparison of this study with other studies.

Adsorbent	Adsorption capacity, mg/g			Ref.
	Cu(II)	Cd(II)	Pb(II)	
Ion imprinted poly(HEMA) based	77.19	86.7	122.7	this study
Magnetic ion imprinted poly(HEMA) based	182.7			this study
Poly(HEMA-co-MAPA)	23.8			[190]
Poly(EGDMA-HEMA) microbeads		9.7	38.3	[191]
Poly(EGDMA-MAH) microbeads	48			[192]
Poly(vinylalcohol)/Cibacron Blue F3GA-poly(propylene) fibers			46	[193]
Polyporous versicolor			118.2	[194]
Shell of lentil	8.98			[195]
Alkali Blue 6B-poly(HEMA) films		41.4	64.5	[196]
Poly(HEMA-VIM) composite cryogel	2.5	5.8	7.6	[197]
Magnetic EDTA-modified Chitosan/SiO <sub>2</sub> / Fe <sub>3</sub> O <sub>4</sub>	3.1	5.06	8.3	[198]
Ca <sub>3</sub> (PO <sub>3</sub> ) <sub>2</sub> -modified carbon		23		[199]
Cd(II)-IIP dual-ligand reagent (2Z)-N,N-bis(2-aminoethyl)but-2-enediamide polymer		32.56		[200]
Cd(II)-IIP phenol-formaldehyde-Cd(II)-2-(p-sulphophenylazo)-1,8-dihydroxynaphthalene-3,6-disulphonate polymer		0.27		[201]
Pb(II)-imprinted 2-vinylpyridine polymer			75.4	[202]
Pb(II)-imprinted 2-aminobenzonitrile-4-vinyl pyridine			38.9	[203]
Cu(II)-imprinted amino-functionalized activated carbon sorbent	26.71			[204]
Cd(II) imprinted mercapto-functionalized silica gel sorbent		83.9		[86]
magnetic Cu(II) ion imprinted composite adsorbent (Cu(II)-MICA)	71.36			[205]
Cu(II) Ion-imprinted chitosan (CS) microsphere	201.6			[206]
Cu(II)-imprinted functionalized silica gel adsorbent	67.3			[207]

## 5. CONCLUSION

Amino acid based functional monomers [N-methacryloyl-L-histidine (MAH), N-methacryloyl-L-cysteine (MAC), and N-methacryloyl-L-aspartic acid (MAAsp)] were used for coordination of heavy metal ions [Cu(II), Cd(II), and Pb(II)] and were used in the synthesis of cryogel networks. These cryogels were characterized by FTIR spectrometry.

The specific surface areas of ion imprinted cryogels for Cu(II) magnetic, Cu(II), Cd(II), and Pb(II) were 106,43.4, 92, and 78 m<sup>2</sup>/g, respectively, the surface areas of non-imprinted cryogels, were 78.5, 18.6, 47, and 29.3 m<sup>2</sup>/g. The pore diameters of cryogels were between 16-33 Å.

The morphology of ion imprinted cryogels and non-imprinted cryogels was examined with a scanning electron microscope (SEM). These cryogels consisted of interconnected cavities and have a macroporous structure. The sizes of these cavities were between 0.4-1.6 µm.

Elemental composition of ion imprinted and non-imprinted cryogels was measured by EDX method. Nitrogen content of non-imprinted cryogels was higher than that of ion imprinted cryogels.

Cd(II) ion imprinted cryogel membranes were prepared by bulk polymerization of HEMA (monomer), N, N'-methylenebisacrylamide (cross linker), and MAC-Cd(II) pre-complex (imprinted molecule). These membranes were prepared for three different compositions (0.05, 0.1, and 0.2 mmol of MAC-Cd (II) pre-complex). With increasing amount of pre-complex, amount of imprinting cavities increased and adsorption capacity of membranes increased as well.

Cu(II) ion imprinted cryogel membranes were prepared in two different forms: magnetic and non-magnetic. Fe<sub>3</sub>O<sub>4</sub> nanoparticles were added to polymerization solution for preparing magnetic imprinted cryogels. These nanoparticles evaluate magnetic effect of membranes and create surface imprinted cavities. Magnetic effect improved adsorption capacity of membranes.

Cu(II) ion imprinted cryogel membranes were prepared by bulk polymerization of HEMA (monomer), N, N'-methylenebisacrylamide (cross linker), and MAH-Cu(II)

pre-complex (imprinted molecule). These membranes were prepared for three compositions (0.05, 0.1, and 0.2 mmol of MAH-Cu(II) pre-complex). With increasing amount of pre-complex, amount of imprinted cavities increased and adsorption capacities of membranes increased.

Cu(II) ion imprinted magnetic cryogel membranes were similarly prepared by bulk polymerization of HEMA (monomer), N, N'-methylenebisacrylamide (cross linker), MAH-Cu (II) pre-complex (imprinting molecule) and Fe<sub>3</sub>O<sub>4</sub> nanoparticles. These membranes were prepared in nine compositions (0.05, 0.1, and 0.2 mmol of MAH-Cu(II) pre-complex and 50, 100, and 150 mg of Fe<sub>3</sub>O<sub>4</sub> nanoparticles). With increasing amount of pre-complex and Fe<sub>3</sub>O<sub>4</sub> nanoparticles, amount of imprinted cavities increased and adsorption capacities of membranes increased.

Pb(II) ion imprinted cryogel membranes were prepared by bulk polymerization of HEMA (monomer), N, N'-methylenebisacrylamide (cross linker), and MAAsp-Pb(II) pre-complex (imprinted molecule). These membranes were prepared in three compositions (0.05, 0.1, 0.2 mmol of MAAsp-Pb(II) pre-complex). With increasing amount of pre-complex, amount of imprinting cavities increased and adsorption capacities of membranes increased.

Non-imprinted cryogel membranes (HEMA-MAH, HEMA-MAC, and HEMA-MAAsp) were prepared by bulk polymerization of HEMA monomer), N, N'-methylenebisacrylamide (cross linker) and 0.1 mmol of MAH, MAC, and MAAsp (functional monomer). Adsorption capacities of these non-imprinted cryogels were less than those of ion imprinted cryogels for the same composition of cryogel and under the same experimental conditions.

Adsorption of metals by cryogels was affected by medium pH, because of the influence of complexation reactions by the electrostatic attractions between the surface charges and the dissolved ions. With decreasing pH of medium (increasing amount of H<sup>+</sup> ions), adsorption of metals decreased.

Initial concentration of metal ions affected the amount of adsorbed metals by cryogel membranes. Initially with increasing initial concentration, amount of adsorbed metal increased but then reached equilibrium because of saturation of cavities by metal ions.



Adsorption capacity of ion imprinted cryogels was affected by medium temperature. With increasing temperature electrostatic interaction of solutes decreased in water and eventually decreased the amount of adsorbed metals. The maximum adsorption capacities for these cryogels were obtained at +4 °C.

Contact time of ion imprinted cryogels and metal ions solution effect the adsorption capacity. Initially rate of adsorption was very fast, and then the adsorption rate slowed down and reached equilibrium because of filling of cavities available for adsorption.

Langmuir and Freundlich isotherms were applied for these adsorption processes. The Langmuir model gave the higher  $R^2$  (correlation coefficient) values; therefore adsorption of metal ions by ion imprinted cryogels was best described by Langmuir model. Also the  $R_L$  values were between 0 and 1, indicating that the adsorption of metal ions on the ion imprinted cryogels was favorable under the conditions being studied.  $1/n$  values obtained from the Freundlich model were below one but were close to one, therefore the adsorption was homogeneous and monolayered (Langmuir model).

Thermodynamic parameters were calculated by Langmuir isotherms of cryogels for different temperatures and Van't Hoff plots ( $\Delta G^\circ$ ,  $\Delta H^\circ$ , and  $\Delta S^\circ$ ).  $\Delta G^\circ$  values indicated the feasibility of process and spontaneous nature of adsorption.  $\Delta H^\circ$  values were negative; this implies the exothermic nature of the adsorption and  $\Delta S^\circ$  values were positive and this indicates that there was an increase in the randomness of heavy metal adsorption at the cryogel–solution interface.

Pseudo first-order and pseudo second-order kinetic models were applied for adsorption of metal ions by ion imprinted cryogels. The correlation coefficients ( $R^2$ ) of the pseudo second-order model were higher than those of the pseudo first-order model. Thus, the second-order model was more suitable to predict the kinetics of adsorption of metal ions onto the ion imprinted cryogels. Also the calculated  $Q_{\max}$  values by second-order model agree very well with the experimental values.

Competitive adsorption of Cu(II) ions by Cu(II) ion imprinted magnetic and non-magnetic cryogels with three other metal ions (Cd, Pb, and Zn) were examined.

The amount of adsorbed Cu(II) ion by magnetic and non-magnetic Cu(II) ion imprinted cryogels was higher than those of the other metal ions, but the amount of Cu(II) ion that was adsorbed for these competitive systems were lower than single ion containing system (without competitive metal ions).

Competitive adsorption of Cd(II) ions by Cd(II) ion imprinted cryogels with three other metal ions (Cu, Pb and Zn) was examined. The amount of adsorbed Cd(II) ion by Cu(II) ion imprinted cryogels was higher than those of the other metal ions, but the amount of Cd(II) ion that was adsorbed for these competitive systems was lower than that of single system (without competitive metal ions).

Competitive adsorption of Pb(II) ions by Pb(II) ion imprinted cryogels with three other metal ions (Cu, Cd and Zn) was examined. The amount of adsorbed Pb(II) ion by Pb(II) ion imprinted cryogels was higher than those of the other metal ions, but the amount of Pb(II) ion that was adsorbed for these competitive systems was lower than that of single system (without competitive metal ions).

Competitive adsorption of Cu(II), Cd(II) and Pb(II) by Cu(II), Cd(II) and Pb(II) ion imprinted cryogels in one system with other metal ions (Zn(II), Ni(II), Ca(II), Co(II) and Fe(III)) was examined. Adsorption capacity order was Pb(II) > Cd(II) > Cu(II) > Zn(II) > Ca(II) > Co(II) > Ni(II) > Fe(III). Adsorbed amounts of imprinted metal ions were higher than the other ions but these amounts were lower than those of single systems.

Reuses of these cryogels were examined for three cycles. Percent of desorption ratios of metal ions after three cycles was about 97%.

## 6. REFERENCES

- [1] Hani, H., The analysis of inorganic and organic pollutants in soil with special regard to their bioavailability, *International Journal of Environmental Analytical Chemistry*, 39(2), 197-208, **1990**.
- [2] Gündüz, T., *Environmental chemistry*, Gazi Kitabevi, Ankara, **2008**.
- [3] Zitka, O., Ryvolova, M., Hubalek, J., Eckschlager, T., Adam, V., Kizek, R., From Amino Acids to Proteins as Targets for Metal-based Drugs Current Drug Metabolism, 13(3 t), 306-320, **2012**.
- [4] Waldron, H.A., Lead poisoning in the ancient world, *Medical History*, 17, 391-399, **1973**.
- [5] Fu, F., Wang, Q., Removal of heavy metal ions from wastewaters, *Journal of Environmental Management*, 92, 3, 407- 418, **2011**.
- [6] Barakat, M.B., New trends in removing heavy metals from industrial wastewater, *Arabian Journal of Chemistry*, 4, 361-377, **2011**.
- [7] Asouhidou, D.D., Lazaridis, N.K., Matis, K.A., Sorbent Materials for Metal Ions Removal from Aqueous Solutions, *Protection and Restoration of Environment*, VII, Mkonos, **2004**.
- [8] Yadla, S.V., Sridevil, V., Lakshmi, M.V., A Review on Adsorption of Heavy Metals from Aqueous Solution, *Journal of Chemical, Biological and Physical Sciences*, 2, 3, 1585-1593, **2012**.
- [9] Ayhan, H., *Polimerik Biyomalzemeler*, TÜBİTAK Bilim ve Teknik, 8-11, **2002**.
- [10] Crini, G., Recent developments in polysaccharide-based materials used as adsorbents in wastewater treatment, *Progress in Polymer Science*, 30, 38–70, **2005**.
- [11] Dainiak, D.A., Kumar, A., Galaev, I.V., Mattiasson, B., Detachment of affinity- captured bioparticles by elastic deformation of a macroporous hydrogel, *PANS*, 103, 4, 849–854, **2006**.
- [12] Kumar, A., Bansal, V., Nandakumar, K, S., Integrated bioprocess for the production and isolation of urokinase from animal cell culture using supermacroporous cryogel matrices, *Biotechnology and Bioengineering*, 93, 4, 636–646, **2006**.
- [13] Wang, X., Min, B.G., Cadmium sorption properties of poly(vinyl alcohol) /hydroxyapatite cryogels: I. kinetic and isotherm studies *Journal of Sol -Gel Science and Technology*, 43, 99, **2007**.
- [14] Sener, G., Uzun, L., Say, R., Denizli, A., Use of molecular imprinted nanoparticles as biorecognition element on surface plasmon resonance sensor, *Sensors and Actuators Chemical*, 160, 1, 791–799, **2011**.

- [15] Lopes, C.S., Descalzo, A.B., Raimundo, I.M., Orellana, G., Moreno-Bondi, M.C., Fluorescent ion-imprinted polymers for selective Cu(II) optosensing, *Anal. Bioanal. Chem*, 402 , 3253–3260, **2012**.
- [16] Mafu, L.D., Msagati, T.A.M., Mamba, B.B., Adsorption studies for the simultaneous removal of arsenic and selenium using naturally prepared adsorbent materials, *Environ. Sci. Pollut. Res.*, 20, 790–802, **2013**.
- [17] Dunnick, J.K., Fowler, B.A., *Handbook on Toxicity of Inorganic Compounds*, Marcel Dekker, New York, 155, **1988**.
- [18] Blais, J, F., Djedidi, Z., Cheikh, R.B., Tyagi, R.D., Mercier, G., Metals Precipitation from Effluents: Review, *Practice Periodical of Hazardous, Toxic, and Radioactive Waste Management ASCE*, 135-149, **2008**.
- [19] Nordberg, G.F., Fowler, B.A., Nordberg, N., Friberg, L., *Handbook on Toxicology of Metals*, Elsevier, U.S.A, 6-10, **2007**.
- [20] Peters, R.W., Bhattacharyya, D., *Environmental Separation of Heavy Metal*, AIChE Symposium Series, 81, 243, 165-203, **1985**.
- [21] Dean, j.G., Bosqui, F.L., Lanouette, K.H., Removing heavy metals from waste water, *Environmental Science & Technology*, 6, 6, 518-522, **1972**.
- [22] Pletcher, D., *New, METAL ION REMOVAL FROM EFFLUENTS*, *Electrosynthesis*, 2, 3, **1996**.
- [23] Atkins, P.W., *Physical Chemistry*, Oxford University Press, **1998**.
- [24] Juang, R.S., Shiau, R.C., Metal removal from aqueous solutions using chitosan-enhanced membrane filtration, *J. Membr. Sci*, 165, 159 –167, **2000**.
- [25] Langmuir, I., The constitution and fundamental properties of solids and liquids, *J. Am. Chem. Soc*, 38(11), 2221, **1916**.
- [26] Freundlich, H.M.F., *Uber die adsorption in losungen*, *Z. Phys. Chem. A*, 57, 385, **1906**.
- [27] Solener, M., Tunali, S., Ozcan, S.A., Ozcan, A., Gedikbey, T., Adsorption characteristics of lead (II) ions onto the clay/ poly (methoxyethyl) acrylamide (PMEA) composite from aqueous solutions, *Desalination*, 223, 308–322, **2008**.
- [28] Moufliha, M., Aklila, A., Sebti, S., Removal of lead from aqueous solutions by activated phosphate. *J. Hazard. Mater*, B119, 183–188, **2005**.
- [29] Essawy, H.A., Ibrahim, H.S., Synthesis and characterization of poly(vinylpyrrolidone-co-methylacrylate) hydrogel for removal and recovery of heavy metal ions from wastewater, *React. Funct. Polym.*, 61, 421–432, **2004**.
- [30] Das, N., Vimala, R., Karthika, P., Biosorption of heavy metals—An overview, *Indian Journal of Biotechnology*, 7, 159-169, **2008**.

- [30] Alinnor, J., Adsorption of heavy metal ions from aqueous solution by fly ash, *Fuel*, 86, 853–857, **2007**.
- [31] Uysal, M., Ar, I., Removal of Cr(VI) from industrial waste by adsorption: Part I: Determination of optimum conditions, *J. Hazard. Mater.*, 149, 482–491, **2007**.
- [32] Kesenci, K., Say, R., Denizli, A., Removal of heavy metal ions from water by using poly(ethyleneglycol dimethacrylate-co-acrylamide) beads, *Eur. Polym. J.*, 38, 1443–1448, **2002**.
- [33] Barakat, M.A., Sahiner, N., Cationic hydrogels for toxic arsenate removal from aqueous environment, *J. Environ. Manage*, 88, 955–961, **2008**.
- [34] Lozinsky, V. I., Galaev, I. Y., Plieva, F. M., Savina, I. N., Jungvid, H., Mattiasson, B., Polymeric cryogels as promising materials of biotechnological interest, *Trends in Biotechnology*, 21, 10, 445–451, **2003**.
- [35] Lozinsky, V.I., Damshkaln, L.G., Shaskol'skii, B.L., Babushkina, T.A., Study of cryostructuring of polymer systems: 27. Physicochemical properties of poly(vinyl alcohol) cryogels and specific features of their macroporous morphology, 69, 6, 747-764, **2007**.
- [36] Tripathi, A., Kathuria, N., Kumar, A., Elastic and macroporous agarose–gelatin cryogels with isotropic and anisotropic porosity for tissue engineering, *Journal of Biomedical Materials Research*, 90, 3, 680–694, **2008**.
- [37] Kathuria, N., Tripathi, A., Kar, K.K., Kumar, A., Synthesis and characterization of elastic and macroporous chitosan–gelatin cryogels for tissue engineering *Acta Biomaterialia*, 5, 1, 406– 418, **2009**.
- [38] Lozinsky, V.L., Cryogels on the basis of natural and synthetic polymers: preparation, properties and application, *Russ. Chem. Rev.*, 71, 489–511, **2002**.
- [39] Hjorth, R., Expanded bed adsorption: elution in expanded bed mode, *EXPAND BED CHROMATOGRAPHY*, 1-9, **1999**.
- [40] Arvidsson, P., Pileva, F.M., Lozinsky, V.I., Galaev, I.Y., Mattiasson, B., Direct chromatographic capture of enzyme from crude homogenate using immobilized metal affinity chromatography on a continuous supermacroporous adsorbent, *J. Chromatography. A.*, 986, 2, 275–290, **2003**.
- [41] Chase, H. A., Purification of proteins by adsorption chromatography in expanded beds, *Trends Biotechnol*, 12, 296–303, **1994**.
- [42] Kokufuta, E., Functional immobilized biocatalysts, *Progress in polymer science*, 17, 4, 647-697, **1992**.
- [43] Hayashi, T., Hyon, S., Lipoprotein lipase immobilization onto porous polyvinyl alcohol beads, *J. Appl. Polym. Sci.*, 49, 12, 2121–2127, **1993**.

- [44] Lozinsky, V., What New opporunites the Use of Viverse Polymeric Cryogels Opens for the Immobilization of Molecules and Cells, *Russian Academy of Science*, 58, 6a, 111-115, **2004**.
- [45] Scardi, V., Immobilization of enzymes and microbial cells in gelatin, *Methods in Enzymology*, 135, 293–299, **1987**.
- [46] Önnby, L., Pakade, V., Mattiasson, B., Kirsebom, H., Polymer composite adsorbents using particles of molecularly imprinted polymers or aluminium oxide nanoparticles for treatment of arsenic contaminated waters, *Water Research*, 46, 13, 4111-4120, **2012**.
- [47] Hajizadeh, S., Kirsebom, H., Mattiasson, B., Characterization of macroporous carbon-cryostructured particle gel, an adsorbent for small organic molecules, *Soft Matter*, 6, 5562–5569, **2010**.
- [48] Tekin, K., Uzun, L., Sahin, C. A., Bektas, S., Denizli, A., Preparation and Characterization of Composite Cryogels Containing Imidazole group and Use in Heavy Metal Removal, *Reactive & Functional Polymers*, 71, 985–993, **2011**.
- [49] Papancea, A., Valente, A.J.M., Patachia, A., PVA cryogel membranes as promising tool for the retention and separation of metal ions from aqueous solutions, *Journal of Applied Polymer Science*, 118, 3, 1567-1573, **2010**.
- [50] Noir, M.A., Plieva, F., Hey, T., Guieysse, B., Mattiasson, B., Macroporous molecularly imprinted polymer/cryogel composite systems for the removal of endocrine disrupting trace contaminants, *Journal of Chromatography A* 1145, 1, 158-164, **2007**.
- [51] Abu Qdaisa, H., Moussab, H., Removal of heavy metals from wastewater by membrane processes: a comparative study, *Desalination*, 164, 105–110, **2004**.
- [52] Zuoa, W., Zhanga, G., Mengb, Q., Zhangb, H., Characteristics and application of multiple membrane process in plating wastewater reutilization, *Desalination* 222, 187–196, **2008**.
- [53] Rether, A., Schuster, M., Selective separation and recovery of heavy metal ions using water-soluble N-benzoylthiourea modified PAMAM polymers, *React. Funct. Polym.*, 57, 13–21, **2003**.
- [54] Petrov, S., Nenov, V., Removal and recovery of copper from wastewater by a complexation–ultrafiltration process, *Desalination*, 162, 201–209, **2004**.
- [55] Barakat, M.A., Removal of Cu(II), Ni(II), and Cr(III) ions from wastewater using complexation–ultrafiltration technique. *J. Environ. Sci. Technol.*, 1, 3, 151–156, **2008**.
- [56] Trivunac, K., Stevanovic, S., Removal of heavy metal ions from water by complexation-assisted ultrafiltration, *Chemosphere*, 64, 3, 486–491, **2006**.

- [57] Ferella, F., Prisciandaro, M., De Michelis, I., Veglio, F., Removal of heavy metals by surfactant-enhanced ultrafiltration from wastewaters, *Desalination*, 207, 125–133, **2007**.
- [58] Arthanareeswaran, G., Thanikaivelan, P., Jaya, N., Mohana, D., Raajenthiren, M., Removal of chromium from aqueous solution using cellulose acetate and sulfonated poly(ether ether ketone) blend ultrafiltration membranes. *J. Hazard. Mater.*, 139, 44–49, **2007**.
- [59] Nagendran, A., Vijayalakshmi, A., Arockiasamy, D.L., Shobana, K.H., Mohan, D., Toxic metal ion separation by cellulose acetate/sulfonated poly(ether imide) blend membranes: effect of polymer composition and additive, *J. Hazard. Mater.*, 155 (3), 477– 485, **2008**.
- [60] Vijayalakshmi, A., Arockiasam, D.L., Nagendran, A., Mohan, D., Separation of proteins and toxic heavy metal ions from aqueous solution by CA/PC blends ultrafiltration membranes, *Sep. Purif. Technol*, 62, 32–38, **2008**.
- [61] Mavrov, V., Erwe, T., Blocher, C., Chmiel, H., Study of new integrated processes combining adsorption, membrane separation and flotation for heavy metal removal from wastewater, *Desalination*, 157, 97–104, **2003**.
- [62] Blocher, C., Dorda, J., Mavrov, V., Chmiel, H., Lazaridis, N.K., Matis, K.A., Hybrid flotation—membrane filtration process for the removal of heavy metal ions from wastewater, *Water Res.*, 37, 4018–4026, **2003**.
- [63] Nenov, V., Lazaridis, N.K., Blocher, C., Bonev, B., Matis, K.A., Metal recovery from a copper mine effluent by a hybrid process, *Chem. Eng. Process*, 47, 596–602, **2008**.
- [64] Klaassen, R., Feron, P., Jansen, A., Membrane contactor applications, *Desalination*, 224, 81–87, **2008**.
- [65] Madaeni, S.S., Mansourpanah, Y., COD removal from concentrated wastewater using membranes, *Filtration Sep.*, 40, 40–46, **2003**.
- [66] Chen, G.H., Electrochemicals technologies in wastewater treatment, *Sep. Purif. Technol.*, 38, 1, 11–41, **2004**.
- [67] Tzanetakis, N., Taama, W.M., Scott, K., Jachuck, R.J.J., Slade, R.S., Varcoe, J., Comparative performance of ion exchange membrane for electro dialysis of nickel and cobalt, *Sep. Purif. Technol.*, 30, 113–127, **2003**.
- [68] Mohammadi, T., Mohebb, A., Sadrzadeh, M., Razmi, A., Modeling of metal ion removal from wastewater by electro dialysis, *Sep. Purif. Technol*, 41, 73– 82, **2005**.
- [69] Barakat, M.A., Adsorption behavior of copper and cyanide ions at TiO<sub>2</sub>-solution interface, *J. Colloid Interface Sci.*, 291, 345–352, **2005**.

- [70] Zhang, F.S., Itoh, H., Photocatalytic oxidation and removal of arsenite from water using slag–iron oxide–TiO<sub>2</sub> adsorbent, *Chemosphere*, 65, 1, 125–131, **2006**.
- [71] Denizli A., Salih B., Pişkin E., Alkali blue 6B-attached poly(EGDMA-HEMA) microbeads for removal of heavy-metal ions, *React. Funct. Polym.*, 29, 1,11-19, **1996**.
- [72] Soutif, J.C., Brosse, J.C., Chemical modification of polymers, *Reactive Polymer*, 13, 1-26, **1990**.
- [73] Flora, S.J.S., Pachauri, V., Chelation in Metal Intoxication, *Int.J.Envirn.Res. Public Health*, 7, 7, 2745-2788, **2010**.
- [74] Ruzicka, J., Arndal, A., Sorbent extraction in flow-injection analysis and its application enhancement of atomic spectrometry, *Analytica Chimica Acta*, 216, 243-255, **1989**.
- [75] Madoni, P., Davoli, D., Gorbi, G., Vescovi, L., Toxic effect of heavy metals on the activated sludge protozoan community , *Water Research*, 30,135-142, **1996**.
- [76] Han, J.X., Shang, Q., Du, Y., effect of environmental cadmium pollution on human health, *Health*, 159-166, **2009**.
- [77] Fernandes, J.C., Henriques, F.C., Biochemical, physiological and structural effects of excess copper in plants, *Bot. Rev.*, 57, 246–273, **1991**.
- [78] Klassen, C., *Casarett & Doull's Toxicology: The Basic Science of Poisons*, 8.Edition, Fulfilled by Amazon, 715-730, **2013**.
- [79] Voluntary Estuary Monitoring Manual Chapter 12: Contaminants and Toxic Chemicals Heavy metals, Pesticides, PCBs, and PAHs, [http://www.water.epa.gov/type/oceb/nep/upload/2009\\_03\\_13\\_estuaries\\_mit\\_orchap12.pdf](http://www.water.epa.gov/type/oceb/nep/upload/2009_03_13_estuaries_mit_orchap12.pdf) (**March 2006**).
- [80] Arnold, H., Egon, W., Nils, W., "*Blei*". *Lehrbuch der Anorganisc Chemie*, Walter de Gruyter, Germany, 801–810, **1985**.
- [81] Golub, M. S., "Summary". Metals, fertility, and reproductive toxicity, Taylor and Francis, 153, ISBN 978-0-415-70040-5, **2005**.
- [82] EPA, Basic Information about Lead in Drinking Water, <http://water.epa.gov/drink/contaminants/basicinformation/lead.cfm> .
- [83] Malachowski, L., Stair, J.L., Holcombe, J.A., FRET Peptidyl Sensors for the Detection of Metal Ions, *UM Microform*, 76, 4, 777-787, **2004** .
- [84] Passerini, A., Punta, M., Ceroni, A., Rost, B., Frasconi, P., <http://citeseerx.ist.psu.edu/viewdoc/download?doi:10.1.1.123.rep>.
- [85] Li, Z.C., Fan, H.T., Zang, Y., Cd(II)-imprinted polymer sorbents prepared by combination of surface imprinting technique with hydrothermal assisted



- sol-gel process for selective removal of cadmium(II) from aqueous solution, *Chemical Engineering Journal*, 171, 2, 730-710, **2011**.
- [86] Buhani, Narsito, Nuryono, Kunarti, E.S., Production of metal ion imprinted polymer from mercapto-silica through sol-gel process as selective adsorbent of cadmium, *Desalination*, 251, 1-3, 83-89, **2010**.
- [87] Bahrami, S., Bassi, A.S., Yanful, E., Polyethyleneimine-containing sol-gels as novel sorbents for the removal of cadmium from aqueous solutions, *The Canadian J. of Chemical Engineering*, 77, 931-935, **1999**.
- [88] Faghihian, H., Nejati-Yazdinejad, M., Sorption Performance of cysteine-modified Bentonite in Heavy Metal Uptake, *J. of Serbian Chemical Society*, 74, 833-843, **2009**.
- [89] Özkütük, E.B., Özalp, E., Ersoz, A., Thiocyanate separation by imprinted polymeric systems, *Microchim Acta*, 169, 129-135, **2010**.
- [90] Candan, N., Magnetic ion-imprinted beads for cadmium removal from aqueous solutions, *Anadolu University Journal of Science and Technology*, 9, 135-146, **2008**.
- [91] Gawin, M., Konefał, J., Trzewik, B., Walas, S., Tobiasz, A., Mrowiec, H., Witek, E., Preparation of a new Cd(II)-imprinted polymer and its application to determination of cadmium(II) via flow-injection-flame atomic absorption spectrometry, *Talanta*, 80, 3, 1305-1310, **2010**.
- [92] Alizadeh, T., An imprinted polymer for removal of Cd<sup>2+</sup> from water samples: Optimization of adsorption and recovery steps by experimental design, *Chinese J. of Polymer Science*, 29, 6, 658-669, **2011**.
- [93] Singh, C.K., Sahu, J.N., Mahalik, K.K., Studies on the removal of Pb(II) from wastewater by activated carbon developed from Tamarind wood activated with sulphuric acid, *J. of Hazardous Materials*, 154, 2-3, 1547-51, **2009**.
- [94] Segatelli, M.G., Santos, V.S., Presotto, A.B.T., Yoshida, I.V.P., Tarley, C.R.T., Cadmium ion-selective sorbent preconcentration method using ion imprinted poly(ethylene glycol dimethacrylate-co-vinylimidazole), *Reactive and Functional Polymers*, 70, 6, 326-333, **2010**.
- [95] Adie, B.D., Okuofu, C.A., Osakwe, C., Comparative Analysis of the Adsorption of Heavy Metals in Wastewater Using Borrassus Aethiopicum and Cocos Nucifera, *International Journal of Applied Science and Technology*, 2, 7, **2012**.
- [96] Abollino, O., Aceto, M., Malandrino, M., Sarzanini, C., Mentasti, E., Adsorption of heavy metals on Na-montmorillonite. Effect of pH and organic substances, *Water Research*, 37, 1619-1627, **2003**.
- [97] Heechan, Ch., Dalyoung, O., Kwanho, K., A study on removal characteristics of heavy metals from aqueous solution by fly ash, *Journal of Hazardous Materials*, 127, 1-3, 187-195, **2005**.

- [98] NiÑă, I., Iorgulescu, M., Spiroiu, M.F., Ghiurea, M., Petcuand, C., Cintează, O., THE ADSORPTION OF HEAVY METAL IONS ON POROUS CALCIUM ALGINATE MICROPARTICLES, *Chimie, Anul XVI (serie nouă)*, 1, 59 – 67, **2007**.
- [99] Zhang, M., Zhang, Z., Liua, Y., Yanga, X., Luoa, L., Chena, L., Yaob, Sh., *Chemical Engineering Journal*, 178, 443– 450, **2011**.
- [100] Zhu, L., Zhu, Z., Zangh, R., Hong, J., Qiu, Y., Synthesis and adsorption performance of lead ion-imprinted micro-beads with combination of two functional monomers, *Journal of Environmental Sciences*, 23,12, 1955–1961, **2011**.
- [101] Boevski, I.V., Daskalova, N., A METHOD FOR DETERMINATION OF TOXIC AND HEAVY METALS IN SUSPENDED MATTER FROM NATURAL WATERS BY INDUCTIVELY COUPLED PLASMA ATOMIC EMISSION SPECTROMETRY (ICP-AES), *Journal of university of Chemical technology and Metallurgy*,42,4 ,419-426, **2007**.
- [102] Welz, B., Sperling, M., *Atomic Absorption Spectrometry*, Wiley-VCH, Weinheim, Germany, ISBN 3-527-28571-7, **1999**.
- [103] Piletska, E, V., Guerreiro, A, R., Whitcombe, M, J., Piletsky, S, A., Influence of the Polymerization Conditions on the Performance of Molecularly Imprinted Polymers, *Macromolecules*, 42, 4921–4928, **2009**.
- [104] Lei, Y., Cormack, P, A, C., Mosbach, K., Molecularly imprinted monodisperse microspheres for competitive radioassay, *Anal. Commun*, 36, 35-38, **1999**.
- [105] Okutucu, B., Önal, S.,Telefoncu, A., Noncovalently galactose imprinted polymer for the recognition of different saccharides, *Talanta*, 78, 1190–1193, **2009**.
- [106] Whitcombe, M, J., Rodriguez, M, E., Villar, P, Vulfson, E., A New Method for the Introduction of Recognition Site Functionality into Polymers Prepared by Molecular Imprinting: Synthesis and Characterization of Polymeric Receptors for Cholesterol, *J. Am. Chem. Soc.*, 117, 7105–7111, **1995**.
- [107] Otero- Romani, J., Moreda- Pineir, A., Bermejo- Barrera, P., Martin- Esteban, A., Synthesis, characterization and evaluation of ionic-imprinted polymers for solid-phase extraction of nickel from seawater, *Analytica Chimica Acta*, 630 ,1-9, **2008**.
- [108] Haupt, K., *Molecularly imprinted polymers in analyticalchemistry*, *Analyst*,126, 747-756, **2001**.
- [109] Sun, H.V., Qiao, F., Recognition mechanism of water-compatible molecularly imprinted solid-phase extraction and determination of nine quinolones in urine by high performance liquid chromatography. *J. Chromatogr., A*, 1212, 1–9, **2008**.

- [110] Sun, H., Qiao, F., Liu, G., Liang, S., Simultaneous isolation of six fluoroquinolones in serum samples by selective molecularly imprinted matrix solid-phase dispersion, *Anal. Chim. Acta*, 625, 154–159, **2008**.
- [111] Yan, H., Tian, M., Row, K. H., Determination of enrofloxacin and ciprofloxacin in milk using molecularly imprinted solid-phase extraction, *J. Sep. Sci.*, 31, 3015–3020, **2008**.
- [112] Benito-Peña, E., Urraca, J.L., Sellergren, B., Moreno-Bondi, M.C., Solid-phase extraction of fluoroquinolones from aqueous samples using a water-compatible stoichiometrically imprinted polymer, *J. Chromatogr. A.*, 1208, 62–70, **2008**.
- [113] Hu, X., Pan, J., Hu, Y., Li, G., Preparation and evaluation of propranolol molecularly imprinted solid-phase microextraction fiber for trace analysis of  $\beta$ -blockers in urine and plasma samples, *J. Chromatogr., A*, 1216, 190–197, **2009**.
- [114] Jing, T., Gao, X., Wang, P., Wang, Y., Lin, Y., Hu, X., Hao, Q., Zhou, Y., Mei, S., Determination of trace tetracycline antibiotics in foodstuffs by liquid chromatography-tandem mass spectrometry coupled with selective molecular-imprinted solid-phase extraction, *Anal. Bioanal. Chem.*, 393, 2009–2018, **2009**.
- [115] González, G.P., Hernando, P.F., Alegría, J.S.D., An optical sensor for the determination of digoxin in serum samples based on a molecularly imprinted polymer membrane, *Anal. Chim. Acta*, 638, 209–212, **2009**.
- [116] Chen, P., Nien, P., Wu, C., Wu, T., Lin, C., Ho, K., Fabrication of a molecularly imprinted polymer sensor by self-assembling monolayer/mediator system, *Anal. Chim. Acta*, 643, 38–44, **2009**.
- [117] Li, Y., Li, X., Li, Y., Dong, C., Jin, P., Qi, J., Selective recognition of veterinary drugs residues by artificial antibodies designed using a computational approach, *Biomaterials*, 30, 3205–3211, **2009**.
- [118] Mosbach, K., Toward the next generation of molecular imprinting with emphasis on the formation, by direct molding, of compounds with biological activity (biomimetics), *Anal. Chim. Acta*, 435, 3-8, **2009**.
- [119] Lingxin, C., Shoufang, X., Jinhua, L., Recent advances in molecular imprinting technology: current status, challenges and highlighted applications, *Chem. Soc. Rev.*, 40, 2922-2942, **2011**.
- [120] Yang, H., Zhang, S., Tan, F., Zhuang, S., Wang, X., Surface Molecularly Imprinted Nanowires for Biorecognition, *J. Am. Chem. Soc.*, 127, 1378–1379, **2010**.
- [121] Qin, L., He, X., Zhang, W., Li, W., Zhang, Y., Surface-modified polystyrene beads as photografting imprinted polymer matrix for chromatographic separation of proteins, *J. Chromatogr. A.*, 1216, 807–814, **2009**.

- [122] Wang, H., Zhou, W., Yin, X., Zhuang, Z., Yang, H., Wang, X., Template Synthesized Molecularly Imprinted Polymer Nanotube Membranes for Chemical Separations, *J. Am.Chem.Soc.*,128, 15954– 15955, **2006**.
- [123] Zhang, Y., Liu, R., Hu,Y., Li, G., Microwave Heating in Preparation of Magnetic Molecularly Imprinted Polymer Beads for Trace Triazines Analysis in Complicated Samples, *Anal. Chem.*,81, 967–976, **2009**.
- [124] Wang, X., Wang, L., He, X., Zhang,Y., Chen, L., A molecularly imprinted polymer-coated nanocomposite of magnetic nanoparticles for estrone recognition, *Talanta*, 78, 327–332, **2009**.
- [125] Wang, H., He, Y., He, X., Li, X., Chen, L., Zhang, y., BSA-imprinted synthetic receptor for reversible template recognition , *J. Sep. Sci.*,32, 1981–1986, **2009**.
- [126] Qin, L., He, X., Zhang, W., Li, W., Zhang, Y., Surface-modified polystyrene beads as photografting imprinted polymer matrix for chromatographic separation of proteins, *J. Chromatogr., A*, 1216, 807–814, **2009**.
- [127] Diltemiz, S.E., Say, R., Buyuktiryaki, Hur, D., Denizlic, A., Ersoz, A, Quantum dot nanocrystals having guanosine imprinted nanoshell for DNA recognition, *Talanta*, 75, 890–896, **2008**.
- [128] Wang, H., He, Y., Ji, T., Yuan, X., Surface Molecular Imprinting on Mn-Doped ZnS Quantum Dots for Room-Temperature Phosphorescence Optosensing of Pentachlorophenol in Water., *Anal. Chem.*, 81, 1615–1621, **2009**.
- [129] Li, Y.,Yin, X., Chen, F., Yang, H., Zhuang, Z., Wang, X.,Synthesis of Magnetic Molecularly Imprinted Polymer Nanowires Using a Nanoporous Alumina Template, *Macromolecules*, 39, 4497–4499, **2006**.
- [130] Hu, Y., Liu, R., Zhang, Y., Li, G.,Improvement of extraction capability of magnetic molecularly imprinted polymer beads in aqueous media via dual-phase solvent system ,*Talanta*, 79, 576–582, **2009**.
- [131] An, Z., Shi, Q., Tang, W., Tsung, C., Hawker, C.J., Stucky, G.D., Facile RAFT Precipitation Polymerization for the Microwave-Assisted Synthesis of Well-Defined, Double Hydrophilic Block Copolymers and Nanostructured Hydrogels, *J. Am. Chem. Soc.*,129, 14493–14499, **2007**.
- [132] Titirici, M., Borje, S., Thin Molecularly Imprinted Polymer Films via Reversible Addition–Fragmentation Chain Transfer Polymerization, *Chem. Mater.*, 18, 1773–1779, **2006**.
- [133] Sulitzky, C., Rückert, B., Hall, a.J., Lanza, F., Unger, K.,Sellergren, B., Grafting of Molecularly Imprinted Polymer Films on Silica Supports Containing Surface-Bound Free Radical Initiators, *Macromolecules*, 35, 79–91, **2002**.

- [134] Southard, G.E., Houten, K.A.V., Edward, W.O., Luminescent sensing of organophosphates using europium(III) containing imprinted polymers prepared by RAFT polymerization, *Anal. Chim. Acta*, 581, 202–207, **2007**.
- [135] Pan, G., Zu, B., Guo, X., Zhang, Y., Li, C., Zhang, H., Preparation of molecularly imprinted polymer microspheres via reversible addition–fragmentation chain transfer precipitation polymerization, *Polymer*, 50, 2819–2825, **2009**.
- [136] Lu, C., Zhou, W., Han, B., Yang, H., Chen, X., Wang, X., Surface-.... Imprinted Core–Shell Nanoparticles for Sorbent Assays, *Anal. Chem.*, 79, 5457–5461, **2007**.
- [137] Chen, Z., Cui, H., Hales, K., Li, Z., Qi, K., Pochan, D.J., Wooley, K.L., Unique Toroidal Morphology from Composition and Sequence Control of Triblock Copolymers, *J. Am. Chem. Soc.*, 127, 8592–8593, **2005**.
- [138] Li, Z., Ding, J., Day, M., Tao, M., Molecularly Imprinted Polymeric Nanospheres by Diblock Copolymer Self-Assembly, *Macromolecules*, 39, 2629–2636, **2006**.
- [139] Zhang, Y., Liu, R., Hu, Y., Li, G., Microwave Heating in Preparation of Magnetic Molecularly Imprinted Polymer Beads for Trace Triazines Analysis in Complicated Samples, *Anal. Chem.*, 81, 967–976, **2009**.
- [140] He, C., Long, Y., Pan, J., Li, K., Liu, F., Molecularly imprinted silica prepared with immiscible ionic liquid as solvent and porogen for selective recognition of testosterone, *Talanta*, 74, 1126–1131, **2008**.
- [141] Lopes Pinheiro, A.B., Descalzo, I.M., Raimundo, G., Orellana, M.C., Moreno- Bondi, Biomimetic Recognition Elements for Sensing Applications, *Anal. Bioanal. Chem.* 402, 3253–3260, **2012**.
- [142] Chen, C.Y., Yang, C.Y., Chen, A.H., Biosorption of Cu(II), Zn(II), Ni(II) and Pb(II) ions by cross-linked metal-imprinted chitosans with epichlorohydrin, *J. Environ. Manage.* 92, 796–802, **2011**.
- [143] Chen, A.H., Yang, C.Y., Chen, C.Y., Chen, C.Y., Chen, C.W., The chemically crosslinked metal-complexed chitosans for comparative adsorptions of Cu(II), Zn(II), Ni(II) and Pb(II) ions in aqueous medium, *J. Hazard. Mater.* 163 1068–1075, **2009**.
- [144] Shawky, H.A., Synthesis of ion-imprinting chitosan/PVA crosslinked membrane for selective removal of Ag(I), *J. Appl. Polym. Sci.*, 114, 2608–2615, **2009**.
- [145] Wang, S., Zhang, R., Selective Solid-Phase Extraction of Trace Copper Ions in Aqueous Solution with a Cu(II)-Imprinted Interpenetrating Polymer Network Gel Prepared by Ionic Imprinted Polymer (IIP) Technique, *Microchim. Acta.*, 154 73–80, **2006**.

- [146] Pan, J., Wang, S., Zhang, R., Trace Metal Chemistry in Arid-zone Field Soils Amended with Sewage Sludge: I. Fractionation of Ni, Cu, Zn, Cd, and Pb in Solid Phases, *Int. J. Environ. Anal. Chem.*, 86, 855–865, **2006**.
- [147] Rao, T.P., Kala, R., Daniel, S., Metal ion-imprinted polymers—Novel materials for selective recognition of inorganics, *Anal. Chim. Acta.*, 578, 105–116, **2006**.
- [148] Alizadeh, T., Ganjali, M.R., Zare, M., Application of an Hg<sup>2+</sup> selective imprinted polymer as a new modifying agent for the preparation of a novel highly selective and sensitive electrochemical sensor for the determination of ultratrace mercury ions, *Anal. Chim. Acta.*, 689, 52–59, **2011**.
- [149] Ganjali, M.R., Alizadeh, T., Azimi, F., Larjani, B., Faridbod, F., Norouzi, P., Bio-Mimetic Ion Imprinted Polymer Based Potentiometric Mercury Sensor Composed of Nano-Materials, *Int. J. Electrochem. Sci.*, 6, 5200–5208, **2011**.
- [150] Ng, S.M., Narayanaswamy, R., Demonstration of a simple, economical and practical technique utilising an imprinted polymer for metal ion sensing, *Microchim. Acta.*, 169303–311, **2011**.
- [151] Segatelli, M.G., Santos, V.S., Presotto, A.B.T., Yoshida, I.V.P., Tarley, C.R.T., Cadmium ion-selective sorbent preconcentration method using ion imprinted poly(ethylene glycol dimethacrylate-co-vinylimidazole), *React. Funct. Polym.*, 70, 325–333, **2010**.
- [152] Baghel, M. Boopathi, B. Singh, P. Pandey, T.H. Mahato, P.K. Gutch, K. Sekhar, Synthesis and characterization of metal ion imprinted nanoporous polymer for the selective recognition of copper, *Biosens. Bioelectron.*, 22, 3326–3334, **2007**.
- [153] Singh, B., Chauhan, G.S., Bhatt, S.S., Kumar, K., Metal ion sorption and swelling studies of psyllium and acrylic acid based hydrogels, *Carbohydrate Polymers*, 64, 1, 50-56, **2006**.
- [154] Fasihi, J., Ammari Alahyari, S., Shamsipur, M., Sharghi, H., Charkhi, A., Adsorption of uranyl ion onto an anthraquinone based ion-imprinted copolymer, *React. Funct. Polym.*, 71, 803–808, **2011**.
- [155] Andaç, A.M., Özyapı, E., Senel, S., Say, R., Denizli, A., Ion-Selective Imprinted Beads for Aluminum Removal from Aqueous Solutions, *Ind. Eng. Chem. Res.*, 45, 1780–1786, **2006**.
- [156] Andac, A.M., Mirel, S., Senel, S., Say, R., Ersoz, A., Denizli, a., Ion-imprinted beads for molecular recognition based mercury removal from human serum, *Int. J. Biol. Macromol.*, 40, 159–166, **2007**.
- [157] Demiralay, E.Ç., Andac, A.M., Say, R., Alsancak, G., Denizli, A., Nickel(II)-imprinted monolithic columns for selective nickel recognition, *J. Appl. Polym. Sci.*, 117, 3704–3714, **2011**.

- [158] Luo, X., Luo, S., Zhan, Y., Shu, H., Huang, Y., Tu, X., Novel Cu (II) magnetic ion imprinted materials prepared by surface imprinted technique combined with a sol–gel process, *J. Hazard. Mater.*, 192, 949–955, **2011**.
- [159] Fu, X.C., Wu, J., Nie, L., Xie, G.G., Liu, J.H., Huang, X.H., Electropolymerized surface ion imprinting films on a gold nanoparticles/single-wall carbon nanotube nanohybrids modified glassy carbon electrode for electrochemical detection of trace mercury(II) in water, *Anal. Chim. Acta.*, 720, 29–37, **2012**.
- [160] Li, T., Wu, L., Chen, S., Li, H., Xu, X., A Simple Scheme for Grafting an Ion-Imprinted Layer onto the Surface of Poly(propylene) Fibers, *Macromol. Chem. Phys.*, 212, 2166–2172, **2012**.
- [161] Milja, T.E., Prathish, K.P., Rao, T.P., Synthesis of surface imprinted nanospheres for selective removal of uranium from simulants of Sambhar salt lake and ground water, *J. Hazard. Mater.*, 188, 384–390, **2011**.
- [162] Dam, H.A., Kim, D., Selective Copper(II) Sorption Behavior of Surface-Imprinted Core–Shell-Type Polymethacrylate Microspheres, *Ind. Eng. Chem. Res.*, 48, 5679–5685, **2009**.
- [163] Li, T., Wu, L., Chen, S., Li, H., Xu, X., A Simple Scheme for Grafting an Ion-Imprinted Layer onto the Surface of Poly(propylene) Fibers, *Macromol. Chem. Phys.*, 212, 2166–2172, **2011**.
- [164] Li, T., Chen, S., Li, H., Li, Q., Wu, L., Preparation of an Ion-Imprinted Fiber for the Selective Removal of Cu<sup>2+</sup>, *Langmuir*, 27, 6753–6758, **2011**.
- [165] Gao, B., An, F., Zhu, Y., Novel surface ionic imprinting materials prepared via couple grafting of polymer and ionic imprinting on surfaces of silica gel particles, *Polymer*, 48, 2288–2297, 2007.
- [166] An, F., Gao, B., Feng, X., Adsorption and recognition properties of ionic imprinted polyamine IIP-PEI/SiO<sub>2</sub> towards Pb<sup>2+</sup> ion, *J. Appl. Polym. Sci.*, 112, 2241–2246, 2009.
- [167] Liu, Y., Liu, Z., Dai, J., Gao, J., Xie, J., Yan, Y., Selective Adsorption of Co(II) by Mesoporous Silica SBA-15-Supported Surface Ion Imprinted Polymer: Kinetics, Isotherms, and Thermodynamics Studies, *Chin. J. Chem.*, 29, 387–398, **2011**.
- [168] Milja, T.J., Prathish, K.P., Rao, T.P., Synthesis of surface imprinted nanospheres for selective removal of uranium from simulants of Sambhar salt lake and ground water, *J. Hazard. Mater.*, 188, 384–390, **2011**.
- [169] Li, F., Jiang, H., Zhang, S., An ion-imprinted silica-supported organic–inorganic hybrid sorbent prepared by a surface imprinting technique combined with a polysaccharide incorporated sol–gel process for selective separation of cadmium(II) from aqueous solution, *Talanta*, 71, 1487–1493, **2007**.

- [170] Liu, Y., Liu, Z., Wang, Y., Dai, J., Gao, J., Xie, J., Yan, Y., A surface ion-imprinted mesoporous sorbent for separation and determination of Pb(II) ion by flame atomic absorption spectrometry, *Microchim. Acta.*, 172, 309–317, **2010**.
- [171] Liu, Y., Gao, J., Li, C., Pan, J., Yan, Y., Xie, J., Synthesis and Adsorption Performance of Surface-Grafted Co(II)-Imprinted Polymer for Selective Removal of Cobalt, *Chin. J. Chem.*, 28, 548–554, **2010**.
- [172] Pan, J., Guan, W., Zhang, Z., Wang, X., Li, C., Yan, Y., Selective Adsorption of Co(II) Ions by Whisker Surface Ion-Imprinted Polymer: Equilibrium and Kinetics Modeling, *Chin. J. Chem.*, 28, 2483–2488, **2010**.
- [173] Fu, X.C., Chen, X., Guo, Z., Xie, C.G., Kong, L.T., Liu, J.H., Huang, X.J., Stripping voltammetric detection of mercury(II) based on a surface ion imprinting strategy in electropolymerized microporous poly(2-mercaptobenzothiazole) films modified glassy carbon electrode, *Anal. Chim. Acta.*, 685, 21–28, **2011**.
- [174] Ren, Y., Zhang, M., Zhao, D., Synthesis and properties of magnetic Cu(II) ion imprinted composite adsorbent for selective removal of copper, *Desalination*, 228, 135–149, **2008**.
- [175] Candan, N., Tüzmen, M., Andac, A. M., Andac, C., Say, R., Denizli, A., Cadmium removal out of human plasma using ion-imprinted beads in a magnetic column, *Mater. Sci. Eng.*, 29, 144–152, **2009**.
- [176] Nishide, H., Deguchi, J., Tsuchida, E., SELECTIVE ADSORPTION OF METAL IONS ON CROSSLINKED POLY(VINYLPYRIDINE) RESIN PREPARED WITH A METAL ION AS A TEMPLATE, *Chem. Lett.*, 169–174, **1976**.
- [177] Rao, T.P., Kala, R., Daniel, S., Metal ion-imprinted polymers—Novel materials for selective recognition of inorganics, *Anal. Chim. Acta.*, 578, 105–116, **2006**.
- [178] Mafu, L.D., Msagati, T.A.M., Mamba, B.B., Ion-imprinted polymers for environmental monitoring of inorganic pollutants: synthesis, characterization, and applications, *Environ. Sci. Pollut. Res.*, 20, 790–802, **2013**.
- [179] Hür, D., Ekti, S.F., Say, R., N-Acylbenzotriazole Mediated Synthesis of Some Methacrylamido Amino Acids, *Lett. Org. Chem.*, 4, 585-587, **2007**.
- [180] Arshady, R., A new synthetic for the preparation of polymer supports based on beaded copolymers of styrene and 2,4,5-trichlorophenyl acrylate: Synthesis and swelling behavior of poly(styrene-co-acrylamide) resins, *Macromol. Chem.*, 185, 2387-2400, **2008**.
- [181] Johnson, B. B., "Effect of pH, Temperature and Concentration on the adsorption of Cadmium on Goethite". *Environ. Sci. Technol.*, 24, 112 – 118, **1990**.



- [182] Freundlich, H.M.F., *Collid and Capillary Chemistry*, Methuen, London, **1926**.
- [183] Bulut, E., Ozacar, M., Sengil, I.A., Adsorption of malachite green onto bentonite:equilibrium and kinetic studies and process design, *Micropor. Mesopor. Mater.*, 115, 234–246, **2008**.
- [184] Weber, T.W., Chakravorti, R.K., Pore and solid diffusion models for fixed-bed adsorbers, *AIChE J.*, 20, 2, 228–238, **1974**.
- [185] Ileri, R., Sumer, B., kinetic and thermodynamic isotherm of biosorption, *çevre journal*, 7, 39-45, **1993**.
- [186] Weber, W.J., *Adsorption in physico-chemical processes for water quality control*, Wiley, NewYork, 199-259, **1972**.
- [187] Cheung, C. W., Porter, J. F., McKay, G., “Sorption kinetic analysis for the removal of cadmium ions from effluents using bone char.” *Water Res.*, 35,3, 605–612, **2001**.
- [188] Ho, Y.S., McKay, G., Pseudo-second order model for sorption processes, *Process Biochemistry*, 34 ,451–465, **1999**.
- [189] Denizli, A., Piskin, E., Dye-ligand affinity systems, *J.biochem. biophys. Methods* 49 (2001) 391-416.
- [190] Denizli.A., Say.R., Patir,S., Arica.Y., heavy Metal Separation capacity of a Porous metahaclramido-Phenylalanine Containing Membrane Based on a Polyhydroxyethyl Methacrylate Matrix, *separation Science and Technology*, 36,10, 2213-2231, **2001**.
- [191] Salih.B., Denizli. A., Kavakli.C., Say.R., Piskin.E., Adsorption of Heavy Metal Ions onto Dithizone-anchored poly(EGDMA-HEMA) Microbeads, *Talanta*, 46, 1205-1213, **1998**.
- [192] Say.R., Birlik.E., Ersoz.A., Yilmaz.F., Gedikbey.T., Denizli.A., Preconcentration of Copper on Ion-Selective Imprinted Polymer Microbeads, *Analytica Chimica Acta.*, 480, 251-258, **2008**.
- [193] Buyuktuncel. E., Bektas.S., Genc. O., Denizli.A., Poly(vinylalchol) coated/Cibracron Blu F3GA-attached Polypropylene Hollow Fiber Membranes for Removal of Cadmium Ions from Aquatic System, *Reactive & Functional.*, 47, 1-10, **2001**.
- [194] Satiroglu, N., Yacinkaya, Y., Denizli. A., Arica, M.Y., Bektas.S., Genc.O., Application of NaOH Plyporuse Versicolor for Removal of Divalent Ions of Group IIB Elements from Synthetic Wastewater, *Process Biochemistry.*, 38, 65-67, **2007**.
- [195] Aydin, H., Bulut, Y., Yerlikaya, C., Removal of Copper(II) from Aqueous Solution by Adsorption onto Low-Cost Adsorbents, *Journal of Environmental Management*, 87, 37-45, **2008**.

- [196] Denizli, A., Kesenci, K., Arica, M.Y., Salih, B., Hasirci, V., Piskin, E., Novel Dye-Attached Macroporous films for Cadmium, Zinc and Lead Sorption: Alkali Blu 6B-Attached Macroporus Poly(Hydroxyethyl Methacrylate), *Talanta*, 46, 551-558, **1998**.
- [197] Tekin, K., Uzun, L., Arpa, Sahin, C., Bektas, S., Denizli, A., Prepartion and Characterization of Composite Cryogels Containing Imidazole Group and Use in Heavy Metal Removal, *Reactive & Functional Polymer*, 71, 985-993, **2011**.
- [198] Ren, Y., Abood, H.A., He, F., Peng, H., Huang, K., Magnetic EDTA-modified chitosan/SiO<sub>2</sub>/Fe<sub>3</sub>O<sub>4</sub> adsorbent: Preparation, characterization, and application in heavy metal adsorption, *Chemical Engineerin Journal*, 226, 300-311, **2013**.
- [199] Tovar-Gomez, A., Rivera-Ramirez, D.A., Hernández-Montoya, V., Bonilla-Petriciolet.A., Synergic adsorption in the simultaneous removal of acid blue 25 and heavy metals from water using a Ca(PO<sub>3</sub>)<sub>2</sub>-modified carbon, *Journal of Hazardous Materials*, 199– 200, 290– 300, **2012**.
- [200] Zhai, Y., Liu, Y., Changa, X., Chena, S., Huang, X., Selective solid-phase extraction of trace cadmium(II) with an ionic imprinted polymer prepared from a dual-ligand monomer, *Analytica Chimica Acta*, 593,123–128, **2003**.
- [201] Singh, D.K., Mishra, S., Synthesis, characterization and removal of Cd(II) using Cd(II)-ion imprinted polymer, *Journal of Hazardous Materials*, 164, 1547–1551, **2009**.
- [202] Behbahani, M., Bagheri, A., Taghizadeh, M., Salarian, M., Sadeghi, O., Adlnasab, L., Jalali, K., Synthesis and characterisation of nano structure lead (II) ion-imprinted polymer as a new sorbent for selective extraction and preconcentration of ultra trace amounts of lead ions from vegetables, rice, and fish samples, *Food Chemistry*,138, 2050–2056, **2013**.
- [203] Jiang, Y., Kim, D., Synthesis and selective adsorption behavior of Pd(II)-imprinted porous polymer particles, *Chemical Engineering Journal*, 232 503–509, **2013**.
- [204] Li,Z., Li, J., Wanga, Y., Wei, Y., Synthesis and application of surface-imprinted activated carbon sorbent for solid-phase extraction and determination of copper (II), *Spectrochimica Acta Part A: Molecular and Biomolecular Spectroscopy*, 117, 422–427, **2014**.
- [205] Ren, Y., Zhang, M., Zhao, D., Synthesis and properties of magnetic Cu(II) ion imprinted composite adsorbent for selective removal of copper, *Desalination*, 228,135–149, **2008**.
- [206] Feng, T., Wang, J., Zhang, F., Shi, X., Removal of Copper(II) from an Aqueous Solution with Copper(II)-Imprinted Chitosan Microspheres, *J. APPL. POLYM. SCI.*, 3631-3638, **2013**.

- [207] Faghihiana, H., Asghari, Kh., Selective Solid-phase Extraction of  $\text{Cu}^{2+}$  by a Novel Cu(II)-imprinted Silica Gel, *J. Chin. Chem. Soc.*, 60, 1491-1499, **2013**.

## CURRICULUM VITAE

### Credentials

Name, Surname : MİTRA JALİLZADEH

Place of Birth : Khoy- Iran

Marital Status : Single

E-mail : mtraj@hacettepe.edu.tr

Address : Beytepe Campuse, Student Home, D Blok, Rome Number: 307, Hacettepe University.

### Education

High School : Somayeh High School

BSc. : Khoy University

MSc. : Tehran Science and Research Branch of Azad University

PhD. : Hacettepe University, Institute of Graduate Studies in Science, Chemistry Department

### Foreign Languages

English : Upper Intermediate

Persian : Advanced

Azerbaijani : Native

Arabic : Intermediate

### Work Experience

Research Assistant in Khoy University

### Areas of Experiences

Cryogels, Atomic Adsorption Spectroscopy, Electrochemistry

Projects and Budgets

Publications

Oral and Poster Presentations

Comparison of different ion-imprinted cryogels and their uses for selective metal adsorption, Frontiers in polymer science, Barcelona, Spain

Kinetics and isotherm studies on heavy metal adsorption onto heavy metal imprinted cryogels, Affinity techniques, Izmir Turkey

Preparation of magnetic and non-magnetic ion imprinted cryogels and use of them for adsorption of  $\text{Cu}^{+2}$ , Chromatography, Bursa, Turkey